

Western  Graduate&PostdoctoralStudies

Western University  
**Scholarship@Western**

---

Electronic Thesis and Dissertation Repository

---

5-2-2012 12:00 AM

# Multi-stage Wireless Signal Identification for Blind Interception Receiver Design

Gejie Liu

*The University of Western Ontario*

Supervisor

Xianbin Wang

*The University of Western Ontario*

Graduate Program in Electrical and Computer Engineering

A thesis submitted in partial fulfillment of the requirements for the degree in Master of Engineering Science

© Gejie Liu 2012

Follow this and additional works at: <https://ir.lib.uwo.ca/etd>

---

## Recommended Citation

Liu, Gejie, "Multi-stage Wireless Signal Identification for Blind Interception Receiver Design" (2012).  
*Electronic Thesis and Dissertation Repository*. 516.  
<https://ir.lib.uwo.ca/etd/516>

This Dissertation/Thesis is brought to you for free and open access by Scholarship@Western. It has been accepted for inclusion in Electronic Thesis and Dissertation Repository by an authorized administrator of Scholarship@Western. For more information, please contact [wlsadmin@uwo.ca](mailto:wlsadmin@uwo.ca).

# Multi-stage Wireless Signal Identification for Blind Interception Receiver Design

(Spine title: Blind Signal Identification)

(Thesis format: Monograph)

by

Gejie Liu

Graduate Program  
in  
Engineering Science  
Electrical and Computer Engineering

A thesis submitted in partial fulfillment  
of the requirements for the degree of  
Master of Engineering Science

School of Graduate and Postdoctoral Studies  
The University of Western Ontario  
London, Ontario, Canada

© Gejie Liu 2012

THE UNIVERSITY OF WESTERN ONTARIO  
SCHOOL OF GRADUATE AND POSTDOCTORAL STUDIES  
**CERTIFICATE OF EXAMINATION**

**Chief Advisor:**

---

Dr. Xianbin Wang

**Examining Board:**

---

Dr. Serguei L. Primak

---

Dr. Abdallah Shami

---

Dr. Liying Jiang

The thesis by

**Gejie Liu**

entitled:

**Multi-stage Wireless Signal Identification for Blind Interception Receiver  
Design**

is accepted in partial fulfillment of the  
requirements for the degree of

**Master of Engineering Science**

Date: \_\_\_\_\_

---

Chair of Examining Board  
Dr. Luiz Capretz

# Abstract

Protection of critical wireless infrastructure from malicious attacks has become increasingly important in recent years, with the widespread deployment of various wireless technologies and dramatic growth in user populations. This brings substantial technical challenges to the interception receiver design to sense and identify various wireless signals using different transmission technologies. The key requirements for the receiver design include estimation of the signal parameters/features and classification of the modulation scheme. With the proper identification results, corresponding signal interception techniques can be developed, which can be further employed to enhance the network behaviour analysis and intrusion detection.

In detail, the initial stage of the blind interception receiver design is to identify the signal parameters. In the thesis, two low-complexity approaches are provided to realize the parameter estimation, which are based on iterative cyclostationary analysis and envelope spectrum estimation, respectively. With the estimated signal parameters, automatic modulation classification (AMC) is performed to automatically identify the modulation schemes of the transmitted signals. A novel approach is presented based on Gaussian Mixture Models (GMM) in Chapter 4. The approach is capable of mitigating the negative effect from multipath fading channel. To validate the proposed design, the performance is evaluated under an experimental propagation environment. The results show that the proposed design is capable of adapting blind parameter estimation, realize timing and frequency synchronization and classifying the modulation schemes with improved performances.

# Acknowledgements

I present my sincerest appreciation to those who made this thesis possible. I would like to first thank my supervisor, Dr. Xianbin Wang, whose encouragement and support from the initial to the final level enabled me to develop a solid understanding of this subject. His guidance and freedom encouraged me to endeavor into this new research area. It has been a true fortune and privilege working with him.

I also owe my deepest gratitude to Dr. Serguei L. Primak and Dr. Vijay Parsa for whose courses greatly improved my work in theoretical analysis, understanding of communication systems, and signal processing.

At the same time, I would like to thank Dr. Abdelkader Ouda, Dr. Reza Azarderakhsh and Dr. Mohammed Alqedra. It is an honor to work as a teaching assistant under their guidance. I also want to thank Graduate Assistant and librarians in Allyn & Betty Taylor Library and The D. B. Weldon Library for their work and help.

Specially, I am indebted to my parents. Even far away, they have been present and supportive through every step of my study, always providing help in difficult times, and enjoying every single accomplishment during my fighting journey.

Lastly, I offer my regards and blessings to all of those who supported me in any respect during the completion of this study.

# Table of Contents

<b>Certificate of Examination</b>	<b>ii</b>
<b>Abstract</b>	<b>iii</b>
<b>Acknowledgements</b>	<b>iv</b>
<b>List of tables</b>	<b>viii</b>
<b>List of figures</b>	<b>ix</b>
<b>Acronyms</b>	<b>x</b>
<b>1 Introduction</b>	<b>1</b>
1.1 Motivation	1
1.2 Objective	3
1.3 Thesis Contributions	4
1.4 Thesis Organization	6
<b>2 Blind Signal Identification with Iterative Cyclostationary Analysis</b>	<b>8</b>
2.1 OFDM Systems	9
2.1.1 General Structure	9
2.1.2 Implementation	11
2.1.2.1 Guard Time and Cyclic Extension	12
2.1.2.2 Windowing	14
2.2 Cyclostationary Signal Analysis	16
2.3 Blind Parameter Estimation	19
2.4 Introduction of the Proposed Approach	22
2.5 System Model	23
2.5.1 Oversampled OFDM System Model	24

## Table of Contents

---

2.5.2	Cyclostationary Analysis in Oversampled OFDM Signals . . .	25
2.6	Iterative Cyclostationary Analysis with Arbitrary Oversampling Ratio	27
2.7	Parameter Estimation Based on Detected Cyclostationary Feature . .	31
2.8	Enhanced Channel Estimation with System Parameters Estimation .	33
2.8.1	Pilot Block Detection . . . . .	33
2.8.2	Iterative Channel Estimation . . . . .	33
2.9	Simulation Results and Discussions . . . . .	35
2.9.1	Enhanced iterative channel estimation . . . . .	37
2.9.2	Complexity Analysis . . . . .	38
2.10	Conclusion . . . . .	40
<b>3</b>	<b>Joint Blind Signal Parameter Estimation and Synchronization . .</b>	<b>42</b>
3.1	Synchronization for OFDM System . . . . .	42
3.1.1	Timing Offset Estimators . . . . .	43
3.1.1.1	Schmidl's Method . . . . .	43
3.1.1.2	Minn's Method . . . . .	44
3.1.1.3	Park's Method . . . . .	45
3.1.1.4	Seung's Method . . . . .	46
3.1.2	Carrier Frequency Offset and Sampling Clock Offset Estimator	47
3.1.2.1	One Dimensional Linear Least Square Estimation . .	47
3.1.2.2	D-Symbols Delay linear Least Square Estimation . .	48
3.1.2.3	Two Dimensional Linear Least Square Estimation . .	49
3.2	Introduction of the Proposed Approach . . . . .	50
3.3	System Model . . . . .	52
3.4	Envelope Spectrum-based Oversampling Ratio Estimation . . . . .	54
3.5	Joint Iterative Blind Parameter Estimation and Synchronization . . .	57
3.5.1	Estimation of the Number of Subcarriers and CP Length . . .	57
3.5.2	Estimation of Carrier Frequency Offset and Timing Offset . .	59
3.6	Experimental Results . . . . .	61
3.6.1	Lab Testing Platform . . . . .	61
3.6.2	Experimental Results . . . . .	63
3.7	Conclusion . . . . .	64

<b>4</b>	<b>GMM-based Automatic Modulation Classification . . . . .</b>	<b>67</b>
4.1	Automatic modulation classification . . . . .	67
4.1.1	Decision Theoretic-based Automatic Modulation Classification	69
4.1.1.1	ALRT-based Algorithms . . . . .	71
4.1.1.2	GLRT- and HLRT-based Algorithms . . . . .	73
4.1.2	Pattern Recognition-based Automatic Modulation Classification	74
4.1.2.1	Instantaneous Features-based Algorithms . . . . .	74
4.1.2.2	Wavelet Transform-based Algorithm . . . . .	76
4.1.2.3	Signal statistics-based Algorithms . . . . .	77
4.2	Introduction of the Proposed Approach . . . . .	79
4.3	Background . . . . .	81
4.3.1	Gaussian Mixture Models (GMM) . . . . .	82
4.3.2	Kullback-Leibler (K-L) Divergence . . . . .	83
4.4	GMM-based Modulation Classification . . . . .	85
4.4.1	Signal Features Extraction . . . . .	86
4.4.2	Modulation Classification Using GMM . . . . .	88
4.5	Iterative MAP Channel Mitigation Modulation Classification . . . . .	90
4.6	Simulation Results and Discussions . . . . .	93
4.7	Conclusion . . . . .	94
<b>5</b>	<b>Conclusion . . . . .</b>	<b>97</b>
5.1	Contributions of This Thesis . . . . .	97
5.2	Future Works . . . . .	99
	<b>References . . . . .</b>	<b>101</b>
	<b>Curriculum Vitae . . . . .</b>	<b>111</b>



# List of Tables

2.1	Physical layer parameters. . . . .	13
2.2	Complexity needed for the proposed method and traditional estimation. . . . .	39
3.1	PAPR Comparison . . . . .	43
3.2	System Parameters for The Generated OFDM Signals. . . . .	62
4.1	Theoretical Values $\Theta$ of GMM for $A_{nor}$ . . . . .	83
4.2	Theoretical Values $\Theta$ of GMM for $\sigma$ . . . . .	84

# List of Figures

2.1	OFDM modulator. . . . .	11
2.2	Block diagram of an OFDM transceiver. . . . .	13
2.3	OFDM frame with cyclic extension and windowing . . . . .	15
2.4	SCF estimate for a baseband OFDM signal. . . . .	27
2.5	SCF for oversampling ratio $q = 2.85$ . . . . .	28
2.6	Cyclic autocorrelation test for CP length estimator at fixed $\tau = N_s$ . .	32
2.7	Different power levels allocated to the pilot block and data block . . .	34
2.8	MSE of oversampling rate $q$ under multipath channel(SNR = 10dB). .	37
2.9	Prob. of the estimation error of number of subcarriers and CP length. .	38
2.10	MSE of Enhanced Channel Estimation with different estimation error .	41
2.11	SER of signal detection with different parameter estimation error . .	41
3.1	The principle of D-symbol estimation. . . . .	48
3.2	Illustration of oversampling structure for blind parameter estimation. .	53
3.3	Spectrum information of oversampled OFDM signal ( $q = 4$ ) . . . . .	56
3.4	Instrument setups for lab testing platform. . . . .	62
3.5	Mean square error of iterative oversampling ratio $q$ . . . . .	64
3.6	Prob. of correct estimation of number of subcarriers and CP length. .	65
3.7	BER of the proposed joint parameter estimation and synchronization. .	66
4.1	$\gamma_{max}$ for different modulation schemes when SNR = 5dB. . . . .	87
4.2	$\sigma_{max}$ for different modulation schemes SNR = 5dB. . . . .	88
4.3	The block diagram for GMM-based modulation classification. . . . .	89
4.4	Comparison of GMM and HOS on $P_{cc}$ for 16QAM and 2FSK. . . . .	94
4.5	Comparison of GMM and HOS on $P_{cc}$ for BPSK and 2ASK. . . . .	95

# Acronyms

<b>AWGN</b>	<i>Additive White Gaussian Noise</i>
<b>ASK</b>	<i>Amplitude Shift Keying</i>
<b>ACF</b>	<i>Autocorrelation Function</i>
<b>AMC</b>	<i>Automatic Modulation Classification</i>
<b>ALRT</b>	<i>Average Likelihood Ratio Test</i>
<b>CFO</b>	<i>Carrier Frequency Offset</i>
<b>CP</b>	<i>Cyclic Prefix</i>
<b>CR</b>	<i>Cognitive Radio</i>
<b>CS</b>	<i>Cyclic Spectrum</i>
<b>DFT</b>	<i>Discrete Fourier Transform</i>
<b>EM</b>	<i>Expectation-Maximization</i>
<b>FDM</b>	<i>Frequency Division Multiplexing</i>
<b>FSK</b>	<i>Frequency Shift Keying</i>
<b>GMM</b>	<i>Gaussian Mixture Model</i>
<b>GLRT</b>	<i>Generalized Likelihood Ratio Test</i>
<b>HLRT</b>	<i>Hybrid Likelihood Ratio Test</i>
<b>LF</b>	<i>Likelihood Functions</i>
<b>MAP</b>	<i>Maximum A Posteriori</i>
<b>ML</b>	<i>Maximum Likelihood</i>
<b>OFDM</b>	<i>Orthogonal Frequency Division Multiplexing</i>
<b>PSK</b>	<i>Phase Shift Keying</i>
<b>PDF</b>	<i>Probability Density Functions</i>
<b>QAM</b>	<i>Quadrature Amplitude Modulation</i>
<b>QPSK</b>	<i>Quadrature Phase Shift Keying</i>
<b>SDR</b>	<i>Software Defined Radio</i>
<b>SFC</b>	<i>Sliding Frequency Correlator</i>
<b>SFO</b>	<i>Sampling Frequency Offset</i>
<b>WT</b>	<i>Wavelet Transform</i>

# Chapter 1

## Introduction

### 1.1 Motivation

Protection of critical wireless infrastructure has become increasingly important in recent years with the widespread deployment of various wireless technologies and dramatic growth in user populations. Wireless communication systems and networks suffer from various security threats, including attacks similar to those in wired networks and those which are specific to the wireless environment. Wireless communication signals are open to intrusion from the outside without the need for a physical connection and, as a result, some techniques that provide to a wired network have proven to be inadequate in wireless networks. This brings substantial technical challenges to the spectrum regulation enforcement oriented signal sensing practice, due to the inherent difficulties in obtaining the content, identification and network behaviour of a signal of interest through conventional spectral analysis only.

The primary motivation of this study is to further develop the necessary enabling technologies required for blind interception receiver design to protect the wireless infrastructure and improve its resilience to various attacks. Proper RF signal sensing and identification, modulation classification are essential to protecting the public services against illegal usage of wireless communications and malicious attacks in addition to detecting the presence of personal wireless devices in classified areas.

Consequently, the study is dedicated to develop a software defined radio (SDR) based interception receiver to enhance the security of wireless communications, with novel multi-stage RF signal identification techniques. The proposed receiver will be capable of identifying, intercepting and analyzing the signal of interest, and reconfiguring its operating parameters depending on the operational objectives of respective user groups.

Another motivation for the thesis work is for cognitive radio application. With the recent rapid growth in wireless applications and systems, the problem of spectrum utilization has become more critical than ever before. As an emerging solution, Cognitive Radio (CR) systems aim to improve the efficiency of spectrum usage with the principle of sharing the available spectrum resources adaptively. Orthogonal frequency division multiplexing, which has been known to be one of the most effective multicarrier techniques, has attracted significant attention in the development of CR systems due to its high spectral efficiency and flexibility in allocating transmission resources in dynamic environments.

However, the existence of dissimilar wireless transmission schemes poses a challenge to the design of CR receivers that can operate with the multi-waveform signals. Therefore, blind system parameter estimation is of significant importance for reliable communication in CR environments. Furthermore, blind estimation is also helpful to reduce signaling overhead in the case of adaptive transmission where the system parameters change depending on the environmental characteristics or the spectrum availability. The capability of identifying system parameters is necessary for spectrum survey with the purpose of monitoring the systems to discover illegal transmissions as well.

Relevant signal identification are originated from SDR, where initial mode identification has to be performed over a large span of the potential frequency spectrum

to identify the user air interface. Once connected, an SDR has to monitor alternative air interfaces to be able to perform inter-standard handover if necessary. To be specific, the signal detection could be realized through signal sensing and identifications which are widely used in cognitive radio communications. Signal sensing provides the capability to sense, learn, and discover the parameters related to the radio channel characteristics, availability of spectrum and operating environment, user requirements and applications, and network availability

## 1.2 Objective

In order to realize the multi-stage signal identification for blind interception receiver design, blind parameter estimation, synchronization and modulation classification are the primary objectives in this study.

To be specific, the first step is to identify the primary parameters of the incoming signal. Since Orthogonal Frequency Division Multiplexing (OFDM) system is primarily considered in the study, the key system parameters we select here are sampling frequency, number of subcarriers, cyclic prefix ratio as well as frequency and timing offset. Since two directions exist in literature for blind parameter estimation, which are nonparametric spectrum based and cyclostationarity based, we analyze the performance for both and develop the approaches to improve the estimation accuracy under two scenarios. With the aid of estimated parameters, Carrier frequency offset (CFO) and timing offset are estimated for the purpose of synchronization. An iterative scheme is employed to increase the estimation accuracy.

Automatic modulation classification (AMC) is used to automatically identify the modulation schemes used in an intercepted communication signal by analyzing the characteristics of the received signal, which is normally corrupted by the noise

and fading channels. The interest in blind modulation classification has been growing since the late eighties. It plays several important roles in both civilian and military applications including signal surveillance, data interception, and confirmation of signal identification, interference monitoring, and counter-measure development. Legitimate signals should be securely transmitted and received, whereas hostile signals from adversaries must be located, identified, and recovered. The transmitting frequencies of these signals may range from high frequency to millimetre frequency band and their format can vary from traditional simple narrowband modulations to newly introduced wideband schemes particularly OFDM. Under such diverse conditions, advanced techniques are needed for real-time signal interception and processing, which are vital for decisions involving electronic warfare operations and other actions.

Furthermore, the lab testing platform is introduced in the thesis to verify the proposed algorithms of blind parameter estimation and modulation classification. The hardware environments include an arbitrary vector signal generator, spectrum analyzer and high speed signal acquisition system. Our proposed algorithms for blind OFDM system parameter estimations and modulation classification are evaluated using the signal generated from Rohde & Schwarz (R&S) and National Instruments (NI) signal acquisition system.

### 1.3 Thesis Contributions

The main contributions of this thesis are summarized as follows:

- In this study, we present an iterative scheme for blind parameter estimation of OFDM interception receiver design, which is based on cyclostationary feature detection. The approach avoids the exploration of a wide range of cyclic frequencies by first narrowing the analysis to a region containing the feature of

interest and performing high resolution exploration in that region to accurately detect the feature. Based on the detected features, system parameter estimation (sampling frequency, number of subcarriers and Cyclic Prefix (CP) duration) can be successfully obtained which provide the essential information for blind identification.

- An iterative blind parameter estimation and synchronization offset cancellation scheme is proposed in the study to perform accurate signal sampling and parameters identification. Specifically, the arbitrary oversampling ratio is estimated at first through time-domain envelope spectrum information, based on which the other system parameters, including the number of subcarriers and the CP length, are calculated sequentially. Synchronization is obtained from the estimated parameters and an iterative algorithm is employed to refine the results until a certain threshold is reached.
- With the purpose of modulation classification, a Gaussian Mixture Model (GMM)-based offline database is established, containing the parameters for different modulation schemes, as the reference to determine the GMM parameters of the received signal. Similar work has been investigated before without considering multipath fading channels. In the thesis, an iterative Maximum A Posteriori (MAP) channel mitigation technique is introduced to mitigate the multipath fading as well as to maintain system performance. Kullback-Leibler (K-L) Divergence is employed to measure the distance between the received signal and the modulation schemes in the database. To further ease the computational complexity, Gaussian approximation is carried out to cope with multivariate Gaussian components. Performance analysis is presented using Monte Carlo simulation to validate the effectiveness of classification accuracy.



## 1.4 Thesis Organization

The organization of this thesis is as follows:

In Chapter 2, a low-complexity approach, with the capability of blind OFDM parameter estimation, is proposed. The design is based on cyclostationary feature detection over a selected cyclic spectrum range using iterative techniques, instead of an exploration of the entire spectrum. Therefore, the computational complexity of signal interception is dramatically reduced. Monte Carlo simulations are conducted to evaluate the performance of the individual modules as well as the interception receiver. Numerical results show that the proposed algorithm is capable of signal detection in blind scenarios with improved performance.

In Chapter 3, an iterative design method for OFDM system parameter estimation and synchronization under a blind scenario for cognitive radio systems is proposed here. A novel envelope spectrum based arbitrary oversampling ratio estimator is presented first, based on which the algorithms are then developed to provide the identification of other OFDM parameters (number of subcarriers, cyclic prefix (CP) length). CFO and timing offset are estimated for the purpose of synchronization with the help of the identified parameters. An iterative scheme is employed to increase the estimation accuracy. To validate the proposed design, the performance is evaluated under an experimental propagation environment and the results show that the proposed design is capable of adapting blind parameter estimation and synchronization for cognitive radio with improved performances.

Chapter 4 considers the classification of digital modulation schemes in the presence of multipath fading channels and additive noise. The chapter presents a novel modulation recognition approach based on GMM. The basic procedure involves parameter estimation using GMM to set up an offline database and then to classify

the received signal into different modulation schemes based on the database by using K-L Divergence. In order to mitigate the negative impact from multipath fading channels, an iterative MAP-based channel estimation is used in conjunction with the Expectation-Maximization (EM) algorithm. Furthermore, Gaussian approximation is carried out to decrease the computational complexity. Monte Carlo simulations are conducted to evaluate the performance of individual modulation scheme classification. Numerical results show that the proposed approach is capable of recognizing various modulated signals with improved performance under Additive white Gaussian noise (AWGN) and multipath fading channels.

Finally, conclusions are drawn and future works are discussed in Chapter 5.

Notations: An upper (lower) case boldfont letter represents a matrix (column vector). The superscripts  $T$  and  $H$  denote the transpose and the Hermitian transpose, respectively.  $[X]_{i,j}$  denotes the  $(i,j)$ th element of matrix  $X$ . The term  $y(n)$  denotes the  $n$ th element of vector  $y$ .  $Tr(\cdot)$ ,  $E(\cdot)$ , and  $R(\cdot)$  stand for the matrix trace, the expectation, the real part and the imaginary part, respectively.  $|y|$  denotes the Euclidean norm of  $y$ .  $diag(x_1, x_2, \dots, x_N)$  represents a diagonal matrix whose  $l$ th diagonal element is  $x_l$  while  $diag(X)$  denotes a vector of the diagonal elements of  $X$ .  $I_N$  is the identity matrix of size  $N \times N$ .

## Chapter 2

# Blind Signal Identification with Iterative Cyclostationary Analysis

Although cyclostationary analysis of OFDM signals has been widely explored for spectrum sensing and signal identification, the associated high computational complexity requires additional processing and detection time, which further prevents the related techniques from fulfilling the demands of real-time military applications. In addition, recognizable and distinctive features of an OFDM signal in standards-based civilian communications may not be available in military communications thus, posing a challenge for accurate identification of the OFDM system parameters. In this chapter, a low-complexity interception receiver, with the capability of blind OFDM parameter estimation, is proposed. The interception receiver design is based on cyclostationary feature detection over a selected cyclic spectrum range using iterative techniques, instead of an exploration of the entire spectrum. Therefore, the computational complexity of signal interception is dramatically reduced. Monte Carlo simulations are conducted to evaluate the performance of the individual modules as well as the interception receiver. Numerical results show that the proposed algorithm is capable of signal detection in blind scenarios with improved performance.

## 2.1 OFDM Systems

OFDM is a wideband digital communications technique in which high-rate data is transmitted in parallel via multiple orthogonal subcarriers. In 1966, the idea of multi-carrier transmission was first brought out by Chang in [1]. Weinstein and Ebert subsequently proposed a complete digital OFDM system that used discrete Fourier transform (DFT) and inverse DFT (IDFT) for baseband modulation and demodulation [2] in 1971. From then on, OFDM systems have been investigated for wideband communications over mobile radio channels [3]. In this chapter, the transmitter and receiver structures for OFDM systems are presented in the sequel. Moreover, the main merits and drawbacks of OFDM system are summarized, followed by the major applications of OFDM systems.

The usage OFDM for high data transmissions has been investigated due to its high spectral efficiency and robustness to multi-path interference. OFDM is an extension to the conventional frequency division multiplexing (FDM) with respect to spectrum usage. In FDM, many parallel carriers are modulated and transmitted in different frequency bands to different users simultaneously. To avoid band interference caused by spectral leakage in conventional FDM, guard bands are inserted between two adjacent frequency bands. However, the utilization rate of available frequency spectrum drops due to the insertion of guard bands. To cope with this inefficient bandwidth usage, OFDM technique was proposed, in which adjacent subcarriers are overlapped orthogonally without interfering each other.

### 2.1.1 General Structure

The basic principle of OFDM is to split a high-rate datastream into a number of lower rate streams that are transmitted simultaneously over a number of subcarriers. The

relative amount of dispersion in time caused by multipath delay spread is decreased because the symbol duration increases for lower rate parallel subcarriers. The other problem to solve is the intersymbol interference, which is eliminated almost completely by introducing a guard time in every OFDM symbol. This means that in the guard time, the OFDM symbol is cyclically extended to avoid intercarrier interference.

An OFDM signal is a sum of subcarriers that are individually modulated by using phase shift keying (PSK) or quadrature amplitude modulation (QAM). The symbol can be written as:

$$s(t) = \text{Re} \left\{ \sum_{i=-\frac{N_s}{2}}^{\frac{N_s}{2}} d_{i+N_s/2} \exp(j2\pi(f_c - \frac{i+0.5}{T})(t - t_s)) \right\}, t_s \leq t \leq t_s + T \quad (2.1)$$

$$s(t) = 0, t < t_s \text{ and } t > t_s + T$$

where:

$N_s$  is the number of subcarriers

$T$  is the symbol duration

$f_c$  is the carrier frequency

The equivalent complex baseband notation is given by:

$$s(t) = \sum_{i=-\frac{N_s}{2}}^{\frac{N_s}{2}} d_{i+N_s/2} \exp(j2\pi(\frac{i}{T})(t - t_s)), t_s \leq t \leq t_s + T \quad (2.2)$$

$$s(t) = 0, t < t_s \text{ and } t > t_s + T$$

In this case, the real and imaginary parts correspond to the in-phase and quadrature parts of the OFDM signal. They have to be multiplied by a cosine and sine of

the desired frequency to produce the final OFDM signal. Figure 2.1 shows the block diagram for the OFDM modulator.

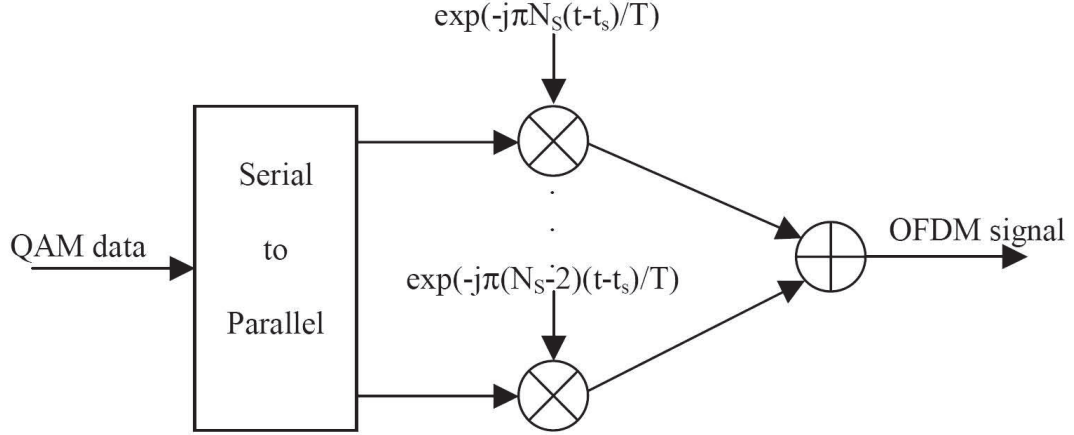


Figure 2.1: OFDM modulator.

The complex baseband OFDM signal defined the equation (2.2) is the inverse Fourier transform of  $N_s$  QAM input symbols. The time discrete case is the inverse discrete Fourier transform. In practice, this transform can be implemented very efficiently by the inverse fast Fourier transform (IFFT). The IFFT drastically reduces the amount of calculations by exploiting the regularity of the operations in the IDFT.

### 2.1.2 Implementation

In practice, the OFDM signal for the standard IEEE 802.11a is generated as follows: In the transmitter, binary input data is encoded by a rate 1/2 convolutional encoder. The rate can be increased to 2/3 and 3/4. After interleaving, the binary values are converted to QAM values. Four pilot values are added each 48 data values, resulting in a total of 52 QAM values per OFDM symbol. The symbol is modulated onto 52 subcarriers by applying the Inverse Fast Fourier Transform (IFFT). The output is converted to serial and a cyclic extension is added to make the system robust to mul-

tipath propagation. Windowing is applied after to get a narrower output spectrum. Using an IQ modulator, the signal is converted to analog, which is upconverted to the 5 GHz band, amplified, and transmitted through the antenna.

Basically, the receiver performs the reverse operations of the transmitter, with additional training tasks. In the first step, the receiver has to estimate frequency offset and symbol timing, using special training symbols in the preamble. After removing the cyclic extension, the signal can be applied to a Fast Fourier Transform to recover the 52 QAM values of all subcarriers. The training symbols and the pilot subcarriers are used to correct for the channel response as well as remaining phase drift. The QAM values are then demapped into binary values, and finally a Viterbi decoder decodes the information bits.

Figure 2.2 shows the block diagram of an OFDM modem, including the transmitter and the receiver. The IFFT modulates a block of input QAM values onto a number of subcarriers. In the receiver, the subcarriers are demodulated by the FFT, which is the reverse operation of the IFFT. These two operations are almost identical. In fact, the IFFT can be made using an FFT by conjugating input and output of the FFT and dividing the output by the FFT size. This makes it possible to use the same hardware for both the transmitter and the receiver. Of course, this saving in complexity is only possible when the modem does not have to transmit and receive simultaneously, which is the case for the standard.

In case of the standard IEEE 802.11a, the parameters for the physical layer (e.g. for OFDM) are listed in Table 2.1

### 2.1.2.1 Guard Time and Cyclic Extension

One of the most important problems in for wireless communications is the multipath delay spread. OFDM deals with it very efficiently. The parallel transmission implies

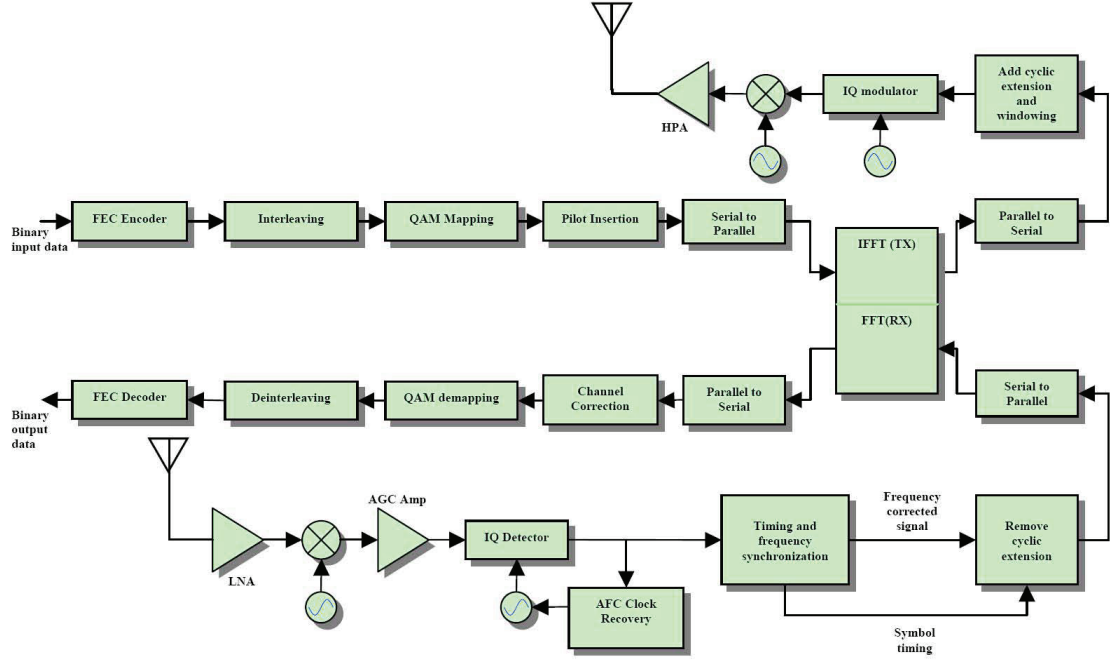


Figure 2.2: Block diagram of an OFDM transceiver.

Table 2.1: Physical layer parameters.

Data rate (Mbits/s)	Modulation	Coding rate (R)	Coded bits subcarrier ( $N_{BPSC}$ )	Coded bits per symbol ( $N_{CBPS}$ )	Data bits per symbol ( $N_{DBPS}$ )
6	BPSK	1/2	1	48	24
9	BPSK	3/4	1	48	36
9	BPSK	3/4	1	48	36
12	QPSK	1/2	2	96	48
18	QPSK	3/4	2	96	72
24	16-QAM	1/2	4	192	96
36	16-QAM	3/4	4	192	144
48	64-QAM	2/3	6	288	192
54	64-QAM	3/4	6	288	216

that the input datastream is divided in  $N_S$  subcarriers and the symbol duration is made  $N_S$  times smaller, which also reduces the relative multipath delay spread, relative to the symbol time, by the same factor.

The intersymbolic interference is almost completely eliminated by introducing



a guard time for a each OFDM symbol. The guard time is chosen larger than the expected delay spread such that multipath components from one symbol cannot interfere with the next symbol. This guard time could be no signal at all but the problem of intercarrier interference (ICI) would arise. Then, the OFDM symbol is cyclically extended in the guard time. Using this method, the delay replicas of the OFDM symbol always have an integer number of cycles within the FFT interval, as long as the delay is smaller than the guard time. Multipath signals with delays smaller than the guard time cannot cause ICI.

If multipath delay exceeds the guard time by a small fraction of the FFT interval (for example 3%), the subcarriers are not orthogonal anymore, but the interference is still small enough to get a reasonable constellation. Considering that the multipath delay exceeds the guard time by 10% of the FFT interval, the constellation is seriously affected and an unacceptable error rate is obtained.

#### **2.1.2.2 Windowing**

Essentially, an OFDM signal consists of a number of unfiltered QAM subcarriers. This means that the out-of-band spectrum decreases rather slowly, following a sinc function. For larger number of subcarriers, the spectrum goes down rapidly in the beginning, which is caused by the fact that the sidelobes are closer together.

To make the spectrum decrease faster, windowing is applied to the OFDM signal. The standard does not specify the kind of window to be used but an example

is included using the following function [4]:

$$W_T(t) = \begin{cases} \sin^2\left(\frac{\pi}{2}\left(0.5 + \frac{t}{T_{TR}}\right)\right), & \text{for } \left(-\frac{T_{TR}}{2} < t < \frac{T_{TR}}{2}\right) \\ 1, & \text{for } \left(\frac{T_{TR}}{2} \leq t \leq T - \frac{T_{TR}}{2}\right) \\ \sin^2\left(\frac{\pi}{2}\left(0.5 - \frac{t-T}{T_{TR}}\right)\right), & \text{for } \left(T - \frac{T_{TR}}{2} \leq t < T + \frac{T_{TR}}{2}\right) \end{cases} \quad (2.3)$$

considering that  $T_{TR}$  is the transition time between two consecutive periods of FFT, as it can be seen in Figure 2.3.

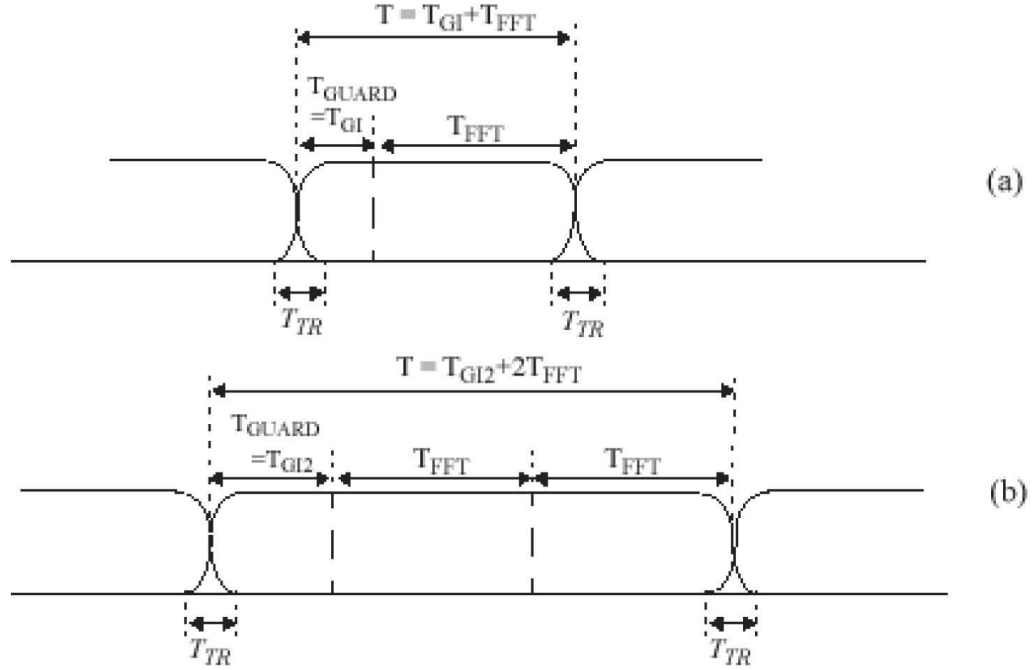


Figure 2.3: OFDM frame with cyclic extension and windowing

Figure 2.3 also illustrates the possibility of extending the windowing function over more than one period,  $T_{FFT}$ , and additionally shows smoothed transitions by application of a windowing function, as exemplified in Equation (2.3). In particular, window functions that extend over multiple periods of the FFT are utilized in the

definition of the preamble.

Several other conventional windows were simulated including raised cosine, Hann, Hamming, Blackman and Kaiser. The best performance was obtained for the Blackman window, considering the resulting stopband attenuation and the transition bandwidth.

## 2.2 Cyclostationary Signal Analysis

Signal cyclostationarity has been used as a statistical tool in many different applications, including spectrum sensing, blind equalization, parameter estimation and modulation recognition [5] - [7]. Communication signals in general exhibit cyclostationarity associated with the symbol period, carrier frequency, chip rate and a combination of these factors [8]. Before discussing the cyclostationarity in OFDM signals, the fundamental concepts of cyclostationary processes will be first introduced.

A cyclostationary signal is a signal having statistical properties which vary cyclically with time. Define the mean and time-varying autocorrelation function (ACF) of a stochastic process  $x(t)$  ( e.g., an OFDM communication signal) as

$$\mu_x(t) = E\{x(t)\} \quad (2.4)$$

and

$$R_x(t_1, t_2) = E\{x(t_1)x^*(t_2)\} \quad (2.5)$$

Here  $E\{\cdot\}$  is the standard expectation operator and  $*$  is the conjugation of the corresponding complex process.

$x(t)$  is wide-sense cyclostationary if its mean and time-varying ACF are periodic in time [9], [10] with a period  $T$ . Namely, for any given integer  $m$ ,

$$\mu_x(t) = \mu_x(t + mT) \quad (2.6)$$

and

$$R_x(t_1, t_2) = R_x(t_1 + mT, t_2 + mT) \quad (2.7)$$

Without loss of generality, define  $t_1 = t + \tau/2$  and  $t_2 = t - \tau/2$ . An alternate definition of the time-varying ACF for a cyclostationary process is

$$R_x(t, \tau) = E\{x(t + \tau/2)x^*(t - \tau/2)\} \quad (2.8)$$

$R_x(t, \tau)$  is referred to as the symmetric form of the time-varying ACF since it considers two points in time separated by  $\tau$  and centred at  $t$ . Due to the clearness and simplicity, (2.8) will be used in the following for further explanation about cyclostationarity.

Analogous to (2.7), wide-sense cyclostationarity in (2.8) can be expressed as

$$R_x(t, \tau) = R_x(t + mT, \tau) \quad (2.9)$$

For any cyclostationary process  $x(t)$  that satisfies (2.9), the time-varying ACF can be expressed as a Fourier series over the corresponding period  $T$

$$R_x(t, \tau) = \sum_{\alpha} R_x^{\alpha}(\alpha, \tau) e^{j2\pi\alpha t} \quad (2.10)$$

where the Fourier series coefficients in (2.10) are given as

$$R_x^\alpha(\alpha, \tau) = \frac{1}{T} \int_{-T/2}^{T/2} R_x(t, \tau) e^{-j2\pi\alpha t} dt \quad (2.11)$$

$R_x^\alpha(\alpha, \tau)$  is referred to as the CCF where  $\alpha$  is the cyclic frequency (CF). If a process is wide-sense stationary, the CCF is identically zero for all  $\alpha$  other than  $\alpha = 0$ . In other words, for a stationary process,  $R_x(t, \tau) = R_x^0(t, \tau)$  and  $R_x(t, \tau)$  can be shortened as  $R_x(\tau)$  because it is no longer dependent upon  $t$ .

The CCF can also be obtained by extending the period of integration in (2.11) to infinite as follows

$$R_x^\alpha(\alpha, \tau) = \lim_{T \rightarrow \infty} \frac{1}{T} \int_{-T/2}^{T/2} R_x(t, \tau) e^{-j2\pi\alpha t} dt \quad (2.12)$$

This expression together with the definition of  $R_x(t, \tau)$  given in (2.8), provide a method for estimating the CCF from observed waveforms. Suppose that samples from the process  $x(t)$  are observed during any observation interval  $T$ , and this observation interval is symmetric with respect to the time origin. An estimate for  $R_x^\alpha(\tau)$  is then given by

$$\hat{R}_x(\alpha, \tau) = \frac{1}{T} \int_{-T/2}^{T/2} x(t + \tau/2) I_T(t + \tau/2) x^*(t - \tau/2) I_T(t - \tau/2) e^{-j2\pi\alpha t} dt \quad (2.13)$$

where  $I$  is the indicator function defined as

$$T = \begin{cases} 1, & |t| \leq T/2 \\ 0, & \text{elsewhere,} \end{cases} \quad (2.14)$$

Moreover, define the Fourier transform of the CCF with respect to  $\tau$  as the cyclic spectrum (CS)

$$S_x(\alpha, f) = \int_{-\infty}^{\infty} R_x^\alpha e^{-j2\pi f\tau} d\tau \quad (2.15)$$

When  $\alpha = 0$ , CS is equal to the power spectrum (or spectral density) defined in the conventional manner [10]. For any wide sense stationary process, the CS is identically zero for all  $\alpha$  other than  $\alpha = 0$ . This follows directly from the equivalence of  $R_\tau^{\alpha=0}$  to  $R(\tau)$  for such a process.

## 2.3 Blind Parameter Estimation

Various blind OFDM system parameters estimation schemes have been studied in recent years for both signal identification and signal behaviour analysis. The existing techniques can be generalized into two categories: with or without sampling frequency at the transmitter as prior information. The first category has been widely explored [11], which focused on the synchronization and other parameters. Furthermore, [12] and [13] present more complete OFDM system parameters extraction which employs the correlation method to explore the system parameters of OFDM systems. However, this category of techniques cannot apply to the considered public security problem due to the unknown information of incoming signals especially for intrusion signal.

Therefore, for signal detection purpose, blind parameter estimation without any prior information is investigated in the PSTP milestone 3. Among those system parameters, the decisive one is the sampling frequency at the transmitter with which the signal can be downsampled from carrier frequency and the subsequent processing is available. There are two primary approaches under current research: cyclostationarity-based and nonparametric spectrum-based estimation. In details, cyclostationary theory, developed for years in various signal processing areas, was first introduced into OFDM system analysis in [11] and based on Dandawat and Giannakis' work [15], the key step to estimate sampling frequency through cyclostationary properties is to examine the cyclo-period of oversampled OFDM signal at the receiver. In literature, Martin and Kedem [16] detected this period through the periodogram associated with the sequence having the similar period to the least common multiple periods of the original cyclostationary signal; Hurd and Gerr [17] obtained the cyclo-period from the bispectrum, which was estimated using the two-dimensional periodogram; Dandawat and Giannakis [15] aimed at the detection of cyclo-stationarity under a broader context, almost cyclo-stationary signals, through a statistical  $\chi^2$  test based on the cyclic covariance and the cyclic spectrum. In [18], cyclostationarity-based sampling frequency estimation through Dandawat and Giannakis approach is presented. However, the above cyclostationarity-based methods failed to fulfill the demands of military communications since computational complexity leads to overly long processing and detection times. As a result, a low complexity OFDM receiver is proposed in the following parts where system parameters, modulation schemes and channel state information (CSI) are jointly estimated based on the cyclic spectrum. Specifically, conventional cyclostationary analysis is replaced by a new scheme where only the samples around specific feature points are computed instead of calculating over the entire spectrum. Therefore, a large computational burden is removed with

negligible performance degradation. Based on the cyclic spectrum features, key system parameters (sampling frequency, cyclic prefix ratio, number of subcarriers and frequency offset as well as timing offset) can be successfully obtained which provide the essential information required for signal identification. Additionally, blind channel estimation is also included such that the signal can be completely demodulated.

On the other hand, a non-parametric spectrum method for blind parameter estimation which is based on spectrum information and autocorrelation is an alternative and complete investigation is provided in [19]. Unfortunately, the method does not work well for upsampling method with raised cosine filter at transmitter which is closer to the practical implementation. We propose a blind estimation method to obtain the key parameters of OFDM system, based on which an iterative channel estimation scheme is proposed to provide CSI as well with enhanced accuracy for potential resource optimization in networks. We establish a novel two-step estimation scheme where accurate results are achieved based on the first step coarse estimation. Other system parameters as mentioned above are subsequently estimated as the input of the channel estimator. Then an iterative channel identification scheme is proposed to improve the performance of traditional pilot-based methods in the hostile environments.

Blind signal interception is a fundamental step of signal intelligence for military applications. However, there are substantial technical challenges to overcome in sensing and identifying various wireless signals due to the existence of many different transmission technologies and standards. The key requirements to achieve blind signal interception include detecting the existence of a signal and identification of its parameters and features. With the proper system parameter identification results, corresponding signal interception and data recovery techniques can be developed.



## 2.4 Introduction of the Proposed Approach

Orthogonal Frequency Division Multiplexing (OFDM) has been widely employed in many civilian and military broadband communication systems due to its high spectral efficiency and robustness to multi-path interference. Various blind OFDM system parameter estimation schemes have been studied recently for signal identification [18]-[21]. Among the existing techniques, cyclostationary estimation is the most commonly used due to its reasonable estimation accuracy for various types of air interface identification. In general, cyclostationarity is an important feature of wireless communication signals which can be used to determine the existence and classification of a signal [8],[22]. Additionally, cyclostationary analysis has been extensively examined as a technique for achieving a wide range of analysis in OFDM systems including signal detection [23], frequency and timing synchronization [24] and channel estimation [25]. Therefore, improving the reliability of cyclostationarity detection will provide more accurate system information for further processing of an intercepted signal.

Most signal detection methods are not suitable to fulfill the demands of military communications since computationally complex receiver design leads to overly long processing and detection times [18]-[20]. In addition, traditional methods require the exploration of a wide range of cyclic frequencies and require a long observation time in order to obtain reliable analysis.

Since the oversampling ratio at the receiver can be arbitrary, it is hard to achieve high estimation accuracy for non-integer oversampling ratios. As a result, a low complexity approach is required to overcome the above challenges. The Zoom Fast-Fourier Transform based method in [21] was proposed to provide a computationally-efficient estimation with high accuracy, however, the observation time required is still long for practical use and may suffer from reduced performance due to sampling clock

frequency instability.

In this chapter, we present an iterative scheme for blind parameter estimation of OFDM interception receiver design, which is based on cyclostationary feature detection. The method avoids the exploration of a wide range of cyclic frequencies by first narrowing the analysis to a region containing the feature of interest and performing high resolution exploration in that region to accurately detect the feature. Based on the detected features, system parameter estimation (sampling frequency, number of subcarriers and Cyclic Prefix (CP) duration) can be successfully obtained which provide the essential information for blind identification. Since the computational complexity of the proposed system is significantly reduced with negligible performance degradation, the usefulness of the entire system is thus increased. The proposed receiver in this chapter is capable of providing reliable signal identification for military signal intelligence applications.

## 2.5 System Model

Due to the time-varying nature of the wireless channel, it is difficult, at times, to determine the presence or existence of a wireless signal. In this case, the periodicity of signal features such as the mean, correlation or spectral descriptors can be used to determine signal existence and is known as cyclostationary analysis [25]. A signal is called second-order cyclostationary if its time-varying auto-correlation function  $R_x(t, \tau)$

$$R_x(t, \tau) = E\{x(t)x(t + \tau)\} \quad (2.16)$$

is periodic in  $t$  for a given delay  $\tau$ . An OFDM signal possesses a periodic auto-correlation function due to the insertion of the cyclic prefix and is thus, second-order

cyclostationary[24].

### 2.5.1 Oversampled OFDM System Model

Consider an OFDM system with  $N_s$  transmission subcarriers. We make the assumption that due to the insertion of the cyclic prefix, there is no inter-symbol interference. Without loss of generality, we focus on one OFDM symbol with duration  $T_s$ . The transmitted OFDM signal in baseband over  $[0, T_s)$  can be represented as

$$s(t) = \frac{1}{\sqrt{N_s}} \sum_{k=0}^{N_s-1} d_k \exp(j2\pi \frac{k}{T_s} t) u(t) \quad (2.17)$$

where  $u(t)$  denotes a raised cosine filter defined in  $[0, T_s)$  and  $d_n$  represents a data symbol with unit average power on the  $n$ th subcarrier. Specifically, letting

$$\mathbf{d} \triangleq [d_0, d_1, \dots, d_{N_s-1}]^T \quad (2.18)$$

the data symbols on  $N_s$  subcarriers satisfy

$$\mathbf{E}[\mathbf{d}\mathbf{d}^H] = \mathbf{I}_{N_s} \quad (2.19)$$

where  $\mathbf{I}_{N_s}$  is an identity matrix of size  $N_s$  by  $N_s$ .

Suppose that  $h(t)$  is an unknown frequency selective multipath channel. The received time-domain signal can be written as

$$x(t) = \sum_m h(m) s(t - mT_s) + w(t) \quad (2.20)$$

where  $w(t)$  is additive white Gaussian noise (AWGN) with zero mean and variance

$\sigma_w^2$ . Assuming that the sampling period at the receiver side is  $T_b$  with  $T_b < T_s$ , the oversampling factor  $q$  is defined as  $q = T_s/T_b$  and the corresponding oversampled OFDM signal can be consequently denoted by

$$x(n) = \sum_m h(m)s(n - qm) + w(n) \quad (2.21)$$

## 2.5.2 Cyclostationary Analysis in Oversampled OFDM

### Signals

If  $t$  and  $\tau$  in (2.16) are replaced with  $t + \tau/2$  and  $t - \tau/2$ , the autocorrelation function can be expressed as

$$R_x(t, \tau) = E\{x(t + \tau/2)x(t - \tau/2)\} \quad (2.22)$$

Therefore, the periodicities can be examined using the cyclic autocorrelation function (CAF) [8],

$$R_x^\alpha(\tau) = \lim_{T \rightarrow \infty} \frac{1}{T} \int_{-T/2}^{T/2} R_x(t, \tau) e^{-j2\pi\alpha t} dt \quad (2.23)$$

for cyclic frequency  $\alpha$  and observation length  $T$ .

Cyclostationary features can be detected from specific correlation patterns which occur in the spectrum of the signal. These patterns can be measured by the normalized correlation between two spectral components of  $x(t)$  at frequencies  $f + \Delta f/2$  and  $f - \Delta f/2$ , where  $\Delta f$  is the spectral resolution size. The spectral correlation function (SCF) is introduced to calculate the cyclic spectrum, which is given by [8]

$$S_x^\alpha(f) = \lim_{\Delta f \rightarrow 0} \lim_{T \rightarrow \infty} \frac{1}{T} \cdot \frac{1}{\Delta f} \cdot \int_{f - \Delta f/2}^{f + \Delta f/2} X_T(t, v + \frac{\alpha}{2}) X_T^*(t, v - \frac{\alpha}{2}) dv \quad (2.24)$$

where

$$X_T(t, v) = \int_{t-T/2}^{t+T/2} x(u) e^{-j2\pi v u} du \quad (2.25)$$

represents the time-variant Fourier transform of  $x(t)$ . Together the CAF and SCF provide a comprehensive means of examining the cyclostationary features of a signal. Gardner [8] proved that in order to obtain satisfactory estimation information, the time-spectral resolution product must exceed unity, i.e.,

$$T\Delta f \gg 1 \quad (2.26)$$

This implies that a lengthy observation time with a high spectral resolution  $\Delta f$  is required to resolve the individual features of the SCF. The SCF for a baseband OFDM signal is shown in Figure 2.4.

Since no prior information is available for a blind OFDM interception receiver, a captured signal must be oversampled for successful reception as well as for correct estimation. Identification of cyclostationary features using an arbitrary oversampling ratio is a challenge for blind OFDM interception receiver design.

Figure 2.5 shows the SCF of the baseband OFDM signal using an oversampling ratio of  $q = 2.85$ . We can see that, due to the oversampling ratio used, the SCF information has been shifted towards the zero spectral frequency axis with the significant peak located at the edge of the signal of interest.

Ideal SCF estimation requires the traversal of the entire cyclic and spectral frequency domains as well as a lengthy observation time with high spectral resolution, resulting in high computational complexity and increased processing delay. In the following sections, an iterative scheme is introduced to determine the cyclostationary features of the received OFDM signal under an arbitrary oversampling ratio. It

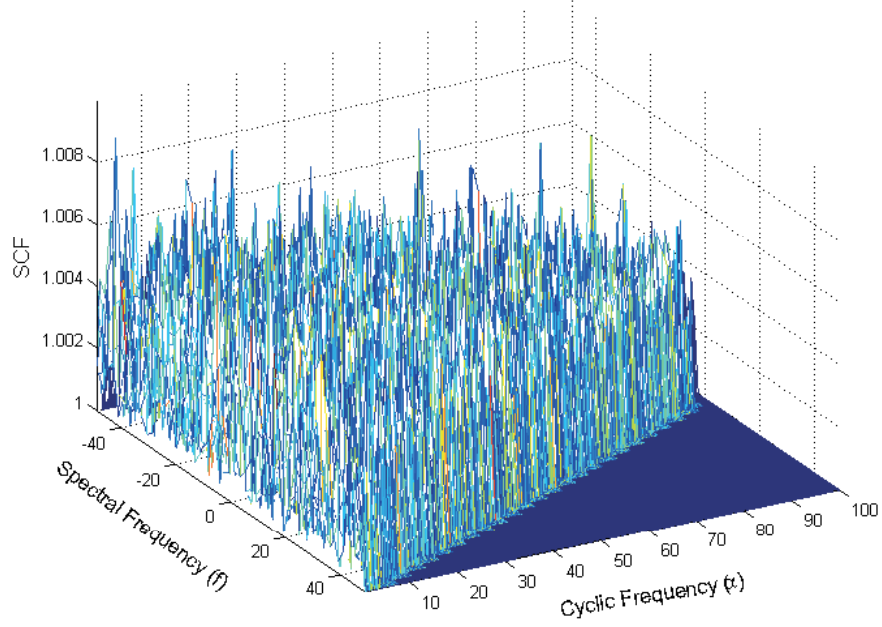


Figure 2.4: SCF estimate for a baseband OFDM signal.

is found, using simulations, that the proposed method reduces the computational load drastically. Blind parameter estimation is realized based on this low-complexity cyclostationary feature analysis.

## 2.6 Iterative Cyclostationary Analysis with Arbitrary Oversampling Ratio

After the detection of an incoming signal, the OFDM interception receiver must identify the desired cyclostationary feature represented as a peak shown in Figure 2.5. Suppose that the index of the peak of the desired cyclostationary feature along the cyclic frequency axis is  $\alpha$  using a spectral resolution size  $\Delta f$ . The length of the cyclic frequency axis is  $L = 1/\Delta f$  and the oversampling ratio  $q = \frac{1}{\alpha \Delta f}$ . Once the

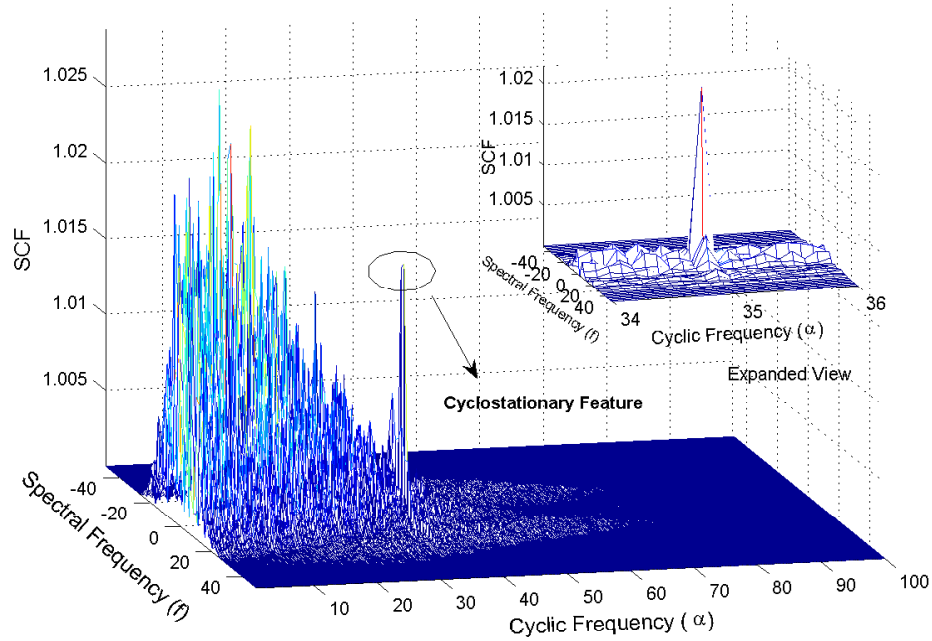


Figure 2.5: SCF for oversampling ratio  $q = 2.85$ .

oversampling ratio  $q$  has been estimated, further parameter estimation can be realized based on this  $q$ . In order to maintain low computational complexity, iterative analysis is used to increase the oversampling ratio estimation accuracy by first performing low, and then high resolution estimation.

For an oversampled OFDM signal, the desired cyclostationary feature is located at the edge of the signal of interest in SCF analysis. One can reduce the computational load by applying an iterative method with increasing observation time as well as decreasing spectral resolution size to only a limited search range of the cyclic frequency axis, which includes the desired peak index.

Low spectral resolution gives coarse SCF information which makes it impossible to detect the cyclostationary feature. However, the edge of signal of interest is still apparent. Therefore, the purpose of the tentative SCF analysis with low spectral

resolution is to identify the relative position of the signal of interest while maintaining a low computational load.

Assume that the tentative short observation time of the SCF for signal detection is  $T_l$  and the low spectral resolution is  $\Delta f_l$ , then the time-spectral resolution product is small and the corresponding  $S_x^\alpha(f)$  is achieved based on (2.24). Therefore, if the existence of an incoming signal is declared, the analysis is then performed on the entire cyclic spectrum using coarse analysis to obtain the spectrum information. We can then detect the edge of the signal of interest and we can assume that this edge is located between  $i$  and  $j$  along the cyclic frequency axis where  $i < j \in (1, 1/\Delta f_l)$ . Two tentative factors are thus decided as

$$\begin{aligned} q_1 &= \frac{1}{j\Delta f_l} \\ q_2 &= \frac{1}{i\Delta f_l} \end{aligned} \quad (2.27)$$

Using  $q_1$  and  $q_2$  we can broadly define the region of interest that contains the exact oversampling ratio  $q$ , i.e.,  $q_1 < q < q_2$ . In order to accurately determine  $q$ , we must increase the time-spectral resolution in the region of interest defined by  $q_1$  and  $q_2$ . Therefore, we can explore a subset of the entire cyclic spectrum instead of exploring the entire cyclic spectrum itself. In this region we now perform a high time-spectral resolution analysis with high estimation accuracy. Let us denote the product of  $\Delta f_h$  and  $T_h$  to be the high time-spectral resolution candidate. The range of interest is now limited to  $\alpha_1$  and  $\alpha_2$ , given as

$$\begin{aligned} \alpha_1 &= \frac{1}{\Delta f_h q_2} \\ \alpha_2 &= \frac{1}{\Delta f_h q_1} \end{aligned} \quad (2.28)$$



We can iteratively improve the estimation accuracy with each iteration increasing in time-spectral resolution within the selected range. Since an arbitrary oversampling ratio scenario is considered, both integer and rational oversampling ratios are possible. Using the iterative approach allows for the efficient estimation of both integer and rational oversampling ratios which can then be used to detect the desired cyclostationary feature accurately.

If the estimated oversampling ratio at  $j - 1$ ,  $j$  and  $j + 1$  steps are  $q^{(j-1)}$ ,  $q^{(j)}$  and  $q^{(j+1)}$ , the final estimation result is achieved if the following conditions are met

$$|q^{(j+1)} - q^{(j)}| < |q^{(j)} - q^{(j-1)}| < \gamma \quad (2.29)$$

where  $\gamma$  is the level of acceptance. Suppose that  $\Delta\hat{f}$  is the spectral resolution size at this step and  $\hat{\alpha}$  is the desired peak index representing the cyclostationary feature. The estimated oversampling ratio  $\hat{q}$  is identified as

$$\hat{q} = \frac{1}{\hat{\alpha}\Delta\hat{f}} \quad (2.30)$$

With this oversampling ratio, the sampling frequency of a transmitted OFDM signal can be determined and the corresponding OFDM symbol length is calculated as well. Therefore, the transmitted OFDM signal is correctly detected by the interception receiver for further analysis.

## 2.7 Parameter Estimation Based on Detected Cyclostationary Feature

After correctly sampling the received continuous signal, the proposed OFDM interception receiver must identify the primary system parameters of the intercepted signal. The parameters defined here are the number of subcarriers as well as the length of the cyclic prefix (CP).

For an OFDM symbol with  $N_s$  subcarriers, the estimated autocorrelation function  $\hat{R}_x(n, \tau)$  of the oversampled signal can be written as

$$\hat{R}_x(n, \tau) = \frac{1}{P} \sum_{n=0}^{P-1} x(n)x^*(n - \tau), \quad \tau \in [0, 1, \dots, P - 1] \quad (2.31)$$

where  $P$  is the length of oversampled incoming signal. The absolute value of  $\hat{R}_x(n, \tau)$  is considered and is given as

$$|\hat{R}_x(\tau)| = \begin{cases} \sum_{n=0}^P |h(n)|^2 + \sigma_w^2, & \tau = 0 \\ \sum_{n=0}^P |h(n)|^2 \frac{N_g}{N_f} + \sigma_w^2, & \tau = N_b, \end{cases} \quad (2.32)$$

where  $h(n)$  stands for the frequency selective channel impulse responses and  $\sigma_w^2$  represents the variance of the AWGN,  $N_g$  is the CP length,  $N_b$  is the OFDM symbol length of the oversampled signal with  $N_b = qN_s$  and  $N_f$  is the length of the OFDM subframe including CP.  $|\hat{R}_x(\tau)|$  will have the most significant peak when  $\tau = N_b$ . Therefore, through peak detection, the estimated number of subcarriers can be achieved by

$$\hat{N}_s = \frac{N_b}{\hat{q}} \quad (2.33)$$

Estimation of the CP length has been discussed in many papers previously ([19], [21], and [41]). However, some implementations use exhaustive autocorrelation analysis [41], some require prior information for accurate results [19] and some techniques are only successful for certain pre-defined CP lengths [21] which are not available for blind interception receiver design. Therefore, in this section, a new approach is developed which utilizes the cyclic autocorrelation information.

Assume that  $N_f = N_g + N_s$  is the length of OFDM subframe. The estimated cyclic autocorrelation is given by

$$R_x^k(\tau) = \frac{1}{P} \sum_{n=0}^{P-1} R_x(n, \tau) e^{-j \frac{2\pi}{P} kn}, \quad (k, \tau) \in [0, 1, \dots, P-1] \quad (2.34)$$

where  $P$  is the length of the oversampled signal. Using the estimated number of subcarriers  $N_s$ , we can obtain the cyclic autocorrelation with delay  $\tau = N_s$ . The cyclic prefix length,  $N_g$ , can be determined by using peak detection on  $R_x^k$  at  $\tau = N_s$ .  $k_{opt}$  represents the first peak with the smallest index above the threshold from the

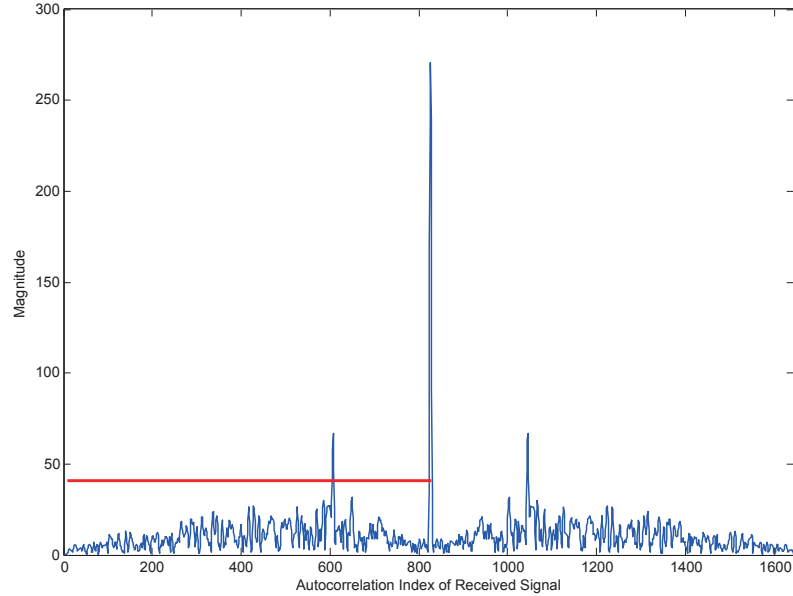


Figure 2.6: Cyclic autocorrelation test for CP length estimator at fixed  $\tau = N_s$ .

cyclic autocorrelation. Therefore,  $N_f$  can be identified as

$$N_f = \frac{2P}{k_{opt}} \quad (2.35)$$

and the CP length  $N_g$  is determined as  $N_g = N_f - N_s$ .

## 2.8 Enhanced Channel Estimation with System Parameters Estimation

After blind parameter estimation for received OFDM signal, further channel identification can be performed based on the necessary parameters. Here we assume the baseband received signal after downsampling is denoted by  $x(n)$ .

### 2.8.1 Pilot Block Detection

In traditional communication system, the power of pilot block is higher than data blocks which is shown in Figure 2.7. Therefore, the pilot block can be detected using the energy detector,

$$E = \sum_n |x(n)|^2. \quad (2.36)$$

which means if the energy of a certain block is higher than the average of other, it can be determined as a pilot block.

### 2.8.2 Iterative Channel Estimation

After detecting the position of pilot block, an enhanced iterative channel estimation scheme is proposed in this section to improve the performance of traditional pilot-aided channel estimation (PACE). It can be assumed that the channel is quasi-static

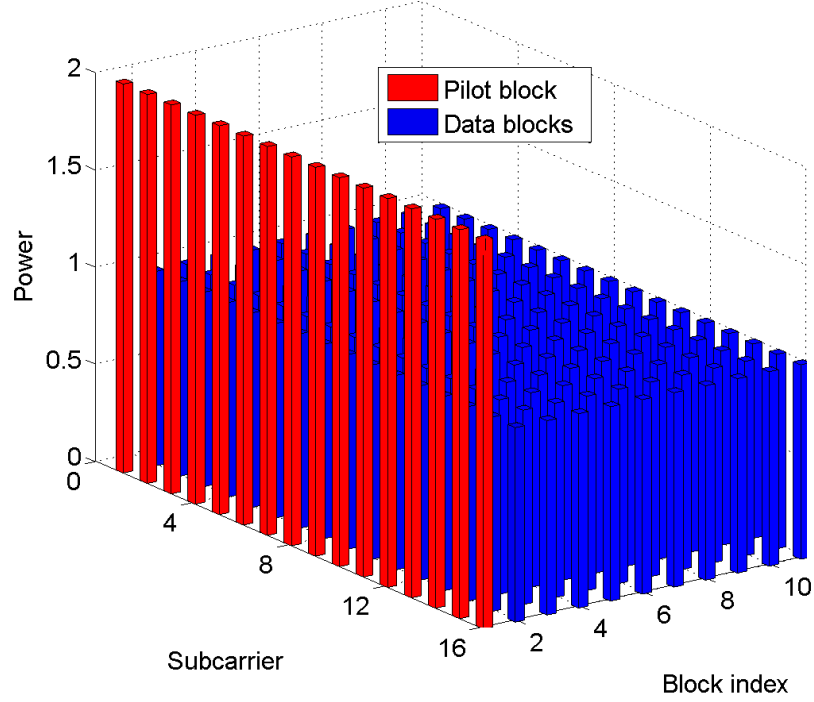


Figure 2.7: Different power levels allocated to the pilot block and data block

over a number of OFDM symbols in common wireless environment. Therefore, the principle of the enhanced channel estimation is that we utilize the initial channel estimate provided by the pilot block to obtain tentative demodulation results of the subsequent OFDM symbols. The demodulated OFDM symbols are combined with the original multiplexed pilot block to enhance the power of the pilot. We summarize the algorithm as follows:

1. Obtain initial channel estimation by using the block-type block through Least Square (LS) estimator:

$$\hat{H}_l = \frac{X_l}{P_l}, \quad l = 0, 1, \dots, N_s - 1, \quad (2.37)$$

where  $\hat{H}_l$  denotes the estimated channel frequency response on the  $l$ th subcar-

rier.  $P_l$  and  $X_l$  denote the pilot symbol and corresponding received sample on the  $l$ th subcarrier.

2. Equalize the subsequent OFDM symbols using the current channel estimate,

$$\tilde{d}_{n,l} = X_{n,l} / \hat{H}_l, \quad n = 1, 2, \dots, B, \quad (2.38)$$

where  $B$  represents the number of OFDM blocks needed for channel estimation accuracy enhancement.

3. Make data decisions on the equalized OFDM symbols and denote them as  $\hat{d}_{n,l}$ . Then update the channel estimation as follows,

$$\hat{H}_l = \frac{1}{1+B} \left( \frac{Y_l}{P_l} + \sum_{n=1}^B \frac{X_{n,l}}{\hat{d}_{n,l}} \right). \quad (2.39)$$

4. Repeat Steps 2) and 3) to simultaneously improve the accuracy of channel estimation and data detection until the estimation results converge or a predefined number of iterations is achieved.

## 2.9 Simulation Results and Discussions

This section provides simulation results for the statistical tests of the proposed system. Monte Carlo simulations are conducted to examine the performance of the above estimation approaches under different scenarios. The parameters of the OFDM system used in the simulation are: number of subcarriers  $N_s = 200$ , length of cyclic prefix  $N_g = 45$  and roll-off factor of raised cosine filter at transmitter is 0.5. The multipath channel considered has an exponentially decaying phase delay profile, comprised of

10 complex Gaussian distributed taps. For any variable  $X$ , the mean square error (MSE) is expressed as  $\text{MSE} = |X' - X|^2$ , where  $X'$  is the estimated value and  $X$  is the original.

$$\text{MSE} = |X' - X|^2 \quad (2.40)$$

where  $X'$  is the estimated value and  $X$  is the original one.

The MSE of an arbitrary oversampling ratio estimation is exhibited in Figure 2.8 under different frequency resolutions. The Signal-to-Noise Ratio (SNR) used is 10 dB. From the figure it is obvious that the spectral resolution is an important factor and that a higher resolution leads to improved accuracy. Based on the Monte Carlo simulation, 0.1 and  $5 \times 10^{-6}$  are chosen as the optimal low spectral resolution and high spectral resolution, respectively. Under such selection, the desired estimation accuracy is realized and low computational complexity is maintained as well.

The simulation results demonstrate the estimation ability of the proposed approach on arbitrary oversampling ratios. Compared with the numerical results of the entire spectrum SCF estimation [21], [40] and [41] the estimation accuracy of the proposed approach is satisfying. Since a higher oversampling ratio provides more signal information, better estimation accuracy is achieved according to the simulation results.

Figure 2.9 illustrates the performance of the introduced approaches for the estimation of the number of subcarriers and the CP length. Instead of using recognizable and distinctive features of an OFDM signal, arbitrary parameters are employed to test the validity of the proposed receiver design. The oversampling ratio used in the simulation is  $q = 5.45$ . The performance is analyzed using both AWGN and multipath channels for different SNR levels. From the results, good performance is achieved for

the estimation of the above two parameters.

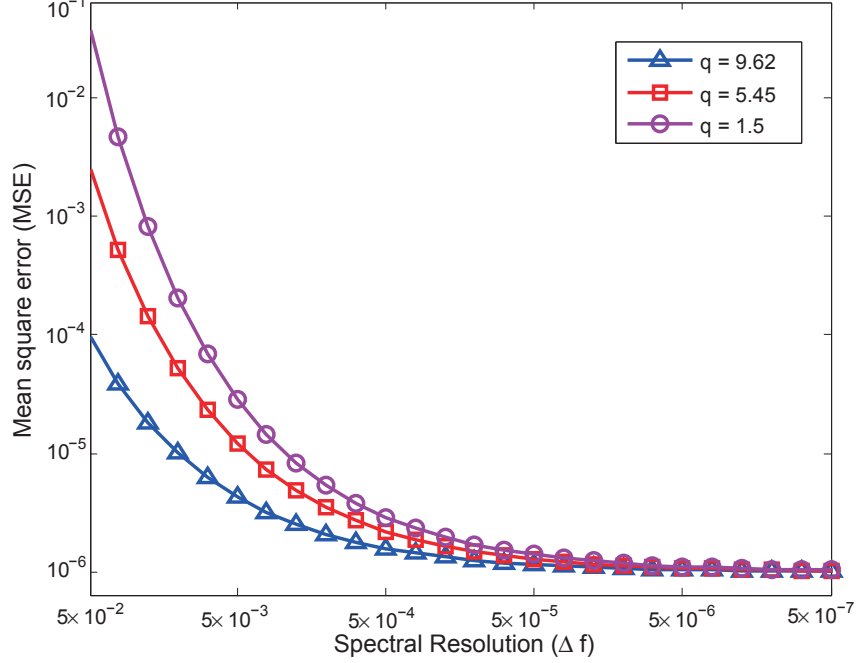


Figure 2.8: MSE of oversampling rate  $q$  under multipath channel( $\text{SNR} = 10\text{dB}$ ).

### 2.9.1 Enhanced iterative channel estimation

The MSE of enhanced iterative channel estimation is simulated in Figure 2.10 which tells that with our proposed OFDM parameters estimation scheme, the performance of traditional PACE is significantly better than those with oversampling rate estimation errors. Around 4dB and 6dB gain can be obtained by the proposed estimation scheme as compared to the estimation error levels (10 samples and 30 samples, respectively). Moreover, by utilizing the proposed enhanced iterative channel estimation scheme, further improvement around 7dB can be observed when the subsequent 5 OFDM data blocks of the pilot block are used as feedback for accuracy enhancement. The same measurement increases to 10dB if 10 OFDM blocks are adopted for "pilot extension". The results indicate that when prior knowledge of channel variation is available,



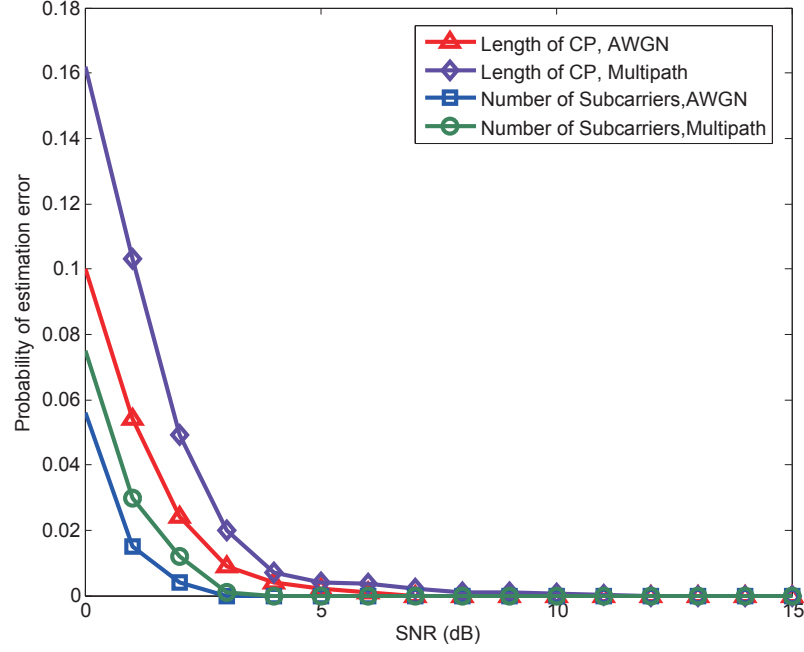


Figure 2.9: Prob. of the estimation error of number of subcarriers and CP length.

the number of OFDM blocks can be automatically chosen to improve the channel estimation results. The corresponding Symbol Error Rate (SER) of OFDM received based on the above channel estimation results is shown in Figure 2.11. It can be found that the performance of data detection with the proposed OFDM parameters estimation greatly outperforms those with the indicated estimation errors. The curve with enhanced iterative channel estimation always leads to the best performance due to the most accurate channel estimation results.

### 2.9.2 Complexity Analysis

In this subsection, the computation reduction of the proposed approach is shown in detail. Let  $\Delta f$  be the size of the spectral resolution under the tentative analysis step. The length of the cyclic frequency axis is  $L = 1/\Delta f$ . The computational load needed

for the entire cyclic spectrum analysis under this step is

$$\text{Real multiplications : } 2L^2 \log_2 L + 5L\Delta f \quad (2.41)$$

$$\text{Real additions : } 2L^2 \log_2 L + 3L\Delta f$$

The observation time  $T_l$  and the spectral frequency resolution  $\Delta f_l$  are chosen to meet  $T_l \Delta f_l \approx 1$  for the coarse estimation step. Even though the entire spectrum is explored, the computational load is still low. Denote  $T_h$  and  $\Delta f_h$  as the length of the observation time and size of the spectral resolution respectively under the condition of  $T_h \Delta f_h \gg 1$ .  $L_h$  is the length of the cyclic frequency axis and  $R$  is the limited cyclic frequency axis range for exploration where  $R \ll L_h$ . In this case, the required computational complexity within the selected range is

$$\text{Real multiplications : } 2L_h R \log_2 L_h + 5R\Delta f_h \quad (2.42)$$

$$\text{Real additions : } 2L_h R \log_2 L_h + 3R\Delta f_h$$

The comparison of the computational complexity between the proposed method and the whole band SCF method based on the simulation parameters is listed in Table 2.2.

Table 2.2: Complexity needed for the proposed method and traditional estimation.

	Real multiplications	Real additions
The proposed method	$2 \times 10^4$	$2.2 \times 10^4$
Whole band SCF estimation	$1.5 \times 10^7$	$1.6 \times 10^7$

## **2.10 Conclusion**

In this chapter we present an OFDM interception receiver that enables parameter estimation with arbitrary oversampling ratios in blind scenarios. Using an iterative cyclostationary feature detection, the computational complexity of the estimation process is dramatically reduced. Through simulations based on AWGN and multi-path channel models, it was verified that the proposed scheme improves the computational efficiency without a large degradation in estimation accuracy. Additionally, the proposed scheme is applicable to not only integer oversampling ratios but also to rational oversampling ratios. Based on the sampling frequency estimation, other primary system parameters are obtained successfully. With the computational load reduction, the proposed method meets the requirements for military communication with a satisfying estimation accuracy for signal interception.

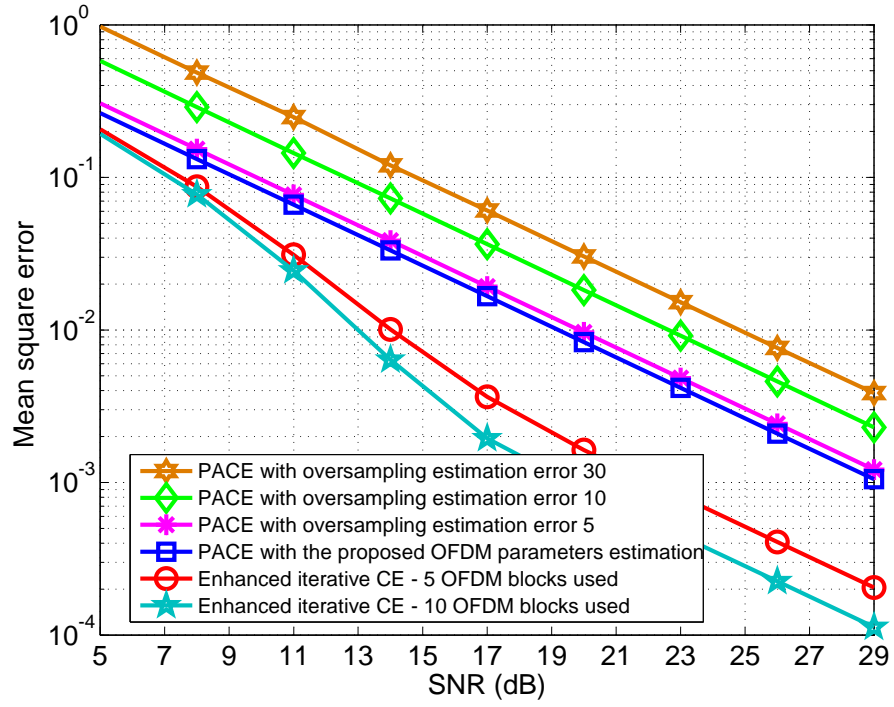


Figure 2.10: MSE of Enhanced Channel Estimation with different estimation error

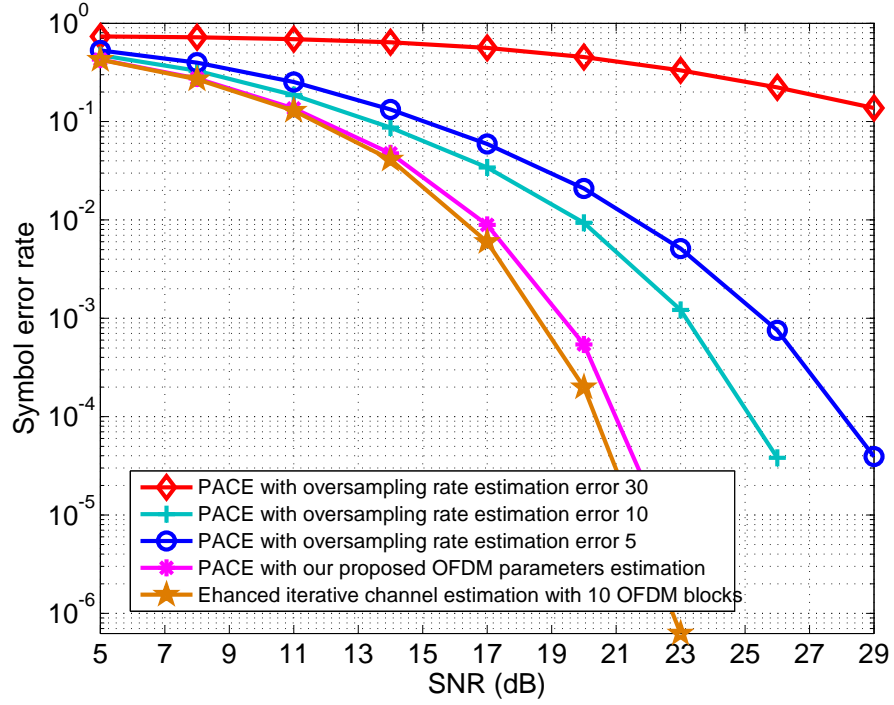


Figure 2.11: SER of signal detection with different parameter estimation error

# Chapter 3

## Joint Blind Signal Parameter Estimation and Synchronization

### 3.1 Synchronization for OFDM System

Synchronization has been one of the crucial research topics in OFDM system because of its sensitivity to the timing and frequency errors [26]. To guarantee the fast and accurate data transmission, the Inter Symbol Interference (ISI) and Inter Carrier Interference (ICI) caused in the transmission have to be eliminated as much as possible. In OFDM system, ISI can be avoided by inserting cyclic prefix with length greater than the channel impulse response, and the ICI can be eliminated by maintaining the orthogonality of carriers under the condition that the transmitter and the receiver have the exact same carrier frequency. But in the real world, frequency offsets will be arising from the frequency mismatch of the transmitter and the receiver oscillators and the existence of Doppler shift in the channel. In addition, due to the delay of signal when transmitting in the channel, the receiver in general starts sampling a new frame at the incorrect time instant. Therefore, it is important to estimate the frequency offset to minimize its impact, and to estimate the timing offset at the receiver to identify the start time of each frame and the FFT window position for each OFDM.

The OFDM synchronization can be divided into data-aided and non-data-aided categories. The data-aided category uses a training sequence or pilot symbols for estimation. It has high accuracy and low calculation, but loses the bandwidth and reduces the data transmission speed. The non-data aided category often uses the cyclic prefix correlation. It does not waste bandwidth and reduce the transmission speed, but its estimation range is too small, not suitable for acquisition. In this chapter, only data-aided methods will be described due to their wide use when researching modern Wireless Local Area Network (WLAN) system. In the reminder of this section, we present review of the synchronization techniques available in the literature.

### 3.1.1 Timing Offset Estimators

#### 3.1.1.1 Schmidl's Method

Two training symbols are placed at the beginning of each frame as preamble. Here, the sequence used to generate the training sequence should be chosen on basis of having a low peak-to-average power ratio so that there is little distortion in the transmitter amplifier [27].

Table 3.1: PAPR Comparison

Type of Sequence	Peak-to-average power ratio
m-sequence	3.5568
Walsh Code	62.0769
Gold Sequence	75.7588

As shown in Table 3.1, the m-sequence has lowest PAPR; therefore it is used to generate the training sequences. The first training symbol has two identical halves in

the time domain. It has the following pattern:

$$S_s = [A, A] \quad (3.1)$$

To detect the frame, the conjugate of a sample from the first half is multiplied by the corresponding sample from the second half, and then at the start of the frame, the products of each of these pairs of samples will have approximately the same phase and the magnitude of the sum will be peaked [28]. The timing metric of this estimator is given by

$$M(d) = \frac{|P(d)|^2}{(R(d))^2} \quad (3.2)$$

where

$$P(d) = \sum_{m=0}^{L-1} (r_{d+m}^* r_{d+m+1}) \quad (3.3)$$

$$R(d) = \sum_{m=0}^{L-1} |r_{d+m+1}|^2 \quad (3.4)$$

Here  $L = N/2$  is the length of complex samples in one half of first training symbol (excluding Cyclic Prefix),  $r_k$  is the received signal, and  $d$  is a time index corresponding to the first sample in a sliding window of  $2L$  samples.

### 3.1.1.2 Minn's Method

Based on Schmidl & Cox' method, Minn et al [29] modified the training sequences pattern and timing metrics definition and designed the first training symbol having four parts with following patterns:

$$S_M = [A, A, -A, -A] \quad (3.5)$$

where  $A$  represents samples of length  $L = N/4$  generated by  $N/4$  point IFFT of  $N_c/4$  length modulated data of a PN sequence. The timing metric used in the evaluation of the technique is given by 3.2 where

$$P(d) = \sum_{k=0}^{L-1} \sum_{m=0}^{L-1} r_{d+2Lk+m}^* r_{d+2Lk_m+L} \quad (3.6)$$

$$R(d) = \sum_{k=0}^{L-1} \sum_{m=0}^{L-1} |r_{d+2Lk_m+L}|^2 \quad (3.7)$$

where  $r_k$  is the received signal, and  $d$  is a time index corresponding to the first sample in a sliding window of  $4L$  samples.

### 3.1.1.3 Park's Method

Minn's method [29] reduces the timing metric plateau found in Schmidl's method but the MSE is still large particularly in ISI channels. This is resulted from the timing metric values around the correct timing point in Minn's method are almost the same. Park et al [30] proposed to increase the difference between the peak timing metric with respect to other metric values. The proposed method entails modifying the training sequence's pattern and timing metric's definition to maximize the different pairs of product between them. The first training symbol having four parts with the following patterns:

$$S_P = [A, B, A^*, B^*] \quad (3.8)$$

where  $A$  represents samples of length  $L = N/4$  generated by IFFT of a PN sequence.  $B$  is designed to be symmetric with  $A$ .  $A^*$  and  $B^*$  are conjugate of  $A$  and  $B$  respec-



tively. The timing metric is given by 3.2, where

$$P(d) = \sum_{k=0}^{N/2} (r_{d-k} r_{d+k}) \quad (3.9)$$

$$R(d) = \sum_{k=0}^{N/2} |r_{d+k}|^2 \quad (3.10)$$

where  $r_k$  is the received signal.

#### 3.1.1.4 Seung's Method

Based on Park's et al method [30], Seung's et al [31] proposed a modified method to define the time domain preamble pattern as follow:

$$S_C = [A, B^*] \quad (3.11)$$

where  $A$  represents the sequence with length of  $N/2$  generated by IFFT of the constant amplitude zero auto-correction (CAZAC) sequence modulated by QPSK and multiplied by a relative large number to maintain an approximately constant signal energy to generate impulse in correct timing point,  $B^*$  represents the conjugate of  $B$ , which is symmetric with  $A$ .

This method then uses zero padding for the guard interval of the preamble instead of the conventional cyclic prefix. The timing metric is given by (3.2) where

$$P(d) = \sum_{k=0}^{N/2} (r_{d-k} r_{d+k+1}) \quad (3.12)$$

$$R(d) = \frac{1}{2} \sum_{k=0}^{N/2} |r_{d+k-N/2}|^2 \quad (3.13)$$

### 3.1.2 Carrier Frequency Offset and Sampling Clock Offset Estimator

Synchronization method conventionally includes the acquisition and tracking processes, also called coarse and fine synchronization, respectively. Several acquisition algorithms by using pre-FFT samples have been proposed in the literature [32], [33], [34]. For OFDM-based DVB-T system, several approaches focusing on joint carrier frequency offset (CFO) and sampling clock offset (SCO) estimation by using the pilots have been presented [35],[36],[37]. In [35], a joint CFO and SCO tracking algorithm was proposed based on linear least square estimation. Unfortunately that channel is assumed to be AWGN channel. In [36], a joint CFO and SCO estimation algorithm was derived from the maximum likelihood (ML) function and two-dimensional least square estimation. Due to the linearization of ML function, estimation performance of the algorithm will degrade when signal SNR becomes large.

#### 3.1.2.1 One Dimensional Linear Least Square Estimation

Applying linear least square estimation to (9) in XXX with  $M$  pilots,  $k_s$ , ( $s = 1, 2, \dots, M$ ) in one symbol, the CFO and SCO estimations yield:

$$\begin{aligned}\Delta\hat{f} &= \frac{\sum_{s=1}^M \theta_1(k_s)}{2\pi N_s T M} \\ \hat{n} &= \frac{\sum_{s=1}^M \theta_1(k_s) C_s}{\sum_{s=1}^M C_s^2}\end{aligned}\tag{3.14}$$

where  $C_s = (k \times 2\pi N_s)/N$ .

As mentioned, in order to get robust estimation, two methods can be used: consecutively observe  $L$  symbols and compute the average of the value estimated by

(3.14); adopt a filter such as PI (proportion integral) filter [37]. If we observe  $L$  consecutive symbols, (3.14) is modified as,

$$\Delta \hat{f} = \frac{\sum_{s=1}^M \theta_1(k_s)}{2\pi N_s T M (L-1)} \quad (3.15)$$

$$\hat{n} = \frac{\sum_{s=1}^M \theta_1(k_s) C_s}{(L-1) \sum_{s=1}^M C_s^2} \quad (3.16)$$

The tracking range of the frequency offset and sampling offset is limited by the condition  $\theta_l(k) < \pi$ , namely,

$$2\pi \Delta f (LN_s + N_g)(1+n)T + 2\pi K (LN_s + N_g)/N + \phi(k) < \pi \quad (3.17)$$

### 3.1.2.2 D-Symbols Delay linear Least Square Estimation

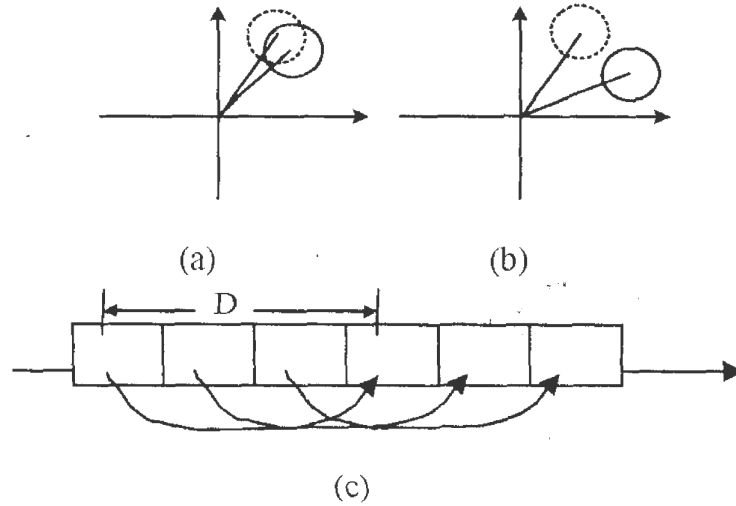


Figure 3.1: The principle of D-symbol estimation.

When the remained CFO and SCO are relatively smaller or the noise is very large, the difference of the rotated phases between two adjacent symbols are very small, as illustrated in Figure 3.1. This may result in poor estimation accuracy and

in some cases may give estimation results of the opposite sign. If we compare the phase rotation of the current symbol with the next  $D$  symbol that delays  $D$  symbol-interval, demonstrated as Figure 3.1.(b) and (c), the effects of noise may be reduced to some extent. In this case, 3.14 is modified as

$$\theta(k) = \phi_l(k) - \phi_{l-D}(k) = 2\pi DN_S T \Delta f + 2\pi DN_S k n / N \quad (3.18)$$

Applying the same least square estimation technique to (3.18), the improved method is presented as (3.19). When  $D$  is equal to  $t/3$ , the RMS (root-mean-square) of estimation error can be minimized [39]

$$\begin{aligned} \Delta \hat{f} &= \frac{\sum_{l=D+1}^L \sum_{s=1}^M \theta_1(k_s)}{2\pi N_S T M D (L - D)} \\ \hat{n} &= \frac{\sum_{l=D+1}^L \sum_{s=1}^M \theta_1(k_s) C_s}{D(L - D) \sum_{s=1}^M C_s^2} \end{aligned} \quad (3.19)$$

### 3.1.2.3 Two Dimensional Linear Least Square Estimation

According to IEEE 802.11a standard, the channel can be estimated at the beginning of a frame (packet), thanks to 2 long training symbols, and the channel is considered as invariant within a frame. So  $\phi_l^H(k)$  are considered as a constant value all over the frame. If we observe  $L$  symbol from  $l$ th symbol, denoted as  $l_i$ , ( $i = 1, 2, \dots, L$ ), the rotated phase is written as [39]:

$$\phi_{l_i}(k_s) = 2\pi \Delta f (l_i N_s + N_g) + 2\pi \Delta f (l_i N_s + N_g) \eta T + (2\pi k / N) (l_i N_s + N_g) \eta + \phi(k_s) \quad (3.20)$$

where  $i = 1, 2, \dots, L$  and  $s = 1, 2, \dots, M$ . Applying two-dimensional least square estimation to (3.20), the CFO and SCO estimations yield:

$$\begin{aligned}\Delta\hat{f} &= \frac{\sum_{l=1}^L \sum_{s=1}^M (l_i N_s + N_g)(\varphi_{l_i, k_s} - \phi(k_s))}{2\pi M T \sum_{i=1}^L (l_i N_s + N_g)^2} \\ \hat{\eta} &= \frac{\sum_{l=1}^L \sum_{s=1}^M (l_i N_s + N_g) k_s (\varphi_{l_i, k_s} - \phi(k_s))}{(2\pi/N) \sum_{s=1}^M k_s^2 \sum_{i=1}^L (l_i N_s + N_g)^2}\end{aligned}\tag{3.21}$$

where  $M$  is the total number of pilots in a symbol.

## 3.2 Introduction of the Proposed Approach

With the recent rapid growth in wireless applications and systems, the problem of spectrum utilization has become more critical than ever before. As an emerging solution, Cognitive Radio (CR) systems aim to improve the efficiency of spectrum usage with the principle of sharing available spectrum resources adaptively. Orthogonal frequency division multiplexing (OFDM), which has been known to be one of the most effective multicarrier techniques, has attracted significant attention in the development of CR systems, due to its high spectral efficiency and flexibility in allocating transmission resources in dynamic environments.

However, the existence of dissimilar wireless transmission schemes poses a challenge to the design of CR receivers that can operate with the multi-waveform signals. Therefore, blind system parameter estimation is of significant importance for reliable communication in CR environments. Furthermore, the blind estimation is also helpful to reduce signaling overhead in the case of adaptive transmission where the system parameters are changed depending on the environmental characteristics

or spectrum availability. The capability of identifying system parameters is necessary for spectrum survey with the purpose of monitoring the systems to discover illegal transmissions as well. In the literature, various blind estimation schemes for CR systems have been presented, which can be generalized into two primary categories: cyclostationary characteristics-based [18], [20], [40] and nonparametric spectrum information-based [41]. Specifically, [18] presented a blind parameter estimation system through the statistical  $\chi^2$  test for the cyclo-period. However, the computational load is comparatively high because of the exploration of entire cyclic spectrum. Moreover, [20] enhanced the work in [18] by introducing a sliding DFT (SDFT) [40] implementation and [41] proposed an iterative cyclostationary analysis for parameter estimation. Both worked on reducing the computational complexity without considering synchronization offset. [19] investigated the non-parametric characteristics for blind estimation. However, the introduced method does not work well under the Nyquist pulse shaping which is closer to the practical implementation. Furthermore, neither of the work above provided the evaluation from a real transmission environment, where the propagation is more complex and the system may fail to maintain performance due to unknown interference.

In this chapter, a blind parameter estimation and synchronization design is proposed to identify the fundamental parameters of an OFDM system and reduce the interference from the carrier frequency offset (CFO) and timing offset. In order to guarantee that the information from the transmitter is completely obtained, an oversampling technique is carried out. Therefore, the decisive step of the proposed approach is to estimate this oversampling ratio, for the purpose of capturing the air interface signal accurately. However, given the lack of the prior information and the existence of synchronization offsets, the oversampling ratio can be arbitrary, which makes the design difficult. Hence, an iterative blind parameter estimation

and synchronization offset cancellation scheme is proposed in this chapter to realize the accurate signal sampling and parameters identification. Specifically, the arbitrary oversampling ratio is estimated at first through time-domain envelope spectrum information, based on which the other system parameters including the number of subcarriers, and the cyclic prefix (CP) length are calculated sequentially. Synchronization is realized with the help of the estimated parameters and iteration is employed to refine the results during each step until certain threshold is reached. In order to test the effectiveness of the proposed approach, an experimental environment is established. The OFDM signal is generated from a signal generator with different system parameters as well as including CFO and timing offsets. The propagation signal is then captured by a high speed digitizer for the application of the proposed iterative blind parameter estimation and synchronization algorithm. Test results are provided to evaluate the performance of the proposed approach under various scenarios of system interference.

### 3.3 System Model

Consider an OFDM system with  $N_s$  transmission subcarriers, which is denoted by  $\{e^{j2\pi\frac{t}{T_s}n}\}_{n=0}^{N_s-1}$  and  $T_s$  is the OFDM symbol period. Assuming that an appended sequence with length of  $N_g$  ( $N_g < N_s$ ) is inserted at the beginning of each block as a cyclic prefix (CP), the transmitted OFDM signal over  $(0, T_s)$  can be represented as,

$$s(t) = \frac{1}{\sqrt{N_s}} \sum_{n=0}^{N_s-1} d_n e^{j\frac{2\pi nt}{T_s}} g_c(t) \quad (3.22)$$

where  $d_n$  is the complex data transmitted on the  $n$ th subcarrier with  $E[d_n d_n^*] = 1$  and  $g_c(t)$  is a Nyquist pulse. The raised cosine waveform is taken into consideration in

this chapter due to its ability to minimize intersymbol interference (ISI) and smooth the sharp edges of baseband signals, which is defined on  $(0, T_s)$  and can be expressed as,

$$g_c(t) = \text{sinc}\left(\frac{t}{T_s}\right) \frac{\cos(\pi\alpha\frac{t}{T_s})}{1 - 4\alpha^2(\frac{t}{T_s})^2} \quad (3.23)$$

where  $\alpha$  stands for the roll-off factor. Denote  $h(t)$  to be an unknown frequency selective multipath channel, the received time-domain signal is,

$$x(t) = \sum_{\lambda} s_{\lambda} h(t - \lambda T_s) + w(t) \quad (3.24)$$

where  $w(t)$  is additive white Gaussian noise (AWGN) with zero mean and variance  $\sigma_w^2$ .

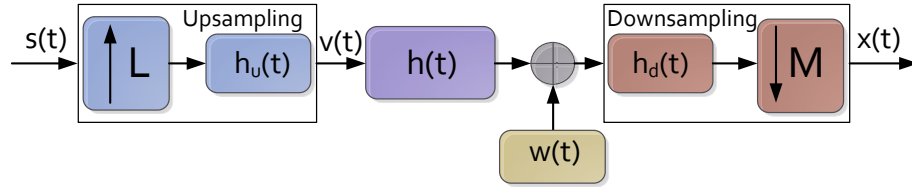


Figure 3.2: Illustration of oversampling structure for blind parameter estimation.

From Figure 3.2, upsampling with a factor  $L$  is used at the transmitter to shape the discrete data into a continuous waveform to be transmitted.  $h_u(t)$  is then employed as an anti-image filter. At the receiver, the signal is downsampled by a factor  $M$  and  $h_d(t)$  is used as an anti-aliasing filter to reduce distortion. Normally  $M < L$  for the consideration of oversampling and the ratio  $q$  is defined as  $q = L/M$ . So the corresponding oversampled OFDM signal at the receiver can be denoted as [18],

$$x(n) = \sum_{\lambda} s_{\lambda} h(n - \lambda q) + w(n) \quad (3.25)$$



### 3.4 Envelope Spectrum-based Oversampling

#### Ratio Estimation

Without considering the interference from the multipath fading and AWGN channels in Figure 3.2, we can denote  $h_T(t) = h_u(t) * h_d(t)$  as the combination of anti-aliasing and anti-image filters, with  $*$  the convolution operation. Then, according to multirate signal processing theory [42], we have,

$$H_T(f) = \begin{cases} 1, & |f| \leq \min(\frac{1}{L}, \frac{1}{M}) \\ 0, & \text{Others} \end{cases} \quad (3.26)$$

where  $H_T(f)$  is the Fourier transform of  $h_T(t)$ . The time-domain relation between  $v(t)$  and  $s(t)$  after upsampling can be expressed as,

$$v(k) = \sum_{n=-\infty}^{\infty} h_T(nL + k \oplus L) s(\lfloor \frac{k}{L} \rfloor - n) \quad (3.27)$$

where  $\oplus$  and  $\lfloor \cdot \rfloor$  denote mod and floor operations, respectively. Let  $V(f_1)$  and  $S(f_1)$  be the Fourier transform of  $v(t)$  and  $s(t)$ , we have,

$$V(f_1) = H_T(f_1) S(f_1 L) \quad (3.28)$$

After the downsampling by a factor  $M$ , the equation for the relationship of  $s(t)$  and  $x(t)$  is,

$$\begin{aligned} x(n) &= v(Mk) \\ &= \sum_{n=-\infty}^{\infty} h_T(nL + Mk \oplus L) s(\lfloor \frac{Mk}{L} \rfloor - n) \end{aligned} \quad (3.29)$$

and assign  $X(f_2)$  as the Fourier transform of  $x(t)$ , the frequency-domain relation then becomes,

$$\begin{aligned} X(f_2) &= \frac{1}{M} \sum_{m=0}^{M-1} V\left(\frac{f_2 - m}{M}\right) \\ &= \frac{1}{M} \sum_{m=0}^{M-1} H_T\left(\frac{f_2 - m}{M}\right) S\left(\frac{(f_2 - m)L}{M}\right) \end{aligned} \quad (3.30)$$

Since  $f_2 = Mf_1$ , we have,

$$X(f_2) = \frac{1}{M} \sum_{m=0}^{M-1} H_T\left(f_1 - \frac{m}{M}\right) S\left(f_1L - \frac{mL}{M}\right) \quad (3.31)$$

From the derivation in [42], after analyzing the properties of  $H_T(f_1)$ , it can be found that when  $m \neq 0$ , we have,

$$H_T\left(f_1 - \frac{m}{M}\right) = 0 \quad (3.32)$$

hence, when  $|f_2| = M|f_1| \leq \min\{\frac{1}{2}, \frac{1}{2q}\}$ ,

$$X(f_2) = \frac{1}{M} S(f_1L) = \frac{1}{M} S(f_2 \frac{L}{M}) = \frac{1}{M} S(qf_2) \quad (3.33)$$

Based on the above relation, a peak can be observed at the frequency component  $1/2q$  of  $X(f_2)$ . In order to separate this peak from the frequency band of OFDM signal, the time-domain envelope spectrum is taken into consideration which can be described as follows.

If the time-domain relation is taken as  $y(n) = |x(n)|^2$ , then the Fourier transform of  $y(n)$  is defined as the envelope spectrum and thus, the frequency relation is,

$$Y(f_2) = X(f_2) * X(-f_2) \quad (3.34)$$

and the desired peak can be observed at the frequency component  $1/q$  of  $Y(f_2)$ . If the Fast Fourier Transform (FFT) is applied, this relation becomes,

$$Y(k) = X(k) * X^*(N - k) \quad (3.35)$$

where  $x^*(n)$  and  $X^*(k)$  represent the conjugation operation. The desired frequency component is located at the index  $k = N/q$  with  $N$  equal to the number of FFT points.

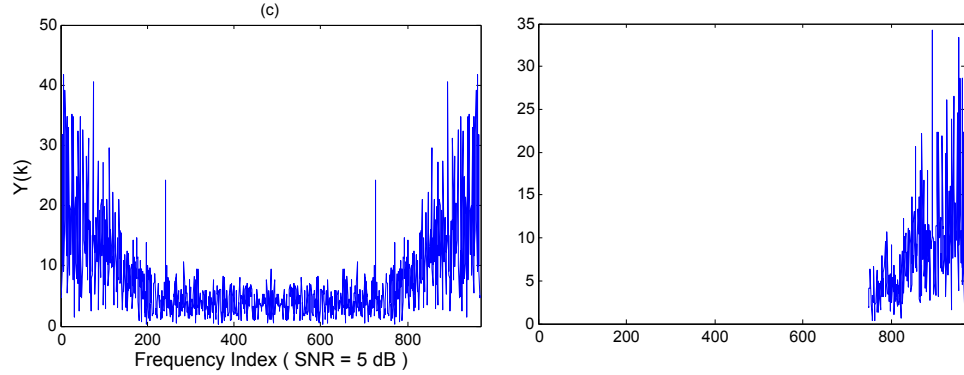


Figure 3.3: Spectrum information of oversampled OFDM signal ( $q = 4$ )

Figure 3.3 exhibits the envelope spectrum of  $x(n)$  as  $Y(k)$ . From the above analysis, the index  $k$  after FFT to indicate oversampling ratio  $q$  is located at  $N/q$  as labeled in different Signal-to-Noise Ratio (SNR) scenarios. Since  $Y(k)$  has a symmetric pattern with a series of peaks, the peak detection algorithm is employed to find

the peak closest to the spectrum center, if denoted as  $\tilde{k}$ , the estimated oversampling factor  $\tilde{q}$  is,

$$\tilde{q} = \frac{N}{\tilde{k}} \quad (3.36)$$

### 3.5 Joint Iterative Blind Parameter Estimation and Synchronization

Through (3.36), the oversampling frequency at the transmitter is obtained and the received signal is sampled accordingly. The next step is to estimate the other OFDM parameters and synchronize the received signals. The number of subcarriers and the CP length are considered in this chapter with the approaches from [41].

#### 3.5.1 Estimation of the Number of Subcarriers and CP Length

For an OFDM symbol with  $N_s$  subcarriers, the estimated autocorrelation function  $\hat{R}_x(n, \tau)$  of the oversampled signal can be written as,

$$\hat{R}_x(n, \tau) = \frac{1}{P} \sum_{n=0}^{P-1} x(n)x^*(n - \tau) \quad (3.37)$$

where  $\tau \in [0, 1, \dots, P - 1]$ ,  $P$  is the length of oversampled incoming signal. The absolute value of  $\hat{R}_x(n, \tau)$  is considered and is given as,

$$|\hat{R}_x(\tau)| = \begin{cases} \sum_{n=0}^P |h(n)|^2 + \sigma_w^2, & \tau = 0 \\ \sum_{n=0}^P |h(n)|^2 \frac{N_g}{N_f} + \sigma_w^2, & \tau = N_b \end{cases} \quad (3.38)$$

where  $h(n)$  is the channel impulse response,  $N_g$  is the CP length,  $N_b$  is the OFDM symbol length of the oversampled signal with  $N_b = qN_s$  and  $N_f = N_s + N_g$ .  $|\hat{R}_x(\tau)|$  will have the most significant peak when  $\tau = N_b$ . Therefore, through peak detection, the estimated number of subcarriers can be achieved by,

$$\tilde{N}_s = \frac{N_b}{\tilde{q}} \quad (3.39)$$

The estimation of the CP length  $N_g$ , is accomplished by the cyclic autocorrelation which is given by,

$$R_x^k(\tau) = \frac{1}{P} \sum_{n=0}^{P-1} R_x(n, \tau) e^{-j\frac{2\pi}{P}kn} \quad (3.40)$$

Using the estimated number of subcarriers  $\tilde{N}_s$ , we can obtain the cyclic autocorrelation with delay  $\tau = \tilde{N}_s$ . The cyclic prefix length,  $N_g$ , can be determined through peak detection on  $R_x^k$  at  $\tau = \tilde{N}_s$ . If we assume that  $k_{opt}$  represents the first peak with the smallest index above the threshold from the cyclic autocorrelation then, the estimated length  $\tilde{N}_f$  can be identified as,

$$\tilde{N}_f = \frac{2P}{k_{opt}} \quad (3.41)$$

and the CP length  $\tilde{N}_g$  is determined to be  $\tilde{N}_g = \tilde{N}_f - \tilde{N}_s$ .

### 3.5.2 Estimation of Carrier Frequency Offset and Timing Offset

For synchronization, the problem can be modeled as follows (no oversampling),

$$x(n) = e^{j(2\pi f_e n)} s(n - n_e) * h(n) + w(n) \quad (3.42)$$

where  $f_e$  is the CFO and  $n_e$  is the timing offset, both of which have an impact on blind OFDM parameter estimation. If  $N_s$  is provided as prior information and the received signal is perfectly sampled, the estimation of  $n_e$  and  $f_e$  can be solved through the Maximum Likelihood (ML) algorithm proposed by [43]. Therefore, in our case, we consider  $N_b$  as the number of subcarriers for the oversampled OFDM symbol and  $f'_e$  and  $n'_e$  are assumed to be the CFO and timing offset respectively. The Log Likelihood estimator is given by [43],

$$\lambda(n'_e, f'_e) = |\hat{R}_x(n'_e, N_b)| \cos \left( \frac{2\pi f'_e}{N_b} + \angle(\hat{R}_x(n'_e, N_b)) \right) - \rho \Phi(n'_e) \quad (3.43)$$

where  $\hat{R}_x(n, N_b)$  is the autocorrelation operation in (3.37) when  $\tau = N_b$ ,  $\angle$  represents the argument of a complex sequence and,

$$\begin{aligned} \Phi(n) &= \frac{1}{2} \sum_{k=n}^{n+P-1} [|x(k)|^2 + |x(k + N_b)|^2] \\ \rho &= \frac{|E\{x(n)x^*(n + N_b)\}|}{E\{|x(n)|^2\}E\{|x(n + N_b)|^2\}} \end{aligned} \quad (3.44)$$

The ML estimation of  $n'_e$  and  $f'_e$  is given by,

$$\begin{aligned}\hat{n}'_e &= \arg_{\max}(n'_e) \{ |\hat{R}_x(n'_e, N_b)| - \rho\Phi(n'_e) \} \\ \hat{f}'_e &= -\frac{\angle \hat{R}_x(\hat{n}'_e, N_b)}{2\pi} + n\end{aligned}\tag{3.45}$$

The above estimator works well under the flat fading channel scenario, accurate sampling as well as the prior information of OFDM system parameters. Under the blind estimation scenario and when the multipath fading channel is considered, the estimator is not optimum. However, the results can be utilized as initial guesses for both the CFO and the timing offset to refine the estimation accuracy of the OFDM parameters in the previous steps. Therefore, an iterative scheme is employed to improve the performance of parameter estimation and synchronization jointly, which is described below:

1. Obtain the initial oversampling ratio  $\tilde{q}$  by setting a downsampling factor  $M$ .  $\tilde{q}$  is calculated through (3.36).
2. Estimate the number of subcarriers  $\tilde{N}_s$  and CP length  $\tilde{N}_g$  through (3.39) and (3.41) based on the oversampling ratio  $\tilde{q}$ .
3. Realize the synchronization from the estimation of the CFO  $\hat{f}_e$  and  $\hat{n}_e$  based on (3.45).
4. Recover the oversampled signal  $x(n)$  with the estimated  $\hat{f}_e$  and  $\hat{n}_e$ . Repeat Steps 1), 2) and 3) to refine the estimation performance in each step and improve the accuracy. If the estimated oversampling ratio at  $j-1$ ,  $j$  and  $j+1$  steps are  $\tilde{q}^{(j-1)}$ ,  $\tilde{q}^{(j)}$  and  $\tilde{q}^{(j+1)}$ , the final estimation result is achieved if the following

conditions are met

$$|\tilde{q}^{(j+1)} - \tilde{q}^{(j)}| < |\tilde{q}^{(j)} - \tilde{q}^{(j-1)}| < \gamma \quad (3.46)$$

where  $\gamma$  is the level of acceptance.

## 3.6 Experimental Results

### 3.6.1 Lab Testing Platform

Experimental testing has been done through a lab testing platform for algorithm verification which contains a vector signal generator, a FSP spectrum analyzer and a high speed digitizer. In our experiments, a R&S<sup>®</sup> SMJ100A vector signal generator is used to generate the OFDM signals, which is used by the proposed blind parameter estimation and synchronization approach. The SMJ100A supports a wide range of possible input values ranging from  $50mV$  to  $30V$  as well as software-selectable  $50ohm$  or  $1Mohm$  input impedance. To intercept the transmitted OFDM signals, a NI PXI 5105 high speed digitizer is used, which is capable of capturing 8 simultaneous channels of data at a rate of  $60Msamples$  per second with a resolution of 12 bits. This high speed digitizer is inserted into a NI PXI-1031 4-Slot 3U Chassis, a high-power PXI chassis with reduced acoustic noise emission and enhanced cooling capacity. In the experiments, the output of the SMJ100A is wired into the input of Channel 0 of the PXI 5105 digitizer. The generated signal is captured, sampled and saved at the PXI 5105 digitizer through the NI LABVIEW interface. The blind system parameter estimation and synchronization approach is performed in MATLAB after loading the saved data from the PXI 5105.



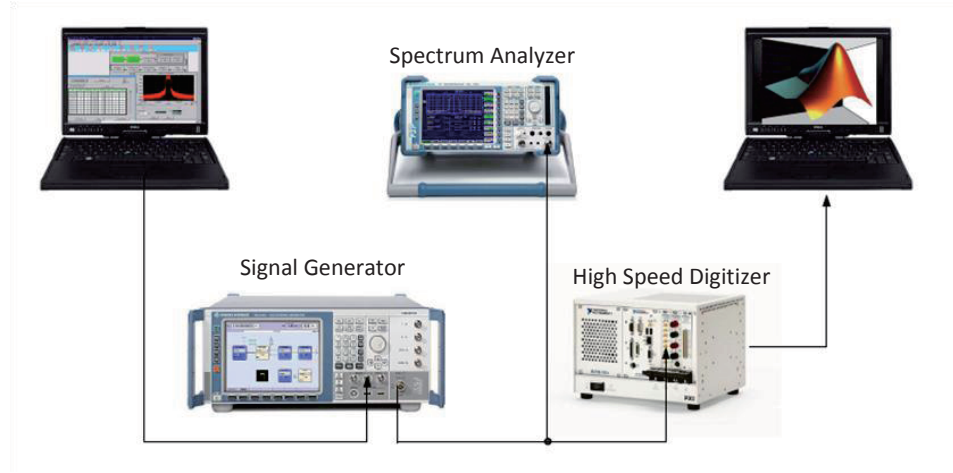


Figure 3.4: Instrument setups for lab testing platform.

Table 3.2: System Parameters for The Generated OFDM Signals.

Data Source	PRBS
Modulation Type	16QAM
Symbol Rate	0.25Mbps
PSDU Rate	24Mbps
Sequence Length	1024 bytes
Number of Data Subcarriers	48
Number of Pilot Subcarriers	4
Subcarriers Frequency Spacing	0.3125 MHz
Impulse Filter	Raised-Cosine Filter
Impulse Length	32
Roll-off Factor	0.5

The parameters employed for OFDM signal generation are listed in Table 4.1. The impairments are also introduced using the SMJ100A with a Rayleigh fading channel scenario and different SNRs, CFO and timing offset levels. The definition of Mean-Square Error (MSE) used in this chapter is,

$$\text{MSE} = |\tilde{x} - x|^2, \quad (3.47)$$

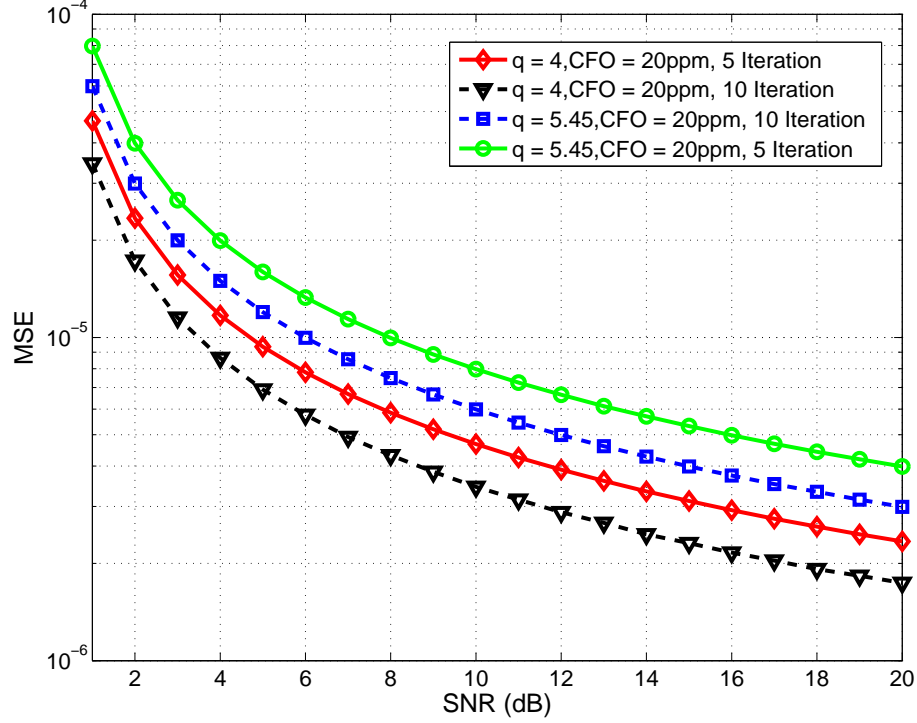
where  $\tilde{x}$  is the estimated value and  $x$  is the original one.

### 3.6.2 Experimental Results

The MSE of the iterative oversampling ratio estimation is exhibited in Figure 3.5 using the lab testing platform. The parameters of the OFDM system are taken from Table 4.1. The CFO is set to  $f_e = 20ppm$  and the timing offset is  $n_e = 10T_s$ . The multipath channel applied is assumed to be Rayleigh fading, where the randomly generated channel coefficients are  $\{h(n)\}_{n=0}^{N_L-1}$  with length  $N_L$ . The channels have an exponentially decaying phase delay profile, comprised of four complex Gaussian distributed taps with average power  $\sigma_h^2 = E[|\sum_n h_n|^2]$ . From the experimental results, it can be seen that low MSE is achieved from the proposed algorithms and the iteration can improve the estimation accuracy efficiently. Moreover, the experimental performance demonstrates the estimation ability of the proposed approach on both integer and rational oversampling ratio scenarios.

Figure 3.6 illustrates the performance of the introduced iterative approach for the estimation of the number of subcarriers and the CP length. The oversampling ratio used in the simulation is  $q = 5.45$ , and  $f_e = 20ppm$ ,  $n_e = 10T_s$ . The performance is analyzed under the same multipath channel environment as above for different SNR levels. From the results, the performance is satisfying and iteration is able to increase the estimation accuracy of the above two parameters.

In order to validate the effectiveness of the proposed approach, the bit error rate (BER) of the received signal is evaluated with different parameters. We assume that the receiver has perfect knowledge of the multipath fading channel and the modulation scheme. The OFDM parameters are the same as above. Three levels of CFO are considered which are  $f_e = 12ppm, 20ppm, 28ppm$ . The results are evaluated for 5 and 10 iteration scenarios separately. From Figure 3.7, it presents the performance of proposed approach for data recovery and validates the iterative scheme.

Figure 3.5: Mean square error of iterative oversampling ratio  $q$ .

### 3.7 Conclusion

In this chapter, we propose a joint iterative blind OFDM parameter estimation and synchronization approach for cognitive radio (CR) systems to operate with multi-waveform signals. The chapter begins with introducing the system model for over-sampled OFDM signals and proposes the envelope spectrum-based arbitrary oversampling ratio estimation. According to the oversampling ratio, the number of subcarriers and the cyclic prefix (CP) length are identified as well, all of which are used to provide the necessary information for carrier frequency offset (CFO) and timing offset estimation. The iterative scheme is then explained to refine the estimation results and increase the accuracy in every step. The proposed approach is evaluated using a lab testing platform and from the experimental results, we can see good performance

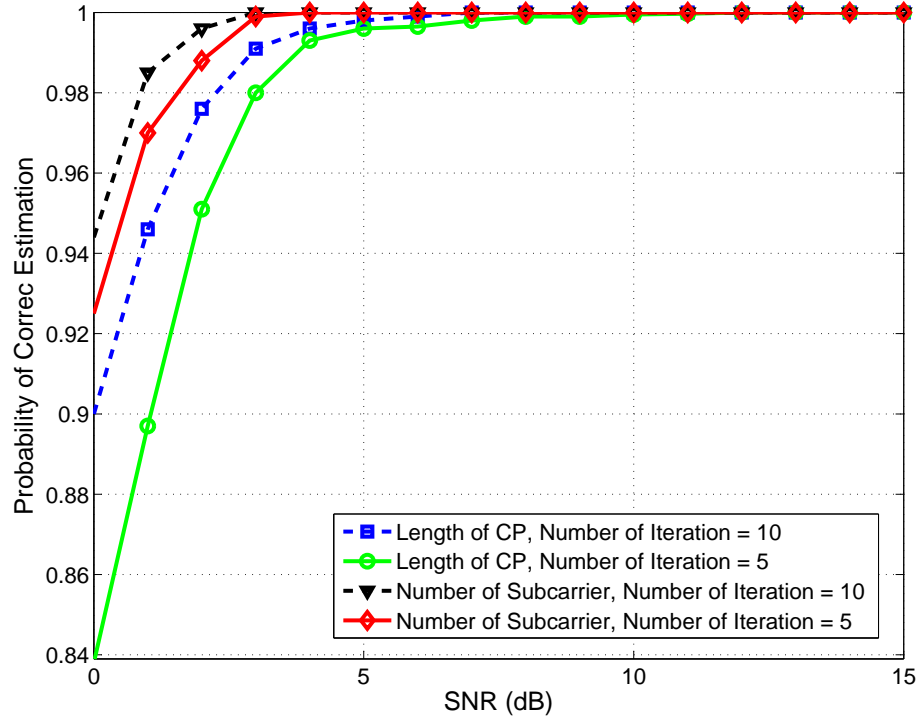


Figure 3.6: Prob. of correct estimation of number of subcarriers and CP length.

on blind parameter estimation and synchronization under the presence of a Rayleigh multipath fading channel and additive noise. Moreover, the bit error rate (BER) for data recovery is satisfying with the prior information of multipath fading channel and modulation scheme.

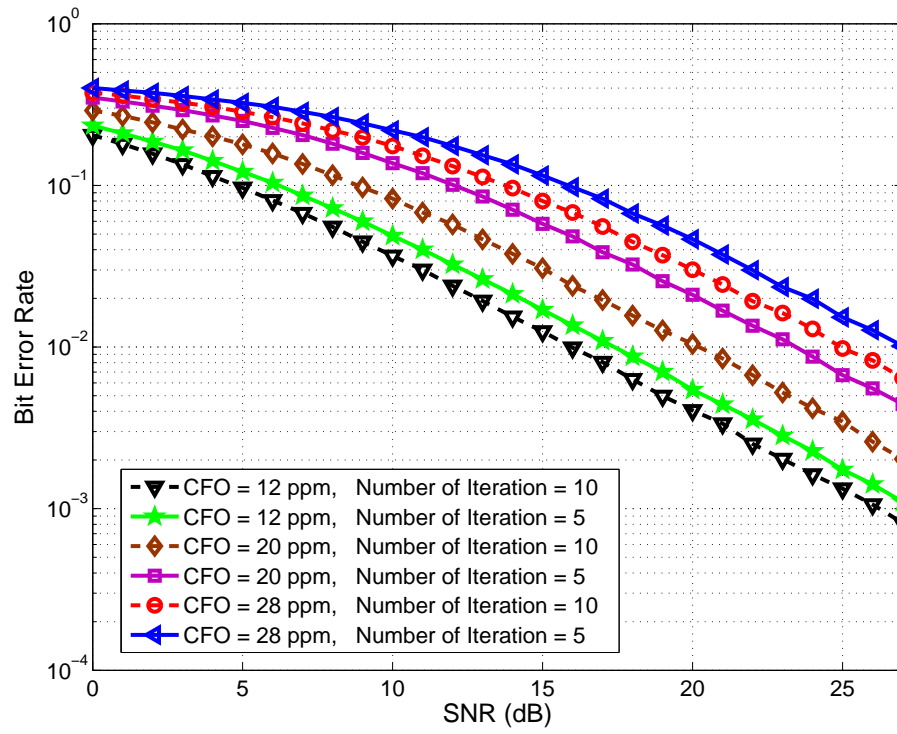


Figure 3.7: BER of the proposed joint parameter estimation and synchronization.

# Chapter 4

## GMM-based Automatic Modulation Classification

### 4.1 Automatic modulation classification

Automatic modulation classification (AMC) is used to automatically identify the modulation scheme used in an intercepted communication signal by analyzing the characteristics of the received signal, which is normally corrupted by the noise and fading channels. The interest in blind modulation classification has been growing since the late eighties. It plays several important roles in both civilian and military applications including signal surveillance, data interception, and confirmation of signal identification, interference monitoring, and counter-measure development. Legitimate signals should be securely transmitted and received, whereas hostile signals from adversaries must be located, identified, and recovered. The transmitting frequencies of these signals may range from high frequency to millimetre frequency band and their format can vary from traditional simple narrowband modulations to newly introduced wideband schemes particularly orthogonal frequency division multiplexing (OFDM). Under such diverse conditions, advanced techniques are needed for real-time signal interception and processing, which are vital for decisions involving electronic warfare operations and other tactical actions [44].

In general, the decision-theoretic methods and the pattern recognition solutions are two typical AMC approaches. Decision-theoretic approach is based on the likelihood function or the approximation thereof [45]-[48], where the modulation classification can be deemed as a multiple-hypothesis test, or can be further converted into a sequence of pair-wise hypothesis tests. Once the appropriate likelihood functions are established, average likelihood ratio test (ALRT), generalized likelihood ratio test (GLRT), or hybrid ALRT/GLRT (HLRT) can be adopted as the potential solutions. The decision-theoretic classifiers with maximum likelihood (ML) are optimal, but the corresponding close-form solutions either are unavailable or involve the numerical search of high computation complexity. This approach is not robust with respect to the model mismatch in the presence of phase or frequency offsets, residual channel effects, and so on [45]-[48].

On the other hand, in the pattern recognition approach [49]-[55], the modulation classification module is composed of two subsystems; the first one is a feature extraction subsystem, which extracts the key features from the received signal; the second subsystem is a pattern recognizer, which processes those features and determines the modulation type of the transmitted signal according to a pre-designed decision rule. The most adopted features are higher-order statistics (HOS), including cumulants and moments. A hierarchical framework based on fourth-order cumulants is proposed in [49]. A combination of second- and fourth-order cyclic cumulants (CC) magnitudes is proposed in [50] while higher-order up to eighth-order CC is adopted in [51] and  $n$ th-order warped CC magnitudes is utilized in [52]. Statistical moments of the signal phase are used in [53]. Obviously, cumulants are preferred due to their favourable properties over moments [56]. In contrast to the decision-theoretic methods, the pattern recognition methods may be non-optimal but simple to implement and can often achieve the nearly optimal performance if carefully designed. Furthermore, the pat-

tern recognition methods can be robust with respect to the aforementioned model mismatches. Thus, we focus on the pattern recognition modulation classification approach in this chapter and two approaches are proposed in both time-domain and frequency-domain.

### 4.1.1 Decision Theoretic-based Automatic Modulation Classification

The decision-theoretic (DT) modulation classification approach provides an optimal solution in the sense that it minimizes the probability of false classification if all assumptions of other system parameters are met. Within the DT approach, AMC is formulated as a multiple composite hypothesis-testing problem, and the corresponding hypothesis is resolved using maximum likelihood techniques. Various methods for the determination of the maximum likelihood have been proposed for DT-AMC based upon different assumptions regarding other unknown signal parameters. An in-depth understanding of validity this assumption is critical to proper selection of an AMC technique for a particular scenario.

Three different decision-theoretic algorithms have been developed in the literature: average likelihood ratio test (ALRT), generalized likelihood ratio test (GLRT) and hybrid likelihood ratio test (HLRT). ALRT is a popular AMC approach applied to phase shift keying (PSK) and quadrature amplitude modulation (QAM). ALRT treats unknown system parameters in the received signal as random variables (R.V.'s) and the likelihood functions (LF) are obtained by an averaging process. This requires a hypothesis for the probability density functions (PDF) of the R.V.'s. If the true PDF coincides with the hypotheses, then the results are optimal. The LF under the



hypothesis  $H_i$ , representative of the  $i$ th modulation,  $i = 1, 2, \dots, N_{mod}$ , is given by

$$\Lambda_A^{(i)}[r(t)] = \int \Lambda[r(t)|v_i, H_i]p(v_i|H_i)dv_i \quad (4.1)$$

where  $\Lambda[r(t)|v_i, H_i]$  is the conditional LF of the noisy received signal  $r(t)$  under  $H_i$ , conditioned on the modulated value for  $i$ th modulation scheme  $v_i$ , and  $p(v_i|H_i)$  is the priori PDF of  $v_i$  under  $H_i$ . The known PDF of  $v_i$  enabled us to reduce the problem to a simple hypothesis-testing problem by integrating over  $v_i$ . The ALRT is computationally intensive but current microprocessors have made the ALRT feasible. In general, the performance of ALRT-AMC is very sensitive to other system parameters such as symbol timing, baud rate, carrier frequency, carrier phase, pulse shape, and noise power. The accuracy of ALRT is also affected by channel fading and the type of noise in presence.

The GLRT treats the modulation scheme candidates as unknown deterministic values and the maximum likelihood test is applied as if the true values were known. The best performance is achieved by the so-called uniformly most powerful (UMP) test [57]. When an UMP test does not exist or hard to derive, a logical procedure is introduced to estimate the unknown quantities. Assuming is true, and then uses these estimates in a likelihood ratio test, as if they were correct. If maximum likelihood (ML) is used for estimates, the test is called GLRT. Obviously, GLRT treats the unknown quantities (including both the parameters and data symbols) as deterministic unknowns, and the LF under is given by

$$\Lambda_G^{(i)}[r(t)] = \max_{v_i} \Lambda[r(t)|v_i, H_i] \quad (4.2)$$

The HLRT is a hybrid approach that treats some of the candidate modulation schemes as random variables with known PDFs and some of the candidate parameters

as unknown deterministic variables. This is a combination of the aforementioned two modulation classification approaches, for which the LF under is given by

$$\Lambda_H^{(i)}[r(t)] = \max_{v_i} \int \Lambda[r(t)|v_{i1}, v_{i2}, H_i] p(v_{i2}|H_i) dv_{i2} \quad (4.3)$$

where  $v_i = [v_{i1}^\dagger, v_{i2}^\dagger]^\dagger$  and  $v_{i1}, v_{i2}$  are vectors of unknown quantities modelled as unknown deterministic and R.V.s, respectively. Usually,  $v_{i1}$  and  $v_{i2}$  consist of parameters and data symbols, respectively.

#### 4.1.1.1 ALRT-based Algorithms

With all other system parameters perfectly known, ALRT leads to a modulation classification algorithm whose performance can be considered as a benchmark. The data symbol  $\{s_k^{(i)}\}_{k=1}^K$  in the received signal are treated as independent and identically distributed (i.i.d.) R.V.'s. The LF under hypothesis  $H_i$  is computed by averaging over the constellation points corresponding to the  $i$ th modulation format. To begin with, consider the ALRT for classifying PSK/QAM modulation signals. For the  $i$ th hypothesis  $H_i$ , the joint log-likelihood function can be expressed as

$$\Lambda_A^{(i)}(H_i|r(t)) = \sum_{k=1}^K T^{(i)}(k) \quad (4.4)$$

where

$$T^{(i)}(k) = \ln \left\{ \frac{1}{M_i} \sum_{j=1}^{M_i} \exp \left\{ -\frac{\|r(k) - b_j^{(i)}\|^2}{2\sigma^2} \right\} \right\} \quad (4.5)$$

and  $r(k)$  is a symbol-based received complex data series of length  $K$ , preprocessed from the intercepted signal emitted from a non-cooperative transmitter through an AWGN channel with a two-sided power spectral density of  $\sigma$ , and  $b_j^{(i)}, j = 1, 2, \dots, M_i$  is a complex number and is the  $j$ th reference state of  $i$ th modulation type. The deci-

sion of modulation classification is achieved based on the following criterion: choose  $1 \leq i \leq M_i$  as the modulation type if  $\lambda_A^{(i)}(H_i|r_k)$  is maximum.

Consider now the histogram test when the received signal is real [76]. This test is very popular in AMC practice for classifying real variables, such as modulation phase, frequencies, or amplitudes. The histogram is constructed from a density table [67] with the intervals shown on the x-axis and the number of occurrences in each interval represented by the height of a rectangle located above the interval. To determine the similarity between the ALRT and histogram test, we choose both  $r(k)$  and  $b_j^{(i)}, j = 1, 2, \dots, M_i$  as real values, where  $b_j^{(i)}$  is the  $j$ th reference of modulation type. A table is constructed by dividing  $T_1^{(i)}, T_2^{(i)}, \dots, T_Q^{(i)}$ , and counting the number of  $T^{(i)}(k)$ s occupying the  $q$ th interval, denoted by  $D_q^{(i)}$ , for  $q = 1, 2, \dots, Q$ . If  $T^{(i)}(k)$  is bounded by  $\{-R_n^{(i)}, R_p^{(i)}\}$ , i.e. for  $-R_n^{(i)} \leq T^{(i)} \leq R_p^{(i)}$  for all  $k$ , we find

$$T_q^{(i)} = \frac{l_q^{(i)} + l_{q+1}^{(i)}}{2}, \text{ If } l_q^{(i)} \leq T^{(i)} \leq l_{q+1}^{(i)} \quad (4.6)$$

where

$$l_q^{(i)} = -R_n^{(i)} + \frac{R_p^{(i)} + R_n^{(i)}}{Q}(q - 1) \quad (4.7)$$

Therefore the quantized version of (4.1) will be

$$\Lambda_A^{(i)}(H_i|r_k) = \sum_{k=1}^Q T_q^{(i)} D_q^{(i)} \quad (4.8)$$

Notice that the data series  $D_q^{(i)}$  is the histogram value of  $r(k)$ , for  $k = 1, 2, \dots, K$ , with  $Q$  bins, and  $T_q^{(i)}$  is the template associated with  $H_i$ . In the limit as  $Q \rightarrow K$ , the results of the histogram test approach the results of the ALRT, showing that the histogram test is a special case of the ALRT. It is remarkable also that (4.4)-(4.8)

provide asymptotic optimal templates for histogram test.

#### 4.1.1.2 GLRT- and HLRT-based Algorithms

As the ALRT algorithm suffers from high computational complexity in most realistic scenarios, GLRT and HLRT algorithms have been investigated as possible solutions to identify linear modulations. In AWGN and with  $v_i = [\theta \{s_k^{(i)}\}_{k=1}^K]^\dagger$ , the LF for GLRT and HLRT are respectively given by [57]

$$\Lambda_G^{(i)}[r(t)] = \max_{\theta} \left\{ \sum_{k=1}^K \max_{s_k^{(i)}} \left( \operatorname{Re}[s_k^{(i)*} r_k e^{-j\theta}] - 2^{-1} \sqrt{ST} |s_k^{(i)}|^2 \right) \right\} \quad (4.9)$$

$$\Lambda_H^{(i)}[r(t)] = \max_{\theta} \left\{ \prod_{k=1}^K E_{s_k^{(i)}} \{ \exp[2\sqrt{S}N_0^{-1} \operatorname{Re}[s_k^{(i)*} r_k e^{-j\theta}] - STN_0^{-1} |s_k^{(i)}|^2] \} \right\} \quad (4.10)$$

$E_{s_k^{(i)}}$  is a finite summation over all the possible constellation points of the  $i$ th modulation, for the  $k$ th interval.  $T$  is the signal length for pulse shaping filter and  $S$  is the signal power.  $N_0$  is the PSD of zero-mean AWGN.  $\theta$  is the carrier frequency offset. GLRT has some implementation advantages over ALRT and HLRT, as it avoids the calculation of exponential functions and does not require the knowledge of noise power to compute the LF.

## 4.1.2 Pattern Recognition-based Automatic Modulation Classification

The design of a feature based (FB) modulation classification algorithm first relies on some features extracted from the intercepted signal followed by a decision-making process [65]. Sample features of the received signal considered for modulation classification includes the variance of the centred normalised signal amplitude, phase and frequency [66], the variance of the zero-crossing interval [67],[68], the variance of the magnitude of the signal wavelet transform (WT) after peak removal [69]-[71], the phase PDF [72]-[74] and its statistical moments [75]-[77], moments, cumulants, and cyclic cumulants of the signal itself [78]-[80], etc.

### 4.1.2.1 Instantaneous Features-based Algorithms

The most intuitive way to identify the modulation scheme used in the incoming signal is to explore the information embedded in its instantaneous amplitude, phase and frequency. To extract such information, different methods have been developed in the literature. The following different features in various modulated signal are often employed for modulation classification:

Frequency shift keying (FSK) signals are characterised by constant instantaneous amplitude, whereas amplitude shift keying (ASK) signals have amplitude fluctuations, and PSK signals have information in the phase. The maximum of the discrete Fourier transform (DFT) output of centred (the term 'centred' specifies that the average is removed from the data set, DC-free signal) normalized instantaneous signal was used as a feature to distinguish between FSK and ASK/PSK modulated signals.

ASK and BPSK signals have no information in their absolute phases, whereas M-PSK has. Therefore, the variance of absolute centred normalised phase was used to distinguish between M-PSK and real-valued constellation.

ASK signals have no phase information by their nature, whereas BPSK has. Variance of direct (not absolute) centred normalised phase was used to distinguish between BPSK and ASK modulation schemes. A binary decision tree structure was employed to discriminate modulation schemes between classes, and furthermore, within each class, as we will briefly mention later. At each node of the tree, the decision was made by comparing a statistic against a threshold.

In [74] and [75], the variance of the zero-crossing interval was used as a feature to distinguish FSK from PSK and the unmodulated waveform (UW). The zero-crossing interval is a measure of the instantaneous frequency, and it is a staircase function for FSK signals, whereas a constant for UW and PSK signals. The AMC is treated as a two hypothesis testing problem:  $H_1$  for FSK and  $H_2$  for UW and PSK. The hypotheses are formulated based on the Gaussian assumption for the estimated feature, that is  $N(\mu_{H_i}, \sigma_{H_i}^2)$ ,  $i = 1, 2$ , with the hypothesis-dependent mean  $\mu_{H_i}$  and variance  $\sigma_{H_i}^2$  (the mean is actually the theoretical value of the feature under whereas the variance is estimated under each hypothesis.). An LRT is used for decision, which due to the Gaussian assumption is simplified to the comparison of the feature with a threshold  $h$ , derived from the LRT. The average probability of classification error is then given by

$$p_e = \frac{\left[ \frac{\text{erfc}(n - \mu_{H_1})}{\sigma_{H_1}^2} + \frac{\text{erfc}(n - \mu_{H_2})}{\sigma_{H_2}^2} \right]}{2} \quad (4.11)$$

where  $\text{erfc}(\cdot)$  is the complementary error function defined as

$$\text{erfc}(x) = (2\pi)^{-1/2} \int_x^{\infty} \exp(-\frac{u^2}{2}) du \quad (4.12)$$

The variance of the instantaneous frequency was also employed in [76],[77] to discriminate FSK from UW and PSK. The decision was made by comparing the feature against a threshold.

#### 4.1.2.2 Wavelet Transform-based Algorithm

The use of the wavelet transform to localize the changes in the instantaneous frequency, amplitude and phase of the received signal was also introduced to AMC. The distinct behaviour of the Haar WT (HWT) magnitude for PSK, QAM and FSK signals was employed for modulation identification in [78]-[80]. For a PSK signal, the HWT magnitude is a constant. On the other hand, because of the frequency and amplitude variations in FSK and QAM, the HWT magnitude is a staircase function with peaks at phase changes. These peaks do not provide useful information for non-continuous phase FSK signals. PSK and FSK signals are of constant amplitude, where amplitude normalization has no effect on their HWT magnitude. Therefore, the variance of the HWT magnitude with amplitude normalization was used to discriminate FSK from PSK and QAM. Furthermore, the variance of the HWT magnitude without amplitude normalization was employed to distinguish between QAM and PSK. The decisions were made by comparing the features against some thresholds, based on the statistical analysis of the features, to minimise the probability of classification error for PSK signals [78]-[80].

### 4.1.2.3 Signal statistics-based Algorithms

To discriminate among BPSK, ASK, M-PSK and QAM, the cumulant-based feature was adopted, where the  $n$ th-order/ $q$ -conjugate cumulant of the output of the matched filter is calculated at the zero delay vectors. To make the decision, an LRT based on the PDF of the sample estimate of the feature was formulated to achieve minimum probability of classification error. The moment-based feature was used in [79], where the  $n$ th-order/ $q$ -conjugate moment of the output of the matched filter is calculated at the zero delay. The goal was to distinguish between PSK and QAM. A joint power estimation and classification was performed in [79]. The decision was made based on the minimum absolute value of the difference between the sample estimate and prescribed values of the feature. [80] combined several normalised moments and cumulants for training a neural network to identify FSK, PSK and QAM in multipath environments.

Cumulant-based features were proposed in [78] with details to identify the order of ASK, PSK, and QAM modulations, which can be summarized as follows: the normalized cumulant of fourth-order/two-conjugate for ASK is  $c_{r,4,2}(0)/c_{r,2,1}^2(0)$ ; the magnitude of the normalized cumulant of fourth-order/zero-conjugate for PSK is  $|c_{r,4,2}(0)|/|c_{r,2,1}^2(0)|$ ; and the normalized cumulant of fourth-order/zero-conjugate for QAM is  $c_{r,4,2}(0)/c_{r,2,1}^2(0)$ . The theoretical values of the  $n$ th-order/ $q$ -conjugate cumulant,  $c_{s(i),n,q}$ ,  $q = 0, \dots, n/2$ ,  $n$  is even, for several linear modulations are given in [44]. These values were computed using the moment to cumulant formula in which the  $n$ th-order moments were calculated as ensemble averages over the noise-free unit-variance constellations with equiprobable symbols. Note that owing to the symmetry of the signal constellations considered, the  $n$ th-order moments for  $n$  odd are zero and hence, using the moment to cumulant formula, it is easy to show that the  $n$ th-



order cumulants for odd are also zero. An LRT was formulated based on the PDFs of the sample estimates of features, which are Gaussian, that is,  $N(\mu_H, \sigma_H^2)$ . With a simplified approximation of equal variances under all the hypotheses, the decision was further reduced to comparing the sample estimate of the chosen feature  $\hat{\omega}$  against a threshold, with  $\omega$  as any of the cumulant-based features previously mentioned. For an  $N_{mod}$  hypothesis testing problem, with the hypotheses ordered such that  $\mu_{H_1} < \mu_{H_2} < \dots < \mu_{H_{N_{mod}}}$ , the decision rule is to choose  $H_i$  if

$$\frac{\mu_{H_{i-1}} + \mu_{H_i}}{2} < \hat{\omega}_i < \frac{\mu_{H_i} + \mu_{H_{i+1}}}{2} \quad (4.13)$$

where  $\mu_{H_0} = -\infty$  and  $\mu_{H_{N_{mod}+1}} = \infty$ .

Note that the cumulant-based features  $c_{r,4,2}(0)/c_{r,2,1}^2(0)$  and  $c_{r,4,0}(0)/c_{r,2,1}^2(0)$  do not depend on a fixed carrier phase  $\theta$ , as for  $q = n/2$  the exponential factors which depend on  $\theta$  cancel each other, whereas for  $q \neq n/2$  the phase dependency is dropped by taking the magnitude.

This above method was extended in [81] to classify linear modulations in frequency-selective channels. The blind alphabet matched equalization algorithm, which was used for equalization, was also employed for modulation classification. Some other cumulant-based features were added [72] to the set of features extracted from the instantaneous amplitude, phase and frequency to include QAM signals in the set of candidate modulations to be recognized.

Signal moments were applied to distinguish between QPSK and 16QAM. Specifically, a linear combination of the fourth-order/two-conjugate moment and the squared second-order/one-conjugate moment were employed, with the coefficients and the delay vector optimised to maximize the probability of correct classification. The signal-moment feature  $m_{r,6,3}(0)/m_{r,2,1}^3(0)$  was employed to identify the order of QAM sig-

nals in [81], with the decision made based on the minimum absolute value of the difference between the sample estimate and prescribed values of the feature.

Signal cyclostationarity was also exploited for linear modulation identification, via two approaches: 1.spectral line generation when passing the signal through different nonlinearities, and 2.periodic fluctuations with time of cumulants up to the  $n$ th-order. We note that the  $n$ th-order cycle frequencies (CFs) are given by  $(n - 2q)/\Delta f + m/T$ , with  $m$  an integer. The  $n$ th-order CF formula also holds for an IF signal, where  $\Delta f$  is replaced by the IF frequency,  $f_{IF}$ . With this property, the cyclostationarity of the received signal was exploited for AMC through a pattern of sine-wave frequencies in signal polynomial transformations. For example, the  $2f_{IF}$  and  $4f_{IF}$  sinusoids that appear in the second and fourth powers of the received signal, respectively, were used in [81] to distinguish between BPSK and QPSK. In [82], the same property was explored for a baseband modulated signal. By increasing the order of the nonlinear signal transformation beyond fourth powers, this argument can be extended to identify modulations of order higher than QPSK. Note that the quasi-optimal algorithm derived within the LB framework for PSK signal classification also exploits such a property, by using the information extracted in time domain. However, the signal cyclostationarity is not exploited in this work, as the sampling is performed at the symbol rate  $T^{-1}$ .

## 4.2 Introduction of the Proposed Approach

Modulation classification is a technique used to automatically identify the modulation scheme used by a transmitter at the receiver side by observing the received signal. The technique was originally used for signal interception in military communications but has received renewed interest recently in other areas including adaptive modulation,

software defined radio and cognitive radio networks. To identify the modulation of an incoming signal, decision-theoretic methods[84]-[86] and pattern recognition [87]-[90] are two primary solutions, both of which involve the following steps: preprocessing of the signal and proper selection of the classification algorithm.

Decision-theoretic approaches are based on the likelihood function or approximation theory [84]-[86]. Although the decision-theoretic classifiers with maximum likelihood (ML) are optimal, the corresponding closed-form solutions are either unavailable or computationally intensive when performing a numerical search. Therefore, these approaches are not robust with respect to the model mismatch in the presence of a fading channel as well as phase or frequency offsets.

Pattern recognition methods [87]-[90] may not be optimal but may be simple to implement and can often achieve nearly optimal performance if designed carefully. Within these methods, the modulation classification consists of two subsystems: feature extraction and pattern recognition. Commonly adopted techniques are higher-order statistics (HOS), including cyclic cumulants [87]-[88], statistical moments [89] and support vector machines[90]. Although these methods can be robust when dealing with model mismatch, the classification performance under low Signal-to-Noise (SNR) scenarios is not satisfactory and the computational complexity can be high. To alleviate the computational load and maintain performance, we propose a pattern recognition method in this chapter based on Gaussian Mixture Models (GMM) to classify the modulation schemes, in the presence of multipath fading channels.

GMM has been used successfully in areas such as statistical analysis and speech processing. Specifically, GMM has been used for speaker identification [91], which represents the distribution of the signal with a weighted sum of several multivariate Gaussian functions. The parameters in the model are the weights, mean values and covariances, which can be estimated using the Expectation-Maximization (EM) algo-

algorithm. Since the estimation is based on statistical characteristics, when it comes to wireless propagation, the approach is not sensitive to the transmission diversity, such as dissimilar carrier frequencies, sampling frequencies or symbol rates, thus, making it more robust for implementation. With the purpose of modulation classification, a GMM-based offline database is established, containing the parameters for different modulation schemes, as the reference to determine the GMM parameters of the received signal. Similar work has been investigated in [92] without considering multipath fading channels. In this chapter, an iterative Maximum A Posteriori (MAP) channel mitigation [94] technique is introduced to mitigate the multipath fading as well as maintain system performance. Kullback-Leibler (K-L) Divergence is employed to measure the distance between the received signal and the modulation schemes in the database. To further ease the computational complexity, Gaussian approximation [93] is carried out to cope with multivariate Gaussian components. Performance analysis is presented using Monte Carlo simulation to validate the effectiveness of classification accuracy.

### 4.3 Background

In this section we present the principle and application of GMM and K-L Divergence for use in modulation classification.

### 4.3.1 Gaussian Mixture Models (GMM)

A GMM [91] is a parametric probability density function represented by a weighted sum of  $K$  Gaussian component densities, which can be formulated as

$$p(x|\Theta) = \sum_{k=1}^K \omega_k g(x|\mu_k, \Sigma_k) \quad (4.14)$$

where  $x = \{x\}_{i=0}^{L-1}$  represents a continuous-valued data sequence with length  $L$ .  $\omega_k$  is the mixture weights and  $g(x|\mu_k, \Sigma_k)$  is the  $k$ th Gaussian density with mean value  $\mu_k$  and covariance matrix  $\Sigma_k$ . The GMM parameters are collectively represented by the notation,

$$\Theta = \{\omega_k, \mu_k, \Sigma_k\}, \quad k = 1, \dots, K \quad (4.15)$$

and can be determined by using the EM algorithm [91]. Each Gaussian component density follows the form

$$\begin{aligned} g(x|\mu_k, \Sigma_k) \\ = \frac{1}{(2\pi)^{K/2} |\Sigma_k|^{1/2}} \exp\left\{-\frac{1}{2}(x - \mu_k)' \Sigma_k^{-1} (x - \mu_k)\right\} \end{aligned} \quad (4.16)$$

Given initial parameters  $\Theta^a$ , we wish to estimate the parameters of the GMM to best match the distribution of  $\{x\}$ . The aim of the EM algorithm is to find the model parameters which maximize the likelihood of the GMM. Beginning with  $\Theta^a$ , a new model  $\bar{\Theta}$  is estimated such that the likelihood  $p(x|\bar{\Theta}) \geq p(x|\Theta^a)$  and the new model then becomes the initial model for the next iteration. The process is repeated until some convergence threshold is achieved or a predefined iteration step is reached. During each EM iteration, the following formulas are used to guarantee an increase in the model's likelihood value [91].

Mixture Weights:

$$\bar{\omega}_k = \frac{1}{L} \sum_{i=1}^L p(k|x_i, \Theta) \quad (4.17)$$

Means:

$$\bar{\mu}_k = \frac{\sum_{i=1}^L p(k|x_i, \Theta) x_i}{\sum_{i=1}^L p(k|x_i, \Theta)} \quad (4.18)$$

Variances (diagonal covariance):

$$\bar{\Sigma}_k^2 = \frac{\sum_{i=1}^L p(k|x_i, \Theta) x_i^2}{\sum_{i=1}^L p(k|x_i, \Theta)} - \bar{\mu}_k^2 \quad (4.19)$$

The a posteriori probability for component  $k$  is given by

$$p(k|x_i, \Theta) = \frac{\omega_k g(x_i|\mu_k, \Sigma_k)}{\sum_{k=1}^K \omega_k g(x_i|\mu_k, \Sigma_k)} \quad (4.20)$$

Table 4.1: Theoretical Values  $\Theta$  of GMM for  $A_{nor}$

2ASK	$\omega_k:0.5056, 0.4944, \mu_k:0.0921, 1.9284, \Sigma_k:0.2205, 0.0457$
2FSK	$\omega_k:1.0000, 0.0000, \mu_k:1.0000, 1.0894, \Sigma_k:0.0263, 0.0003$
BPSK	$\omega_k:1.0000, 0.0000, \mu_k:1.0000, 1.1173, \Sigma_k:0.0413, 0.0004$
16QAM	$\omega_k:0.0394, 0.0917, 0.0965, 0.0521, 0.0013, 0.0177$ $0.0720, 0.3958, 0.0102, 0.0142, 0.0034, 0.0122$ $0.0923, 0.0321, 0.0255, 0.0437$ $\mu_k:0.4742, 0.4838, 0.4779, 0.5939, 0.8517, 1.2161$ $1.0699, 1.0802, 0.9470, 1.2887, 1.7136, 1.6107$ $1.4899, 1.3639, 1.4015, 1.4277$ $\Sigma_k:0.0060, 0.0176, 0.0567, 0.1933, 0.0046, 0.0236$ $0.0111, 0.0522, 0.0128, 0.0247, 0.0267, 0.0357$ $0.0396, 0.0244, 0.0095, 0.0075$

### 4.3.2 Kullback-Leibler (K-L) Divergence

After the parameter estimation of GMM, the K-L Divergence is employed to estimate the directed distance between any two probability distribution functions (p.d.f.),  $f$

Table 4.2: Theoretical Values  $\Theta$  of GMM for  $\sigma$ 

2ASK	$\omega_k:0.3783, 0.6217, \mu_k:24.371, 84.716, \Sigma_k:15.303, 23.803$
2FSK	$\omega_k:0.3071, 0.6929, \mu_k:13.977, 53.751, \Sigma_k:9.0016, 17.576$
BPSK	$\omega_k:0.4804, 0.5196, \mu_k:52.720, 154.54, \Sigma_k:32.416, 35.138$
16QAM	$\omega_k:0.0128, 0.0350, 0.0519, 0.0241, 0.1495, 0.0233$ $0.0587, 0.0247, 0.0701, 0.0289, 0.0432, 0.1801$ $0.0721, 0.1327, 0.0609, 0.0318$ $\mu_k:1.1435, 5.8910, 14.157, 24.299, 40.212, 55.875$ $65.682, 88.544, 77.774, 110.23, 131.93, 109.47$ $144.82, 164.73, 184.06, 193.24$ $\Sigma_k:2.0008, 2.0853, 7.5928, 2.2688, 13.965, 9.1713$ $12.232, 2.2568, 8.9860, 5.4923, 8.1922, 1.8935,$ $9.5590, 6.1339, 4.2782, 2.1165$

and  $q$  [93] and the distance is a measure of the dissimilarity between them. The definition of the K-L Divergence is

$$D(f||q) \simeq \int f(i) \log \frac{f(i)}{q(i)} di \quad (4.21)$$

Denote the GMM parameters for  $f$  and  $q$  as

$$\begin{aligned}
 f(i) &= \sum_k \omega_{f,k} g(i|\mu_{f,k}, \Sigma_{f,k}) \\
 q(i) &= \sum_k \omega_{q,k} g(i|\mu_{q,k}, \Sigma_{q,k})
 \end{aligned} \quad (4.22)$$

The K-L distance for GMM parameters is calculated as

$$\begin{aligned}
 D(\hat{f}||\hat{q}) &= \\
 &\frac{1}{2} [\log \left( \frac{|\Sigma_{\hat{f}}|}{|\Sigma_{\hat{q}}|} \right) + \text{Tr}[\Sigma_{\hat{f}}^{-1} \Sigma_{\hat{q}}] + (\mu_{\hat{f}} - \mu_{\hat{q}})^T \Sigma_{\hat{q}} (\mu_{\hat{f}} - \mu_{\hat{q}})]
 \end{aligned} \quad (4.23)$$

where  $\mu_{\hat{f}}$ ,  $\Sigma_{\hat{f}}$ ,  $\mu_{\hat{q}}$  and  $\Sigma_{\hat{q}}$  are the Gaussian approximation [93] of the mean and covariance of the GMM parameters for  $f$  and  $q$ , which is given by (taking  $f$  as an

example)

$$\mu_{\hat{f}} = \sum_{k=1}^K \omega_{f,k} \mu_{f,k} \quad (4.24)$$

$$\Sigma_{\hat{f}} = \sum_{k=1}^K \omega_{f,k} [\Sigma_{f,k} + (\mu_{f,k} - \mu_{f,s})(\mu_{f,k} - \mu_{f,s})^T] \quad (4.25)$$

where  $(\cdot)^T$  denotes the transpose operation and  $\text{Tr}[\cdot]$  represents the trace of a matrix. Therefore, the goal of modulation classification is to find the minimum  $D(\hat{f}||\hat{q})$  of the received signal to one of the considered modulation schemes, and the classification is realized accordingly.

## 4.4 GMM-based Modulation Classification

When considering multipath fading channels, the transmission model can be expressed as

$$r_{e,i} = \sum_{m=0}^{M-1} h_m s_{i-m} + n_i \quad (4.26)$$

where  $\{h_m\}_{m=0}^{M-1}$  are the complex coefficients for a multipath fading channel with length  $M$ .  $\{s_i\}_{i=0}^{L-1}$  is the transmitted modulated symbol with length  $L$ , which constitutes an independently identically distributed (i.i.d.) process.  $\{r_i\}_{i=0}^{L-1}$  is the absolute value of received signal sequence  $\{r_{e,i}\}_{i=0}^{L-1}$  and  $\{n_i\}_{i=0}^{L-1}$  is the additive Gaussian noise with a zero mean and a variance of  $\sigma_n^2$ .

Modulations with Amplitude Shift Keying (ASK), Frequency Shift Keying (FSK), Phase Shift Keying (PSK) and Quadrature amplitude modulation (QAM) are considered since they are most commonly used in digital communications. 2ASK, 2FSK, BPSK and 16QAM are chosen for analysis in this chapter as examples. Hence, the first step is to identify the signal features adopted for modulation classification.



#### 4.4.1 Signal Features Extraction

The features selected here are the instantaneous amplitude and the instantaneous phase of the received signal. The details are described as follows.

##### 1). Instantaneous Amplitude

The instantaneous amplitude  $\{A_i\}_{i=0}^{L-1}$  is defined as [92]

$$A_i = |r_i + j\hat{r}_i| = |r_i + jr_i * \frac{1}{i\pi}| \quad (4.27)$$

where  $\{\hat{r}_i\}_{i=0}^{L-1}$  is the Hilbert Transform of  $\{r_i\}_{i=0}^{L-1}$  and  $*$  denotes the convolution operation. In order to compensate the channel gain, the instantaneous amplitude is normalized by

$$\hat{A}_i = \frac{A_i}{E\{A_i\}} \quad (4.28)$$

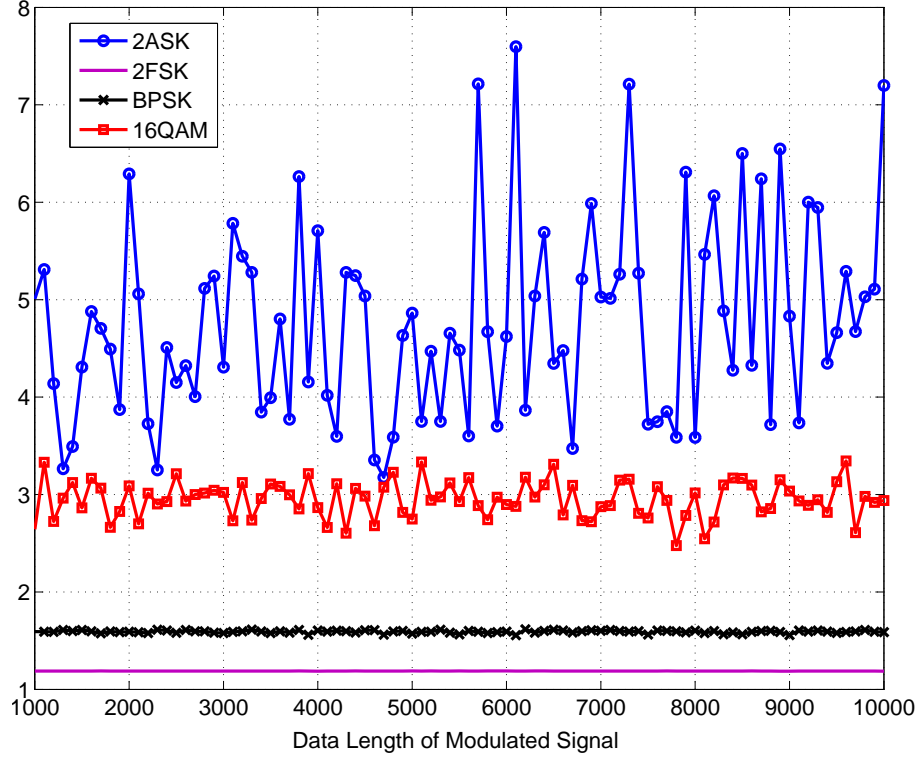
where  $E\{A_i\}$  is the average value of the  $\{A_i\}_{i=0}^{L-1}$ .  $\{\hat{A}_i\}_{i=0}^{L-1}$  is used to discriminate 2FSK and BPSK modulations from 2ASK and 16QAM. Assuming that  $\gamma_{max} = \max_i |\hat{A}_i|^2$ , Figure 4.1 shows the values of  $\gamma_{max}$  for different modulation schemes under variable data length when the SNR is 5dB and there is no fading channel interference. It can be seen that the instantaneous amplitude is capable of distinguishing the signal with FSK and BPSK modulation.

##### 2). Instantaneous Phase

The instantaneous phase  $\{\varphi_i\}_{i=0}^{L-1}$  is given by [92]

$$\varphi_i = \arg\{r_i + j\hat{r}_i\} \quad (4.29)$$

The second signal feature for modulation classification is the standard deviation of the centered non-linear component of the instantaneous phase  $\{\varphi_i\}_{i=0}^{L-1}$ , which is

Figure 4.1:  $\gamma_{max}$  for different modulation schemes when SNR = 5dB.

defined as

$$\sigma_i = \sqrt{\frac{1}{L_1}(\Omega_i^2) - \left(\frac{1}{L_1}|\Omega_i|\right)^2} \quad (4.30)$$

where  $\{\Omega_i\}_{i=0}^{L_1-1}$  is the instantaneous phase  $\{\varphi_i\}_{i=0}^{L_1-1}$  for which  $A_i$  exceeds the mean value in order to remove the  $\{\varphi_i\}$  that are very sensitive to noise.  $\{\sigma_i\}_{i=0}^{L_1-1}$  is used to discriminate between 2ASK, 2FSK and phase modulations (BPSK and 16QAM). Denoting  $\sigma_{max} = \max_i\{\sigma_i\}$ , we can see that Figure 4.2 illustrates the value of  $\sigma_{max}$  for different modulation schemes under different data length when the SNR is 5dB, from which it is clear that  $\sigma_{max}$  is a useful feature to distinguish 2ASK and 2FSK.

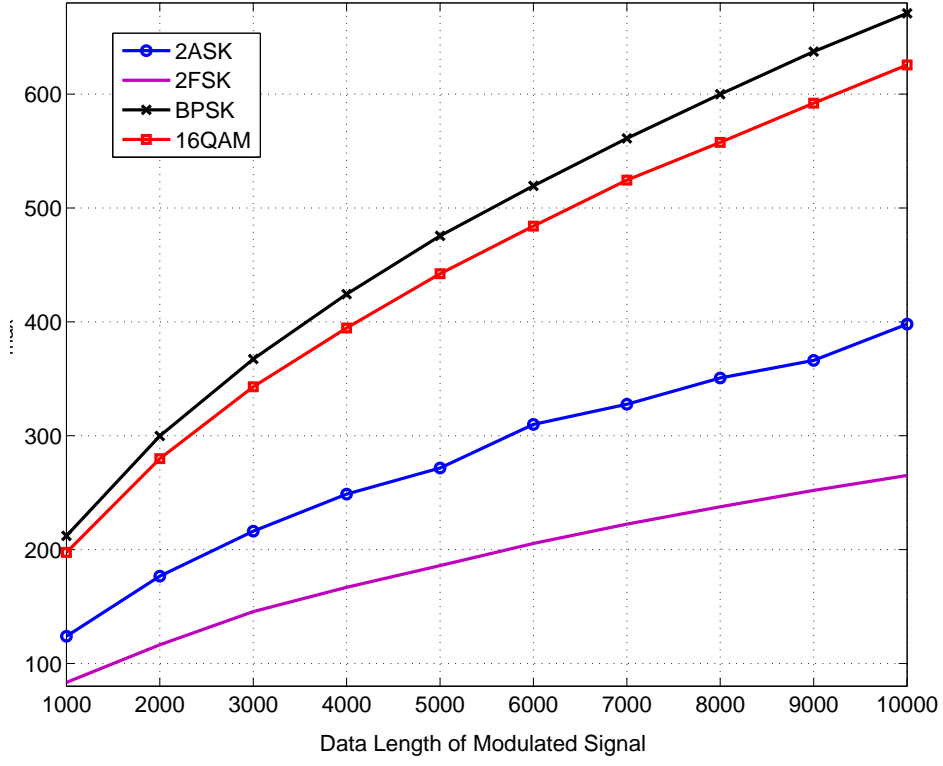


Figure 4.2:  $\sigma_{max}$  for different modulation schemes SNR = 5dB.

#### 4.4.2 Modulation Classification Using GMM

Similar to the application in speech identification [91], an offline GMM database needs to be established for different modulation schemes based on  $\{\hat{A}_i\}$  and  $\{\sigma_i\}$ , which acts as a reference for the received signal to estimate the GMM parameters. The block diagram is showed in Figure 4.3.

As mentioned before, the pattern recognition methods are robust with respect to the model mismatch, therefore, we setup the offline database from the combination of various transmission parameters for different modulation schemes. In detail, the carrier frequency and symbol rate vary from 10 MHz to 50 MHz and 500 kHz to 1 MHz, respectively, in the simulation and the sampling frequency used is 100 MHz. All signals are analyzed as band-limited signals. The choice of GMM configuration

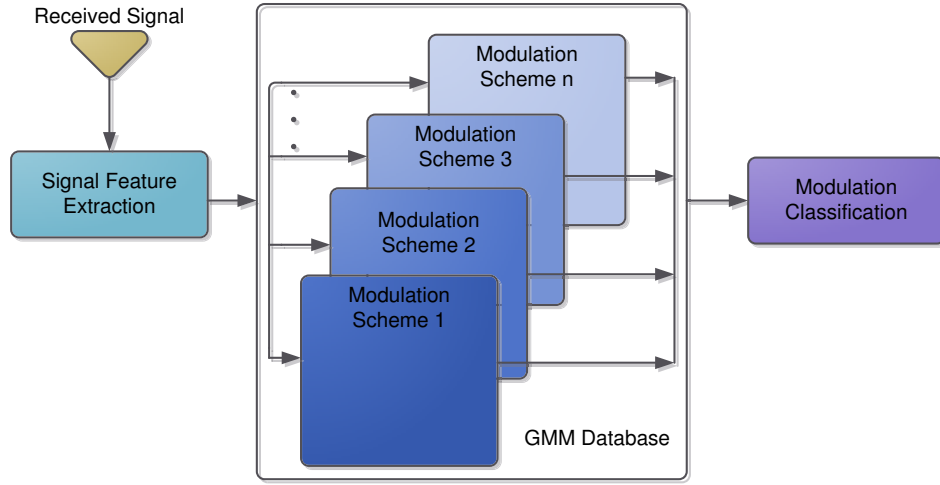


Figure 4.3: The block diagram for GMM-based modulation classification.

(number of components, mean values and covariance matrices) are decided by the diversity of the modulation schemes. Specifically, the selection of Gaussian components in the chapter are  $K = 2$  for 2ASK, 2FSK and BPSK and  $K = 16$  for 16QAM. We assume that the parameters in the GMM database for different modulation schemes are

$$\Theta_p = \{\omega_{p,k}, \mu_{p,k}, \Sigma_{p,k}\}, \quad k = 1, \dots, K \quad (4.31)$$

where  $p = \{1, 2, 3, 4\}$  represents the modulation schemes  $\{2\text{ASK}, 2\text{FSK}, 2\text{PSK}, 16\text{QAM}\}$ .

If we denote  $\mathcal{F} = \{f_i\}_{i=1}^L$  as the  $\{\hat{A}_i\}$  or  $\{\sigma_i\}$  of the received signal and  $\mathcal{Q} = \{q_i\}_{i=1}^L$  as the  $\{\hat{A}_i\}$  or  $\{\sigma_i\}$  of the transmitted signal, the objective function becomes

$$\begin{aligned} P(\mathcal{Q}|\mathcal{F}, \Theta_p^a) &= \prod_{i=1}^L p(q_i|f_i, \Theta_p^a) \\ &= \prod_{i=1}^L \frac{\omega_{q_i}^a p_{q_i}(f_i|\mu_{q_i}^a, \Sigma_{q_i}^a)}{\sum_{k=1}^K \omega_{p,k}^a p_k(f_i|\mu_{p,k}^a, \Sigma_{p,k}^a)} \end{aligned} \quad (4.32)$$

where  $\Theta_p^a = (\omega_{p,1}^a, \dots, \omega_{p,K}^a; \mu_{p,1}^a, \dots, \mu_{p,K}^a; \Sigma_{p,1}^a, \dots, \Sigma_{p,K}^a)$  are the reference parameters from the database for different modulation schemes. The target is to maximize the

likelihood of  $P(\mathcal{Q}|\mathcal{F}, \Theta_p^a)$  by investigating the GMM parameters for  $\{f_i\}_{i=1}^L$  through the EM algorithm based on (4.17)-(4.20). Then, the modulation classification is performed according to the K-L Divergence in (4.23).

Distinct from speech recognition systems, the challenge for the application of GMM to wireless communication is the interference from multipath fading channels, as shown in (4.26), which severely reduces the classification performance. Therefore, in order to improve the classification accuracy, an iterative MAP channel estimation [94] is introduced to mitigate the multipath fading interference, for which the details are described in Section IV.

## 4.5 Iterative MAP Channel Mitigation Modulation Classification

Since  $\{s_i\}_{i=0}^{L-1}$  in (4.26) is an i.i.d. process, it satisfies

$$E\{s(i)s(i-\tau_1)s(i-\tau_2)s(i-\tau_3)\} = \gamma^4 \delta(\tau_1, \tau_2, \tau_3) \quad (4.33)$$

where  $\gamma^4 \equiv E\{s_i^4\}$ . According to HOS theory [95], the fourth-order moment of the received signal  $r(i)$  is chosen in this chapter to explore its underlying characteristics, which can be denoted as

$$\begin{aligned} m_r^4(\tau_1, \tau_2, \tau_3) &= E\{r(i)r(i-\tau_1)r(i-\tau_2)r(i-\tau_3)\} \\ &= \gamma^4 \sum_{m=0}^{M-1} h(m)h(m-\tau_1)h(m-\tau_2)h(m-\tau_3) \end{aligned} \quad (4.34)$$

When  $\tau_1 = \tau_2 = M-1$ , and  $\tau_3 = m$ , for  $m = 0, 1, \dots, M-1$  and  $M$  is the

channel length,  $m_r^4(M-1, M-1, m)$  can be written as

$$m_r^4(M-1, M-1, m) = \gamma^4 h(0)h(M-1)h(M-1)h(m) \quad (4.35)$$

and when  $m = 0$ , we obtain

$$m_r^4(M-1, M-1, 0) = \gamma^4 h(0)h(M-1)h(M-1)h(0) \quad (4.36)$$

Therefore, the normalized multipath fading coefficients  $\tilde{h}(m)$  are

$$\tilde{h}(m) = \frac{m_r^4(M-1, M-1, m)}{m_r^4(M-1, M-1, 0)}, \quad m = 0, 1, \dots, M-1 \quad (4.37)$$

$\tilde{h}(m)$  is used as the initial channel coefficients for the iterative MAP channel estimation. When  $\tilde{h}(m)$  is modeled as a Gaussian p.d.f., we have  $f(\tilde{h}) = g(\tilde{h}|\mu_{\tilde{h}}, \Sigma_{\tilde{h}})$  where  $\mu_{\tilde{h}}$ ,  $\Sigma_{\tilde{h}}$  are the mean and covariance matrix of the channels separately. Based on the MAP channel estimation [94], the required information is the mean value and covariance matrix of the transmitted signal  $\{s_i\}_{i=0}^{L-1}$ , which can be obtained from the offline database through Gaussian approximation [93].

Therefore, if we denote  $\mu_{p,s}$  and  $\Sigma_{p,s}$  as the mean value and covariance matrix of the  $p$ th modulation scheme in the database, the MAP channel estimation can be realized by [94]

$$\hat{h} = (\Sigma_{p,s} + \Sigma_{\tilde{h}})^{-1} \Sigma_{\tilde{h}} (r - \mu_{p,s}) + (\Sigma_{p,s} + \Sigma_{\tilde{h}})^{-1} \Sigma_{p,s} \mu_{\tilde{h}} \quad (4.38)$$

and the channel interference is diminished by

$$\hat{r} = \text{IFFT}\left\{\frac{R}{\hat{H}}\right\} \quad (4.39)$$

where  $R$  and  $\hat{H}$  are the Fast Fourier Transform (FFT) of  $\{r_i\}_{i=0}^L$  and  $\hat{h}$ , respectively, and  $\text{IFFT}\{\cdot\}$  denotes Inverse Fast Fourier Transform. Extracted from  $\hat{r}$ , the instantaneous amplitude and phase are modeled by GMM based on the pre-processed database.

In order to increase the estimation accuracy, iteration is employed to alleviate the multipath channel interference. The proposed iteration procedure can be generalized in the following steps

1. Obtain the initial multipath channel coefficients  $\{\tilde{h}_m\}$  through (4.37).
2. Carry out the MAP channel estimation based on (4.38) to achieve the channel impulse response  $\hat{h}$  and reduce the channel interference through (4.39) to acquire  $\hat{r}$ .
3. Using  $\hat{r}$ , two signal features, namely, instantaneous amplitude and instantaneous phase are calculated from (4.28) and (4.30). GMM parameter estimation is performed from (4.32) as well as the EM algorithm through (4.17)-(4.20).
4. With the estimated parameters, K-L Divergence in (4.23) is employed to measure the distance between the received signal and the modulation scheme in the database.
5. Repeat step 1) - 4) for each modulation scheme in the database until the K-L distance converges to a certain threshold or a predefined number of iteration steps is reached. At this point, the modulation classification is achieved.

## 4.6 Simulation Results and Discussions

In this section, we evaluate our proposed algorithm through Monte Carlo experiments, in terms of the correct classification probability  $P_{cc}$  versus SNR. The parameters of the transmitted signal are selected as: the symbol rate  $f_b$  is chosen to be 1MHz, the carrier frequency  $f_c$  is 20MHz, the shifted frequencies for 2FSK are  $f_1 = 5\text{KHz}$  and  $f_2 = 10\text{KHz}$  and the sampling frequency  $f_s$  at the receiver is 100MHz. The multipath channel applied is assumed to be Rayleigh fading, where the randomly generated channel coefficients are  $\{h(m)\}_{m=0}^{M-1}$  with length  $M$ . Without loss of generality, we set  $h(0)=1$  for channel mitigation. The channels have an exponentially decaying phase delay profile, comprised of four complex Gaussian distributed taps with average power  $\sigma_h^2 = E[|\{\sum_m h_m\}|^2]$ . Traditional HOS-based modulation classification is compared under the same simulation environment as the proposed approach and a Monte Carlo simulation using 10000 operations is carried out with the results analyzed below.

Figure 4.4 and Figure 4.5 depict the simulation results for the proposed algorithm and HOS-based modulation classification. The curves labeled as “with Estimated Channel Info.” present the performance with the estimation of the normalized channel coefficients. It can be seen that the the classification performance of the proposed GMM with 10 iteration outperforms the HOS under AWGN as well as multipath channels when  $\text{SNR} > 0\text{dB}$ . Furthermore, compared to the curves without iteration, the iterative approach can improve the  $P_{cc}$  results considerably under multipath channels, which exhibit the effectiveness of the proposed iteration technique to increase the estimation accuracy.



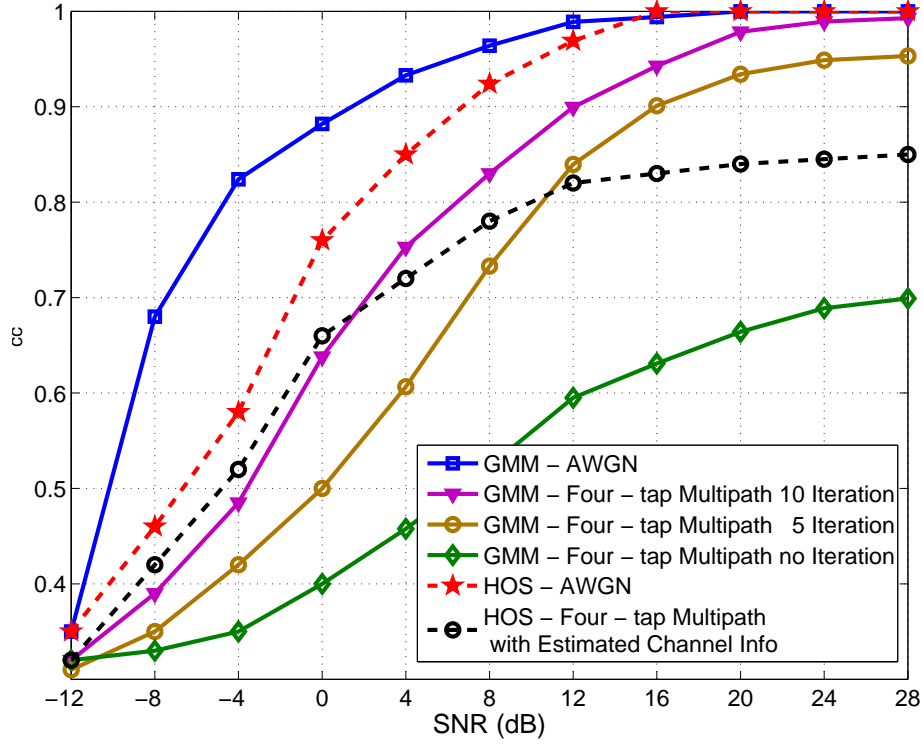


Figure 4.4: Comparison of GMM and HOS on  $P_{cc}$  for 16QAM and 2FSK.

## 4.7 Conclusion

Classification of the modulation scheme used in the intercepted signal of interest is a major step of blind interception receiver design. Accurate identification of the modulation scheme will naturally improve the reliability of the blind data recovery.

To achieve this goal, various modulation classification algorithms have been investigated in this chapter to overcome various difficulties associated with the modulation classification process. One major challenge here is how to limit the negative impact on the blind modulation classification from many factors, which include unknown system parameters of the transmitter and receiver involved, and the unknown signal propagation conditions. Without prior knowledge of the system parameters of

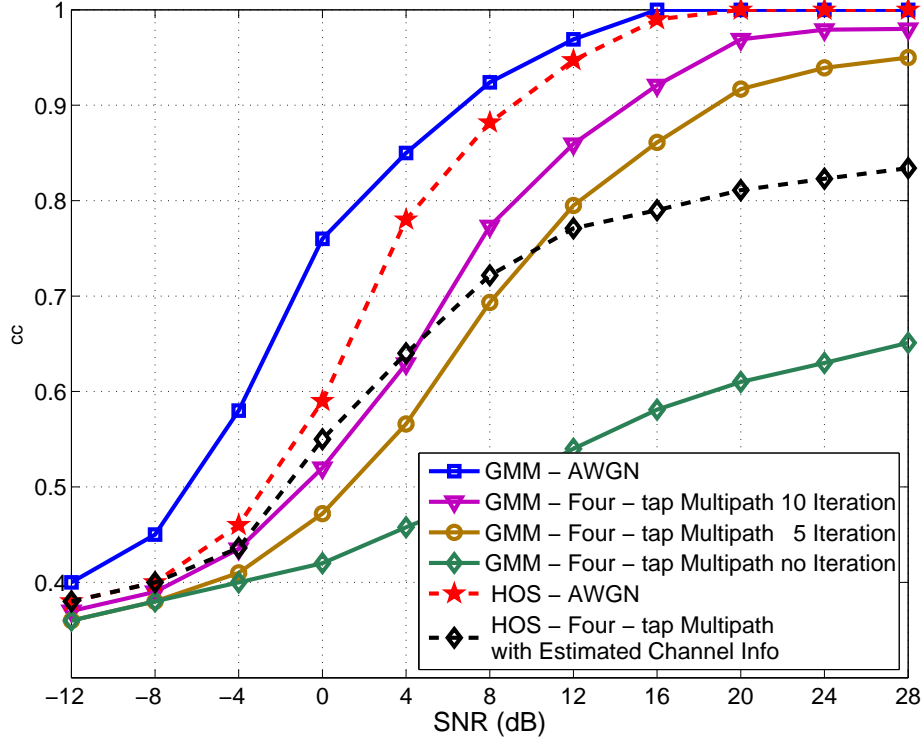


Figure 4.5: Comparison of GMM and HOS on  $P_{cc}$  for BPSK and 2ASK.

transmitter and receiver, for instance, clock mismatch, carrier frequency and phase offsets, and timing error, blind identification of the modulation can be a difficult task. This becomes even more challenging in real-world scenarios from the wireless signal propagation environment with multipath fading, frequency-selectivity and time-variation.

The chapter starts with a comprehensive survey of different modulation recognition techniques in a systematic way. The two general classes of automatic modulation identification algorithms are presented in details, which rely on the likelihood function and features of the received signal, respectively. Moreover, modulation classification based on GMM for digital communications is proposed in this chapter with an iterative MAP multipath channel mitigation algorithm. An offline database is established

according to the GMM parameter estimation for different modulation schemes, which is applied as the reference to model the received signal. K-L Divergence is then employed to measure the distance between the received signal and the database to realize the modulation classification. From the simulation results, the instantaneous amplitude and phase are confirmed to be useful tools for extracting the signal features for different modulation schemes. In addition, the proposed iterative approach can be utilized to increase the classification performance in the presence of multipath fading channels.

# Chapter 5

## Conclusion

### 5.1 Contributions of This Thesis

Three main contributions have been achieved in this thesis, including an iterative cyclostationary analysis for blind signal identification, the joint estimation of signal parameters and synchronization under envelope spectrum information, and the Gaussian Mixture Models (GMM)-based modulation classification under multipath fading channels.

The algorithms for different parameters estimation of OFDM system under a blind scenario are investigated. The OFDM system parameters considered include sampling frequency, number of subcarriers, cyclic prefix ratio as well as frequency and timing offset. Since two directions exist in literature for blind parameter estimation which are nonparametric spectrum based and cyclostationarity based, the thesis analyzed the performance for both and developed the approaches to improve the estimation accuracy under two scenarios. With the aid of estimated parameters, channel identification is performed to provide CSI as well with enhanced accuracy for potential resource optimization in networks. Monte Carlo simulations and experimental measurements are conducted to evaluate the performance of the individual modules as well as the overall algorithms. Current results show that the proposed algorithm is capable of adapting to communication with improved performance.

Considering the synchronization, we propose a joint iterative blind OFDM parameter estimation and synchronization approach for the interception receiver to operate with multi-waveform signals. The thesis begins with introducing the system model for oversampled OFDM signals and proposes the envelope spectrum-based arbitrary oversampling ratio estimation. According to the oversampling ratio, the number of subcarriers and the cyclic prefix (CP) length are identified as well, all of which are used to provide the necessary information for carrier frequency offset (CFO) and timing offset estimation. The iterative scheme is then explained to refine the estimation results and increase the accuracy in every step.

Classification of the modulation scheme used in the intercepted signal of interest is a major step of blind interception receiver design. Accurate identification of the modulation scheme will naturally improve the reliability of the blind data recovery. To achieve this goal, various modulation classification algorithms have been investigated in this thesis to overcome various difficulties associated with the modulation classification process. One major challenge here is how to limit the negative impact on the blind modulation classification from many factors, which include unknown system parameters of the transmitter and receiver involved, and the unknown signal propagation conditions. Without prior knowledge of the system parameters of transmitter and receiver, for instance, clock mismatch, carrier frequency and phase offsets, and timing error, blind identification of the modulation can be a difficult task. This becomes even more challenging in real-world scenarios from the wireless signal propagation environment with multipath fading, frequency-selectivity and time-variation.

This thesis starts with a comprehensive survey of different modulation recognition techniques in a systematic way. The two general classes of automatic modulation identification algorithms are presented in details, which rely on the likelihood function and features of the received signal, respectively. Moreover, we proposed one

modulation classification scheme based on Gaussian Mixture Models for digital communications with an iterative MAP multipath channel mitigation algorithm. An offline database is established according to the GMM parameter estimation for different modulation schemes, which is applied as the reference to model the received signal. K-L Divergence is then employed to measure the distance between the received signal and the database to realize the modulation classification. From the simulation results, the instantaneous amplitude and phase are confirmed to be useful tools for extracting the signal features for different modulation schemes. In addition, the proposed iterative approach can be utilized to increase the classification performance in the presence of multipath fading channels.

## 5.2 Future Works

Reliable signal sensing and identification techniques are fundamental to the proposed blind interception receiver design. New techniques in this domain need to be developed, while some existing signal sensing and identification techniques may be customized to meet the specific purposes of this study. With the development of cooperative communication and compressive sensing techniques, the future work can be done in the following directions:

- Signal identification is currently one of the most challenging design problems in cognitive radio. A robust spectrum sensing technique is important in allowing implementation of a practical dynamic spectrum access in noisy and interference uncertain environments. In addition, it is desired to minimize the sensing time, while meeting the stringent cognitive radio application requirements. To cope with this challenge, concept of compressed sensing can be applied by utilizing the sparsity of the two-dimensional cyclic spectrum. Compressive sampling is

used to reduce the sampling rate and a recovery method is developed for reconstructing the sparse cyclic spectrum from the compressed samples. The reconstruction solution used, exploits the sparsity structure in the two-dimensional cyclic spectrum domain which is different from conventional compressed sensing techniques for vector-form sparse signals.

- Software Defined Radio (SDR) is considered as the next evolutionary step in the mobile communications. One of the most crucial properties of a SDR terminal is that it is capable of using a wide range of air interface standards, providing a seamless interoperability between different standards and an enhanced roaming capability, paving way to a more flexible and efficient use of spectral resources. Cooperative cyclostationary analysis is a possible solution in order to detect and distinguish different systems since those signals have different patterns in the cyclic spectrum under the cyclostationary analysis. Cooperative scheme can be utilized to improve the performance and reduce the complexity and delay. Each user only measures signal power at a single cyclic frequency (CF) and exchange its information with the others for further decision. The use of parallel SC detectors at different CFs by different receivers can reduce the computational complexity and delay as compared to the use of multiple-cycle detector in each receiver. Since each receiver sees independent noise, fading and shadowing, effectively, decision based on the information related to the signal powers simultaneously measured by all receivers search at different CFs, can offer a better performance enhanced by multi-user diversity, in a short period of time.

## References

- [1] R. Chang, "Synthesis of band-limited orthogonal signals for multichannel data transmission," *Bell Sys. Tech. J.*, vol. 45, pp. 1775 - 1796, 1966.
- [2] S. Weinstein and P. Ebert, "Data transmission by frequency-division multiplexing using the discrete Fourier transform," *IEEE Trans. on Communication Technology*, vol. 19, no. 5, pp. 628 - 634, 1971.
- [3] L. Cimini Jr, "Analysis and simulation of a digital mobile channel using orthogonal frequency division multiplexing," *IEEE Trans. on Communications*, vol. 33, no. 7, pp. 665 - 675, 1985.
- [4] Wireless LAN Medium Access Control (MAC) and Physical Layer (PHY) Specification, IEEE Standard, Supplement to Standard 802 Part II: Wireless LAN, New York, NY, 1999.
- [5] M. Oner and F. Jondral, "Cyclostationarity based air interface recognition for software radio systems," in *IEEE Radio and Wireless Conference*, 2004, pp. 263 - 266.
- [6] B. Wang and L. Ge, "A novel algorithm for identification of OFDM signal," in *Proc. IEEE Intl. Conf. on Wireless Communications, Networking and Mobile Computing*, 2005, vol. 1. pp. 261 - 264.
- [7] W. Akmouche, "Detection of multicarrier modulations using 4th-order cumulants," in *Proc. IEEE Military Communications Conference (MILCOM)*, 1999. vol. 1. pp. 432 - 436.
- [8] W. A. Gardner, *Cyclostationarity in Communications and Signal Processing*. New Jersey, NY, USA, IEEE Press, 1993.
- [9] A. Papoulis and S. Pillai, *Probability, Random Variables and Stochastic Processes*. McGraw-Hill Education (India) Pvt Ltd, 2002.



- [10] W. Gardner, Introduction to Random Processes: with applications to signals and systems. McGraw-Hill, 1990.
- [11] H. Bolcskei, "Blind estimation of symbol timing and carrier frequency offset in wireless OFDM systems," IEEE Trans. on Communications, vol. 49, Issue 6, pp. 988 - 999, June 2001.
- [12] H. Ishii, G.W. Wornell, "OFDM Blind Parameter Identification in Cognitive Radios", in Proc. IEEE Int. Symp. Personal, Indoor and Mobile Radio Communications (PIMRC), Sept. 2005, vol. 1, pp. 700 - 705.
- [13] P. Liu, B. Li, Z. Lu, F. Gong, "A Blind Time-parameters Estimation Scheme for OFDM in Multi-path Channel," in Prof. Int. Conf. IEEE Wireless Communications, Networking and Mobile Computing, Sept. 2005, vol. 1, pp. 242 - 247.
- [14] M. Oner and F. Jondral, "Cyclostationarity based air interface recognition for software radio systems," IEEE Radio and Wireless Conf., Sept. 2004, pp. 263 - 266.
- [15] A.V. Dandawate and G.B. Giannakis, "Statistical tests for presence of cyclostationarity," IEEE Trans. on Signal Processing, vol. 42, Issue 9, pp. 2355 - 2369, Sept. 1994.
- [16] D. E. K. Martin and B. Kedem, "Estimation of the period of periodically correlated sequences," J. Times Ser. Anal., vol. 14, no. 2, pp. 193 - 205, 1993.
- [17] H. L. Hurd and N. L. Gerr, "Graphical methods for determining the presence of periodic correlation," J. Times Ser. Anal., vol. 12, no. 4, pp. 337 - 350, 1991.
- [18] M. Shi, Y. Bar-Ness and W. Su, "Blind OFDM systems parameters estimation for software defined radio," in Proc. of IEEE Intl. Symp. on New Frontiers in Dynamic Spectrum Access Networks (DySPAN), Apr. 2007, pp. 119 - 122.
- [19] V. L. Nir, T. V. Waterschoot, M. Moonen and J. Duplcy, "Blind CP-OFDM and ZP-OFDM Parameter Estimation in Frequency Selective Channels," EURASIP J. on Wireless Communication and Networking, no. 11, vol. 2009, Jan. 2009.

- [20] Q. Chen, X. Wang, P. Ho, Y. Wu, "Progressive Automatic Detection of OFDM System Parameters for Universal Mobile DTV Receiver," in Proc. IEEE Vehicular Technology Conference (VTC-Fall), Sept. 2010, pp.1 - 5.
- [21] Q. Chen, X. Wang, D. Fan and S. Guo, "Computation-efficient blind estimation of OFDM signal parameters for interception and data recovery," in Proc. SPIE 8061, April, 2011, doi:10.1117/12.886862.
- [22] A. V. Dandawaté and G. B. Giannakis, "Statistical tests for presence of cyclostationarity," IEEE Trans. on Signal Processing, vol. 42, no. 9, pp. 2355 - 2369, Sept. 1994.
- [23] S. Sohn, N. Han, J. Kim, J. Kim, "OFDM Signal Sensing Method Based on Cyclostationary Detection," in Proc. ICST Conference on Cognitive Radio Oriented Wireless Networks and Communications, Aug. 2007, pp. 63 - 68.
- [24] H. Bolcskei, "Blind estimation of symbol timing and carrier frequency offset in wireless OFDM systems," IEEE Trans. on Communication, Vol. 49, Issue 6, pp. 988 - 999, June 2001.
- [25] R. W. Heath Jr. and G. B. Giannakis, "Exploiting input cyclostationarity for blind channel identification in OFDM systems," IEEE Trans. on Signal Processing, vol. 47, pp. 848 - 856, March 1999.
- [26] T. Pollet, M. Van Bladel, and M. Moeneclaey, "Ber sensitivity of OFDM systems to carrier frequency offset and wiener phase noise," IEEE Trans. Commun., vol. 43, pp. 191 - 193, Feb. 1995
- [27] T. Schmidl and D. Cox, "Robust frequency and timing synchronization for OFDM," IEEE Trans. Commun., vol. 45, no.12, 1997, pp. 1613 - 1621.
- [28] Y. H. Kim, Y. K. Hahm, H. J. Jung, I. Song, "An Efficient Frequency offset Estimator for Timing and Frequency Synchronization in OFDM system," in Proc. IEEE Pacific Rim Conf. on Communications, Computers and Signal Processing, August 2002, pp. 580 - 583.
- [29] H. Minn, M. Zeng, and V. K. Bhargava, "On Timing Offset Estimation for OFDM Systems," IEEE Communications Letters, vol. 4, no. 7, July 2000, pp 242 - 244.

- [30] B. Park, H. Cheon, C. Kang, and D. Hong "A Novel Timing Estimation Method for OFDM Systems," IEEE Communications Letters, vol. 7, no. 5, May 2003, pp.239 - 241.
- [31] S. D. Choi, J. M. Choi, and J. H. Lee, "An Initial Timing Offset Estimation Method for OFDM Systems in Rayleigh Fading Channel," in Proc. IEEE Vehicular Technology Conference (VTC-Fall), 2006, pp. 1 - 5.
- [32] P.H. Moose. "A technique for orthogonal frequency division multiplexing Frequency offset correction," IEEE Trans. Communications, vol.42, no. 10, pp. 2908 - 2914, October 1994.
- [33] J.J. Van de Beek, "ML-estimation of time and frequency offset in OFDM systems," IEEE Trans. Signal Processing, Vol.45, No.7, pp. 1800 - 1805, July 1997.
- [34] T.M. Sctunidl. D.C. Coxi, "Robust Frequency and timing synchronization for OFDM," IEEE Trans. Communications, vol. 45, no. 12, pp. 1613 - 1621, December 1977.
- [35] I.H. Hwang, H.S. Lce and K.W. Kang, "Frequency and timing period offset estimation Techniques for OFDM systems," IEE Electronics Letter, vol. 34. no. 6, pp. 520-521, March 1978.
- [36] S. Siinoens. V Bnzenac and M.D. Courville, "A new method for joint cancellation of clock and carrier frequency offsets in OFDM receivers over frequency selective channels," in Proc. IEEE Vehicular Technology Conference (VTC-Spring), vol. 1, pp. 390-394, May 2000.
- [37] M. Speth. S. Feclitel. G. Fock and H. Meyr, "Optiinum receiver design for OFDM-based broadband transmission part II : A case study," IEEE Trans. Communications, vol. 49, no. 4, pp. 571 - 578, April 2001.
- [38] J.K. Wolf and J.W. Schwartz, "Comparison or estimation for frequency offset," IEEE Trans. Commmunications, vol. 38, no. 1, pp. 124 - 127, January 1990.
- [39] S. Y. Liu, J. W. Chong, "A study of joint tracking algorithms of carrier frequency offset and sampling clock offset for OFDM-based WLANs," IEEE Int.

- Conf. Communications, Circuits and Systems and West Sino Expositions, June 2002, vol. 1, pp. 109 - 113.
- [40] E. Jacobsen, R. Lyons, "The Sliding DFT," IEEE Signal Processing Magazine, vol.20, no. 2, pp. 74-80, Mar. 2003.
- [41] J.-G. Liu, X. Wang, J. Nadeau and P. Ho, "Blind parameter estimation for OFDM interception receiver with iterative cyclostationary analysis," in Proc. IEEE Int. Conf. for Military Communications (MILCOM), Nov. 2011, pp. 2211 - 2215.
- [42] F.-J. Harris, Multirate Signal Processing. Upper Saddle River, NJ: Prentice-Hall, 2004.
- [43] J.-J. van de Beek, M. Sandell, P.-O. Borjesson, "ML estimation of time and frequency offset in OFDM systems," IEEE Trans. on Signal Processing, vol. 45, issue 7, pp. 1800 - 1805, July 1997.
- [44] O.A. Dobre, A. Abdi; Y. Bar-Ness, W. Su, "Survey of automatic modulation classification techniques: classical approaches and new trends ," IET Communications, vol. 1, pp. 137 - 156, 2007.
- [45] P. Panagiotou, A. Anastasopoulos and A. Polydoros, "Likelihood ratio tests for modulation classification," in Proc. IEEE Military Communication Conf. (MILCOM), vol. 2, Oct. 2000, pp. 670 - 674.
- [46] W. Wei and J. M. Mendel, "Maximum-likelihood classification for digital amplitude-phase modulations," IEEE Trans. on Communications, vol. 48, no. 2, pp. 189 - 193, Feb. 2000.
- [47] T. Yucek and H. Arslan, "A novel sub-optimum maximum-likelihood modulation classification algorithm for adaptive OFDM systems," in Proc. of IEEE Wireless Communications and Networking Conf. (WCNC), vol. 2, March 2004, pp.739 - 744.
- [48] Z. Zhao and L. Tao, "A MPSK modulation classification method based on the maximum likelihood criterion," in Proc. Int. Conf. on Signal Processing, vol. 2, Aug. 2004, pp. 1805 - 1808.

- [49] A. Swami and B. M. Sadler, "Hierarchical digital modulation classification using cumulants," *IEEE Trans. on Communications*, vol. 48, no. 3, pp. 416 - 429, March 2000.
- [50] P. Marchand, C. Le Martret and J. L. Lacoume, "Classification of linear modulations by a combination of different orders cyclic cumulants," in *Proc. IEEE Signal Processing Workshop on Higher-Order Statistics*, July 1997, pp. 47 - 51.
- [51] O. A. Dobre, Y. Bar-Ness and Wei Su, "Higher-order cyclic cumulants for high order modulation classification," in *Proc. IEEE Military Communication Conf. (MILCOM)*, vol. 1, Oct. 2003, pp. 112 - 117.
- [52] O. A. Dobre, Y. Bar-Ness and W. Su, "Robust QAM modulation classification algorithm using cyclic cumulants," in *Proc. IEEE Wireless Communications and Networking Conference (WCNC)*, vol. 2, March 2004, pp. 745 - 748.
- [53] S. S. Soliman and S.-Z. Hsue, "Signal classification using statistical moments," *IEEE Trans. on Communications*, vol. 40, no. 5, pp. 908 - 916, May 1992.
- [54] S. Kadambe and Q. Jiang, "Classification of modulation of signals of interest," *IEEE Proc. Digital Signal Processing Workshop*, Aug. 2004, pp. 226 - 230.
- [55] H. B. Guan, C. Z. Ye and X. Y. Li, "Modulation classification based on spectrogram, in *Proc. Intl. Conf. on Machine Learning and Cybernetics*, Aug. 2004, pp. 3551 - 3556.
- [56] C. L. Nikias and A. P. Petropuou, *Higher-order Spectra Analysis*, Prentice-Hall, New Jersey, 1993.
- [57] H.L. van Trees, *Detection, estimation and modulation theoryPart I*, Wiley, New York, 2001.
- [58] L. Hong and K.C. Ho, "An antenna array likelihood modulation classifier for BPSK and QPSK signals," in *Proc. IEEE Int. Conf. Military Communication (MILCOM)*, Oct. 2002, vol. 1, pp. 647 - 651.
- [59] K.M. Chugg, C.S. Long, and A. Polydoros, "Combined likelihood power estimation and multiple hypothesis modulation classification," in *Proc. Asilomar*

- Conf. on Signals, Systems and Computers (ASILOMAR), Oct. 1995, vol. pp. 1137 - 1141.
- [60] L. Hong, and K.C. Ho, "BPSK and QPSK modulation classification with unknown signal level," in Proc. 21st Century Military Communications Conf. (MILCOM), Oct. 2000, vol. 2, pp. 976 - 980.
- [61] N. Lay, and A. Polydoros, "Per-survivor processing for channel acquisition, data detection and modulation classification," in Proc. Asilomar Conf. on Signals, Systems and Computers (ASILOMAR), Oct. 1994, vol. 2, pp. 1169 - 1173.
- [62] N. Lay, and A. Polydoros, "Modulation classification of signals in unknown ISI environments," in Proc. IEEE Military Communication Conf. (MILCOM), Nov. 1995, vol. 1, pp. 170 - 174.
- [63] O.A. Dobre, J. Zarzoso, Y. Bar-Ness, and W. Su, "On the classification of linearly modulated signals in fading channel," Proc. CISS Conf., Princeton, March 2004.
- [64] A. Abdi, O.A. Dobre, R. Choudhry, Y. Bar-Ness, and W. Su, "Modulation classification in fading channels using antenna arrays," in Proc. Military Communication Conf. (MILCOM), October 2004, vol. 1, pp. 211 - 217.
- [65] A.K. Jain, R.P.W. Duin, and J. Mao, "Statistical pattern recognition: A review," IEEE Trans. Pattern Anal. Mach. Intell., 2000, 22, pp. 34 - 37.
- [66] E.E. Azzouz, and A.K. Nandi, "Automatic modulation recognition of communication signals" (Kluwer Academic, 1996).
- [67] S.Z. Hsue, and S.S. Soliman, "Automatic modulation recognition of digitally modulated signals," in Proc. IEEE MILCOM, 1989, pp. 645 - 649.
- [68] S.Z. Hsue, and S.S. Soliman, "Automatic modulation classification using zero crossing," in IEE Proc. Radar Signal Process., 1990, 137, pp. 459 - 464.
- [69] K.C. Ho, W. Prokopiw, and Y.T. Chan, "Modulation identification by the wavelet transform," in Proc. Military Communication Conf. (MILCOM), October 1995, pp. 886 - 890.

- [70] K.C. Ho, W. Prokopiw, and Y.T. Chan, "Modulation identification of digital signals by the wavelet transform," in IEE Proc., Radar, Sonar Navig., 2000, 47, pp. 169 - 176.
- [71] L. Hong, and K.C. Ho, "Identification of digital modulation types using the wavelet transform," in Proc. Military Communication Conf. (MILCOM), October 1999, pp. 427 - 431.
- [72] Y. Yang, and S.S. Soliman, "Optimum classifier for M-ary PSK signals," in Proc. IEEE Int. Conf. Communications, June 1991, vol. 3, pp. 1693 - 1697.
- [73] Y. Yang, and C.H. Liu, "An asymptotic optimal algorithm for modulation classification," IEEE Communication Letter, issue 5, vol. 2, pp. 117 - 119, May 1998.
- [74] Y. Yang, and S.S. Soliman, "A suboptimal algorithm for modulation classification," IEEE Trans. Aerospace Electronics System, issue 1, vol. 33, pp. 38 - 45, January 1997.
- [75] Y. Yang, and S. S. Soliman, "Statistical moments based classifier for MPSK signals," in Proc. IEEE Global Telecommunications Conf. (GLOBECOM), Dec. 1991, vol. 1, pp. 72 - 76.
- [76] S.S. Soliman, and S.Z. Hsue, "Signal classification using statistical moments," IEEE Trans. Communications, issue 5, vol. 40, pp. 908 - 916, May 1992.
- [77] Y. Yang, and S.S. Soliman, "An improved moment-based algorithm for signal classification," Signal Processing, 43, pp. 231 - 244, 1995.
- [78] A. Swami, and B.M. Sadler, "Hierarchical digital modulation classification using cumulants," IEEE Trans. Communications, issue 3, vol. 48, pp. 416 - 429, March 2000.
- [79] W. Dai, Y. Wang, and J. Wang, "Joint power and modulation classification using second- and higher statistics," in Proc. IEEE Wireless Communications and Networking Conference (WCNC), 2002, pp. 155 - 158.

- [80] G. Hatzichristos, and M.P. Fargues, "A hierarchical approach to the classification of digital modulation types in multipath environments," in Proc. Asilomar Conf. on Signals, Systems and Computers (ASILOMAR), 2001, pp. 1494 - 1498.
- [81] A. Swami, S. Barbarossa, and B. Sadler, "Blind source separation and signal classification," in Proc. Asilomar Conf. on Signals, Systems and Computers (ASILOMAR), 2000, pp. 1187 - 1191.
- [82] H. Deng, M. Doroslovacki, H. Mustafa, J. Xu, and S. Koo, "Instantaneous feature based algorithm for HF digital modulation classification," in Proc. CISS Conf., Baltimore, March 2003.
- [83] Y. Yang, C. Liu, and T. Soong, "A log-likelihood function-based algorithm for QAM signal classification," *Signal Processing*, vol. 70, no. 1, pp. 61 - 71, Oct. 1998.
- [84] D. Boiteau and C. Le Martret, "A generalized maximum likelihood framework for modulation," in Proc. IEEE Int. Conf. on Acoustic, Speech and Signal Processing (ICASSP), May 1998, vol.4, pp. 2162 - 2168.
- [85] Y. Lin and C.-C.J. Kuo, "Classification of quadrature amplitude modulated (QAM) signals via sequential probability ratio test (SPRT)," *Signal Processing*, vol. 60, no.3, pp. 263 - 226, August 1997.
- [86] Y. Lin and C.J. Kuo, "Sequential modulation classification dependent samples," in Proc. IEEE Int. Conf. on Acoustic, Speech and Signal Processing (ICASSP), May 1996, vol.5, pp. 2690 - 2627.
- [87] O. A. Dobre, Y. Bar-Ness and W. Su, "Higher-order cyclic cumulants for high order modulation classification," in Proc. IEEE Int. Conf. for Military Communications (MILCOM), Oct. 2003, vol. 1, pp. 112 - 117.
- [88] O. A. Dobre, Y. Bar-Ness and W. Su, "Robust QAM modulation classification algorithm using cyclic cumulants," in Proc. of IEEE Wireless Communications and Network. Conf. (WCNC), March 2004, vol. 2, pp. 745 - 748.
- [89] S. S. Soliman and S.-Z. Hsue, "Signal classification using statistical moments," *IEEE Trans. on Communication*, vol. 40, no. 5, pp. 908 - 916, May 1992.



- [90] G. Han, J. Li, and D. Lu, "Study of modulation recognition based on HOCs and SVM" in Proc. IEEE Vehicular Technology Conf. (VTC-2004 Spring), May 2004, vol.2 pp. 898 - 902.
- [91] L. Rabiner and B.H. Juang, Fundamentals of Speech Recognition. Prentice Hall Signal Processing Series, 1993.
- [92] A. Kubankova, H. Atassi and D. Kubanek1, "Gaussian Mixture Models-based Recognition of Digital Modulations of Noisy Signals," Electrotechnics magazine, vol.2, no.1, Apr. 2011.
- [93] J. R. Hershey and P. A. Olsen, "Approximating the Kullback Leibler Divergence Between Gaussian Mixture Models," in Proc. IEEE Int. Conf. on Acoustic, Speech and Signal Processing (ICASSP), Apr. 2007, vol.4, pp. 317 - 320.
- [94] M. Siala and D. Duponteil, "Maximum a posteriori multipath fading channel estimation for CDMA systems," in Proc. IEEE Vehicular Technology Conf. (VTC-1999 Fall), Jul. 1999, vol. 2, pp. 1121 - 1125.
- [95] S. Xi and H.-C. Wu, "Robust automatic modulation classification using cumulant features in the presence of fading channels," in Proc. IEEE Wireless Communications and Network. Conf. (WCNC), Apr. 2006, vol. 4, pp. 2094 - 2099.

## Curriculum Vitae

**Name:** Gejie Liu

**Place of birth:** Anqing, Anhui, P.R. China

**Year of birth:** 1986

**Post-secondary Education and Degrees:** 2010–2012, Candidate, Master of Engineering Science  
Faculty of Engineering  
The University of Western Ontario  
London, Ontario, Canada

2005–2009, Bachelor of Engineering  
School of Electronic Engineering  
Xidian University  
Xi'an, Shaanxi, P.R. China

### Publications:

- [1] G. Liu, X. Wang, and J.Y. Chouinard, "Iterative Blind OFDM Parameter Estimation and Synchronization for Cognitive Radio Systems," to appear in *Proc. IEEE Vehicular Technology Conference (IEEE VTC'12 Spring)*.
- [2] G. Liu, X. Wang, J. Nadeau, and P. Ho, "Blind Parameter Estimation for OFDM Interception Receiver with Iterative Cyclostationary Analysis," in *Proc. Intl. Conf. for Military Communication (MILCOM)*, Nov. 2011, pp. 2211 - 2215.
- [3] E. Christopher, G. Liu, X. Wang, J. Samarabandu, "Low-complexity OFDM Channel Predictor Design in Time-varying Wireless Channels," in *Proc. IEEE Canadian Conf. on Electrical and Computer Engineering (CCECE)*, May 2011, pp. 1032 - 1035.
- [4] W. Hou, X. Wang and G. Liu, "ML Detection with Successive Group Interference Cancellation for Interleaved OFDMA Uplink," *IEEE Communication Letter*, issue 99, pp. 1 - 3, Nov. 2011.